Part I: Folds and Bifurcations in the Solutions of Semi-Explicit Differential-Algebraic Equations

Part II: The Recursive Projection Method Applied to Differential-Algebraic Equations and Incompressible Fluid Mechanics

Thesis by
Harald von Sosen

In Partial Fulfillment of the Requirements for the Degree of
Doctor of Philosophy

California Institute of Technology
Pasadena, California
1994

(Submitted May 5, 1994)

Acknowledgements

The work of this thesis could not have been accomplished without the support of the people around me. In particular, I would like to thank my advisor, Professor Herbert Keller, for his patience and guidance. His high expectations have brought out the best in me. I am also grateful to Andrew Conley for the many interesting and productive discussions we had about the material in this thesis.

I wish to thank my parents, Bernd and Charlotte von Sosen, for their love and support over the years, and for teaching me the value of education. Special thanks go to my wife, Valerie, for providing balance in my life and making my years as a graduate student enjoyable.

Abstract

Part I: Folds and Bifurcations in the Solutions of Semi-Explicit Differential-Algebraic Equations

A general existence theory for the solutions of semi-explicit differential-algebraic equations (DAEs) is given. Theorems on the form and number of solutions in a neighborhood of an initial value are presented. A set of bifurcation equations is derived, from which the tangents of these solutions can be computed. The phenomena of folds and bifurcation are studied. It is shown that solutions near fold points and pitchfork bifurcation points can be represented smoothly if an appropriate parametrization is introduced. Moreover, it is shown that the complex analytic extension of a real DAE often has complex solutions near a real initial value, and existence theorems on these complex solutions are given. Examples from electrical engineering are presented in support of the theory. Methods for adapting existing numerical DAE solvers to handle fold and bifurcation points are introduced. These methods are tested on a nonlinear electric circuit problem.

Part II: The Recursive Projection Method Applied to Differential-Algebraic Equations and Incompressible Fluid Mechanics

The Recursive Projection Method (RPM) was originally invented by Schroff and Keller for the stabilization of unstable fixed point iterations. A direct application of RPM lies in the computation of unstable steady states of nonlinear ordinary differential equations (ODEs) via time integration. Here, the method is generalized to handle algebraic constraints so that it can be applied to certain differential-algebraic equations (DAEs). This is accomplished by reformulating the DAE as an ODE. In particular, this approach applies to DAEs obtained by semi-discretization of the incompressible Navier-Stokes equations by use of the method of lines. The method is applied to compute unstable steady states of the flow between concentric rotating cylinders.

Contents

List of Figures

List of Tables

Part I

Folds and Bifurcations in the Solutions of Semi-Explicit Differential-Algebraic Equations

Chapter 1

Introduction

Consider the implicit differential equation

$$\mathbf{F}(\mathbf{x}, \mathbf{x}', t) = \mathbf{0}, \tag{1.1}$$

where $\mathbf{F} : \mathbb{R}^n \times \mathbb{R}^n \times \mathbb{R} \rightarrow \mathbb{R}^n$, and prime ($'$) notation represents differentiation with respect to t. A differential equation of the form (1.1) is usually called a differential-algebraic equation (DAE) if the partial derivative $\mathbf{F}_{\mathbf{p}}(\mathbf{x}, \mathbf{p}, t)$ is singular for all values of its arguments. Because DAEs occur in many practical problems, much effort has recently been devoted to the development of numerical methods to solve such systems. A good numerical treatment requires some knowledge of the analytical background of DAEs, and in particular, an existence theory. However, the existence theory of DAEs is as yet quite incomplete.

The classical approach in the analysis of DAEs is to differentiate (1.1) until it is reduced, at least locally, to an explicit ordinary differential equation

(ODE). The usual assumption in this reduction process is that $\mathbf{F}_{\mathrm{p}}(\mathrm{x}, \mathrm{p}, t)$ has constant rank in some open neighborhood of $\mathbf{F}^{-1}(\mathbf{0})$, and that all derivatives of $\mathbf{F}$ generated in the reduction process satisfy a similar constant rank condition (see [22] for details). If (1.1) can indeed be shown to be equivalent to an ODE in this way, then the DAE is called "nonsingular." The number of times that a nonsingular DAE (1.1) must be differentiated in order to obtain an explicit ODE is called the *index* of the problem (see [2],[19],[23] for definitions of the index). Since nonsingular DAEs can be reduced to ODEs, the existence and uniqueness of their solutions follows from the classical existence and uniqueness theory for ODEs. In fact, Rabier and Rheinboldt have used this idea to develop existence and uniqueness theories for certain subclasses of DAEs, all of which satisfy a constant rank condition (see [22],[26],[27]).

If a DAE fails to satisfy the constant rank condition, we call it "singular." Singular ODEs cannot be reduced to explicit ODEs, and therefore the standard existence and uniqueness theorem for ODEs cannot be applied directly. It is known that solutions of singular DAEs may not be unique, that is they may bifurcate. Furthermore, it is possible that after a finite time, the finite solution of the DAE may have an infinite derivative. The solution may or may not exist for times beyond such points. If the solution cannot be continued into the future, such points are called "impasse points" in the electrical engineering literature. Impasse points have been studied by Chua and Deng in [4] and by Rabier and Rheinboldt in [24] and [25]. As we shall see, they are closely related to what we shall call "simple fold points" in Chapter 5. Although simple fold points are the most common and the most simple type of singularity in a DAE, there are many others for which there

is yet no theory.

In the work presented here, we extend the existence theory for DAEs to cases which do not satisfy any constant rank condition and beyond simple fold points. The work can be viewed as a generalization of the bifurcation theory for algebraic nonlinear equations. Algebraic nonlinear equations are a special case of (1.1) where $\mathbf{F}_{\mathrm{p}}(\mathbf{x}, \mathbf{p}, t)$ is identically zero. We therefore expect to find all phenomena of algebraic nonlinear equations (including folds, bifurcations and complex bifurcations) in DAEs. We confine our analysis to initial value problems of the *semi-explicit* form

$$\frac{d\mathbf{u}}{dt} = \mathbf{f}(\mathbf{u}, \mathbf{v}), \tag{1.2a}$$

$$\mathbf{0} = \mathbf{g}(\mathbf{u}, \mathbf{v}), \tag{1.2b}$$

$$\mathbf{u} = \mathbf{0} \text{ and } \mathbf{v} = \mathbf{0} \text{ at } t = 0, \tag{1.2c}$$

where $\mathbf{u} \in \mathbb{R}^n$, $\mathbf{v} \in \mathbb{R}^m$, $t \in \mathbb{R}$, $\mathbf{f} : \mathbb{R}^n \times \mathbb{R}^m \to \mathbb{R}^n$, $\mathbf{g} : \mathbb{R}^n \times \mathbb{R}^m \to \mathbb{R}^m$, and $\mathbf{g}(\mathbf{0}, \mathbf{0}) = \mathbf{0}$. Without loss of generality, we have written the equations in autonomous form and with homogeneous initial data. If either $\mathbf{f}$ or $\mathbf{g}$ depend on t, then the problem can be transformed to autonomous form by letting $\tilde{\mathbf{u}} = (\mathbf{u}, t)^T$ and adding the equation $t' = 1$.

We use throughout the notation $\mathbf{x} \equiv (\mathbf{u}, \mathbf{v}, t)^T$. Also, in the remainder of this paper, superscript "0" denotes that the superscripted quantity is evaluated at $\mathbf{x} = \mathbf{0}$.

If the partial derivative $\mathbf{g}_{\mathbf{v}}^0$ is nonsingular, then (1.2) is nonsingular with index 1 (by the generally accepted definition of the index). If $\mathbf{g}_{\mathbf{v}}^0$ is singular and of constant rank in a neighborhood about $\mathbf{x} = \mathbf{0}$, then (1.2) may be of index 2 or higher. If $\mathbf{g}_{\mathbf{v}}^0$ is singular without constant rank, then (1.2) is

singular and the index is not defined. When (1.2) is a nonsingular DAE, the local existence and uniqueness of a real solution of (1.2) is well covered in the existing literature (see [22],[26],[27]). The theory presented here covers not only these cases, but also the case when (1.2) is a singular DAE.

Definition 1.3 *If* g_v^0 *is nonsingular, then* $x = 0$ *is called a* regular point.

Definition 1.4 *If* g_v^0 *is singular, then* $x = 0$ *is called a* critical point.

Definition 1.5 *If* $\dim\{\mathcal{N}(g_v^0)\} = 1$, *then* $x = 0$ *is called a* simple critical point.

We shall see that, if $x = 0$ is a critical point, bifurcations or folds may occur at $x = 0$. In addition, (1.2) may have complex solutions passing through a critical point. The theory is analogous to the well known bifurcation theory for algebraic nonlinear equations (as in [7], [13], [11], [15] and [18]). Our theory is also consistent with Rabier's analysis of singular implicit differential equations in [21] and Rabier and Rheinboldt's theory for impasse points of quasilinear DAEs in [24]. In Chapter 7, we present some numerical methods which are useful in computing solutions of singular DAEs.

Before we begin, we list some definitions and assumptions used throughout this paper.

Definition 1.6 *If* $x_0 \in I\!R^k$ *and* $\rho \in I\!R$, *let* $B_\rho(x_0) \equiv \{x \in I\!R^k : \| x - x_0 \| < \rho\}$

Assumption 1.7 $\exists \rho_u > 0, \rho_v > 0$ *such that* $\forall u \in B_{\rho_u}(u^0)$ *and* $v \in B_{\rho_v}(v^0)$, f, g, g_u, g_v, f_u, f_v *exist and are continuous.*

Assumption 1.8 $\exists \rho_u > 0, \rho_v > 0$ *such that* $\forall \mathbf{u} \in B_{\rho_u}(\mathbf{u}^0)$ *and* $\mathbf{v} \in B_{\rho_v}(\mathbf{v}^0)$, $\mathbf{f}, \mathbf{g}, \mathbf{g_u}, \mathbf{g_v}, \mathbf{f_u}, \mathbf{f_v}, \mathbf{g_{uu}}, \mathbf{g_{uv}}, \mathbf{g_{vv}}$ *exist and are continuous.*

Assumption 1.9 $\exists \rho_u > 0, \rho_v > 0$ *such that* $\forall \mathbf{u} \in B_{\rho_u}(\mathbf{u}^0)$ *and* $\mathbf{v} \in B_{\rho_v}(\mathbf{v}^0)$, $\mathbf{g_{uuu}}, \mathbf{g_{uuv}}, \mathbf{g_{uvv}}, \mathbf{g_{vvv}}$ *exist and are continuous.*

Chapter 2

Regular Points

We first consider the case when $\mathbf{x} = \mathbf{0}$ is a regular point, i.e., $\mathrm{g}_{\mathrm{v}}^{0}$ is nonsingular. Although this case is well covered in the existing literature, we include it here for completeness.

If $\mathrm{g}_{\mathrm{v}}^{0}$ is nonsingular, then the Implicit Function Theorem (as stated in [14]) can be applied to (1.2b) to obtain the following lemma:

Lemma 2.1 $\exists \rho_1 > 0, \rho_2 > 0$ *such that* $\forall \mathbf{u} \in B_{\rho_1}(\mathbf{0}), \exists \mathbf{V}(\mathbf{u}) \in B_{\rho_2}(\mathbf{0})$ *such that*

(a) $\mathbf{V}(\mathbf{0}) = \mathbf{0}$;

(b) $\mathrm{g}(\mathbf{u}, \mathbf{V}(\mathbf{u})) = \mathbf{0}$;

(c) $\mathbf{v} = \mathbf{V}(\mathbf{u})$ *is the only solution of* $\mathrm{g}(\mathbf{u}, \mathbf{v}) = \mathbf{0}$ *in* $B_{\rho_2}(\mathbf{0})$ *for* $\mathbf{u} \in B_{\rho_1}(\mathbf{0})$;

(d) $\mathbf{V}(\mathbf{u})$ *has the same modulus of continuity with respect to* $\mathbf{u}$ *as* $\mathrm{g}(\mathbf{u}, \mathbf{v})$.

So, for $\mathbf{u} \in B_{\rho_1}(\mathbf{0})$, we have that $\mathbf{v}=\mathbf{V}(\mathbf{u}) \in B_{\rho_2}(\mathbf{0})$, and (1.2) reduces to the initial value problem:

$$\frac{d\mathbf{u}}{dt} = \mathbf{f}(\mathbf{u}, \mathbf{V}(\mathbf{u})) \tag{2.2a}$$

$$\mathbf{u} = \mathbf{0} \text{ at } t = 0. \tag{2.2b}$$

Since the right-hand side of (2.2a) is only a function of $\mathbf{u}$, (2.2a) is simply an ordinary differential equation (ODE). Lemma 2.3 below is a direct application of the standard existence and uniqueness theory for autonomous ODEs.

Lemma 2.3 *$\exists t_a < 0$ and $t_b > 0$ such that $\forall t \in (t_a, t_b)$, there exists a unique function $\mathbf{u}(t)$ solving (2.2) such that*

(a) $\mathbf{u}(t)$ is continuously differentiable;

(b) $\mathbf{u}(t) \in B_{\rho_1}(\mathbf{0})$, and $\mathbf{V}(\mathbf{u}(t)) \in B_{\rho_2}(\mathbf{0})$.

From Lemma 2.1, we know that the only solution of (1.2b) in $B_{\rho_2}(\mathbf{0})$ is $\mathbf{v} = \mathbf{V}(\mathbf{u})$ for $\mathbf{u}$ in $B_{\rho_1}(\mathbf{0})$. Using $\mathbf{u}(t)$ from Lemma 2.3 in $\mathbf{v} = \mathbf{V}(\mathbf{u})$ we obtain:

$$\mathbf{v}(t) = \mathbf{V}(\mathbf{u}(t)) \tag{2.4}$$

which, by the continuity of $\mathbf{V}(\mathbf{u})$ and $\mathbf{u}(t)$, is continuous and has at least one continuous derivative. Since both $\mathbf{V}(\mathbf{u})$ and $\mathbf{u}(t)$ exist and and are unique for all $t \in (t_a, t_b)$, $\mathbf{v}(t)$ exists and is unique in that interval. Thus, we arrive at Theorem 2.5 below.

Theorem 2.5 *If $\mathbf{f}$ and $\mathbf{g}$ satisfy Assumption 1.7, and $\mathbf{g}_{\mathbf{v}}^0$ is nonsingular, then $\exists$ constants $t_a < 0$ and $t_b > 0$ such that $\forall t \in (t_a, t_b), \exists$ unique real functions $\mathbf{u}(t)$ and $\mathbf{v}(t)$ satisfying:*

(a) $\mathrm{u}(0) = 0,\ \mathrm{v}(0) = 0,$

(b) $\mathrm{g}(\mathrm{u}(t), \mathrm{v}(t)) = 0,$

(c) $\frac{d\mathrm{u}}{dt}(t) = \mathrm{f}(\mathrm{u}(t), \mathrm{v}(t)),$

(d) $\frac{d\mathrm{u}}{dt}(t)$ *and* $\frac{d\mathrm{v}}{dt}(t)$ *exist and are continuous.*

As we have stated earlier, Theorem 2.5 is a well known result. For example, we could have obtained the same result by applying Rheinboldt's theory of semi-implicit DAEs in [27] to (1.2).

Chapter 3

Real Solutions Near Critical Points

We now turn to the case when the initial value $\mathbf{x} = \mathbf{0}$ is a critical point. A special case of critical points occurs when $\mathbf{g}_{\mathbf{v}}^{0}$ has a one-dimensional nullspace, so that $\mathbf{x} = \mathbf{0}$ is a simple critical point. In that case, the theory developed in this chapter simplifies considerably, and we shall consider it in subsequent chapters.

Although a real DAE may have complex solutions which pass through a real critical point, we only look for real solutions in this chapter. Then, in Chapter 4, we shall study the phenomenon of complex bifurcation.

3.1 The Nullspaces

Let $r \in \{1, 2, \ldots, m\}$ be the dimension of the nullspace of $\mathrm{g}_{\mathrm{v}}^0$. Let $\Phi = [\phi_1, \phi_2, \ldots, \phi_r] \in \mathbb{R}^{m \times r}$ and $\Psi = [\psi_1, \psi_2, \ldots, \psi_r] \in \mathbb{R}^{m \times r}$ be orthonormal bases for the right and left nullspaces of $\mathrm{g}_{\mathrm{v}}^0$. Thus,

$$\mathrm{g}_{\mathrm{v}}^0 \Phi = 0,$$

$$\Psi^T \mathrm{g}_{\mathrm{v}}^0 = 0,$$

$$\Phi^T \Phi = \Psi^T \Psi = I_r.$$

Let $Z \in \mathbb{R}^{m \times (m-r)}$ denote an orthonormal basis for the orthogonal complement in $\mathbb{R}^m$ of the right nullspace of $\mathrm{g}_{\mathrm{v}}^0$. Thus, the compound matrix $[\Phi\ Z] \in \mathbb{R}^{m \times m}$ is orthogonal. Now any $\mathrm{v} \in \mathbb{R}^m$ can be uniquely written as

$$\mathrm{v} = \Phi \mathrm{y} + Z \mathrm{z}, \tag{3.1}$$

where $\mathrm{y} = \Phi^T \mathrm{v} \in \mathbb{R}^r$ and $\mathrm{z} = Z^T \mathrm{v} \in \mathbb{R}^{m-r}$. The following relations then hold:

$$\frac{\partial}{\partial \mathrm{y}} \mathrm{g}(\mathrm{u}, \Phi \mathrm{y} + Z \mathrm{z}) = \mathrm{g}_{\mathrm{v}} \Phi,$$

$$\frac{\partial}{\partial \mathrm{z}} \mathrm{g}(\mathrm{u}, \Phi \mathrm{y} + Z \mathrm{z}) = \mathrm{g}_{\mathrm{v}} Z,$$

$$\mathcal{R}(\mathrm{g}_{\mathrm{v}}^0 Z) = \mathcal{R}(\mathrm{g}_{\mathrm{v}}^0).$$

Let $W \in \mathbb{R}^{m \times (m-r)}$ denote an orthonormal basis for the orthogonal complement in $\mathbb{R}^m$ of the left nullspace of $\mathrm{g}_{\mathrm{v}}^0$. Thus, the compound matrix

$[\Psi\ W] \in \mathbb{R}^{m\times m}$ is orthogonal and we have two distinct direct sum decompositions of $\mathbb{R}^m$:

$$\mathbb{R}^m = \mathcal{R}(\Phi) \oplus \mathcal{R}(Z),$$

$$\mathbb{R}^m = \mathcal{R}(\Psi) \oplus \mathcal{R}(W).$$

They will be used to reduce (1.2b) to a problem in $\mathbb{R}^r$. We have used the first decomposition to yield (3.1).

3.2 The Lyapunov-Schmidt Reduction

Since $[\Psi\ W]$ is orthogonal, the equation $\mathbf{g}(\mathbf{u},\mathbf{v}) = \mathbf{0}$ is the same as $W^T\mathbf{g}(\mathbf{u},\mathbf{v}) = 0$ and $\Psi^T\mathbf{g}(\mathbf{u},\mathbf{v}) = 0$. Thus, (1.2b) is equivalent to the system

$$\mathbf{g}_1(\mathbf{u},\mathbf{y},\mathbf{z}) \equiv W^T\mathbf{g}(\mathbf{u},\mathbf{v}) = \mathbf{0}, \tag{3.2a}$$

$$\mathbf{g}_2(\mathbf{u},\mathbf{y},\mathbf{z}) \equiv \Psi^T\mathbf{g}(\mathbf{u},\mathbf{v}) = \mathbf{0}, \tag{3.2b}$$

where $\mathbf{v} = \Phi\mathbf{y} + Z\mathbf{z}$. Immediately we can apply the Implicit Function Theorem to (3.2a) to solve for $\mathbf{z} = \mathbf{z}(\mathbf{u},\mathbf{y})$:

Lemma 3.3 *Suppose* $\mathbf{x} = \mathbf{0}$ *is a critical point and Assumption 1.8 is satisfied. Then* $\exists$ *constants* $\rho_1 > 0, \rho_2 > 0, \rho_3 > 0$ *such that* $\forall \mathbf{u} \in B_{\rho_1}(\mathbf{0})$ *and* $\mathbf{y} \in B_{\rho_2}(\mathbf{0}), \exists$ *unique* $\mathbf{z} = \mathbf{z}(\mathbf{u},\mathbf{y}) \in B_{\rho_3}(\mathbf{0})$ *such that*

(a) $\mathbf{z}(\mathbf{0},\mathbf{0}) = \mathbf{0}$;

(b) $\mathbf{g}_1(\mathbf{u},\mathbf{y},\mathbf{z}(\mathbf{u},\mathbf{y})) = \mathbf{0}$;

(c) $\mathbf{z}(\mathbf{u},\mathbf{y})$ *is twice continuously differentiable.*

Proof: $\mathbf{g_1}(0,0,0) = W^T\mathbf{g}(0,0) = 0$, and the partial derivative

$$\left(\frac{\partial \mathbf{g_1}}{\partial \mathbf{z}}\right)^0 = W^T \mathbf{g}_\mathbf{v}^0 Z \in \mathbb{R}^{(m-r)\times(m-r)}$$

is nonsingular by the definition of W and Z. By Assumption 1.8, $\mathbf{g}$ is twice continuously differentiable. Hence, by the Implicit Function Theorem, the result follows. □

In view of Lemma 3.3, the solution set of $\mathbf{g}(\mathbf{u},\mathbf{v}) = 0$ is, in a neighborhood of $\mathbf{x} = 0$, the same as the solution set of (3.2b) with $\mathbf{z} = \mathbf{z}(\mathbf{u},\mathbf{y})$:

$$\mathbf{g_3}(\mathbf{u},\mathbf{y}) \equiv \mathbf{g_2}(\mathbf{u},\mathbf{y},\mathbf{z}(\mathbf{u},\mathbf{y})) \equiv \Psi^T\mathbf{g}(\mathbf{u},\Phi\mathbf{y} + Z\mathbf{z}(\mathbf{u},\mathbf{y})) = 0. \tag{3.4}$$

The above reduction of (1.2b) to (3.4) is called the Lyapunov-Schmidt reduction.

3.3 Parametrization of Solutions

The solution trajectory of a system of the form (1.2) in which $\mathbf{g}_\mathbf{v}^0$ is singular cannot in general be represented by a unique smooth function of t. Just consider the following example:

Example 3.5 *Let $n = m = 1$ and consider the DAE initial value problem*

$$\frac{du}{dt} = f(u,v) \equiv 1,$$

$$0 = g(u,v) \equiv u - v^2,$$

$$u = v = 0 \text{ at } t = 0.$$

Here: $g_v^0 = -2v|_{v=0} = 0$, *so the initial value is a critical point. Real solutions (plotted in Figure 3.6) exist only for* $t \geq 0$ *and they are:*

$u = t,$

$v = \pm\sqrt{t}.$

In addition, there are two complex solutions for $t < 0$*:*

$u = t,$

$v = \pm i\sqrt{-t},$

where $i = \sqrt{-1}$. *There are two real solutions for* $t > 0$ *and no real solutions for* $t < 0$. *If we include the complex solutions, then there are two solutions on either side of* $t = 0$.

The solution of Example 3.5 is clearly not a single-valued function of t. Further, the t-derivative of v becomes unbounded as $|t| \to 0$. We note, however, that the entire real solution set can be parametrized smoothly by a single scalar parameter, s, as follows:

$$u = s^2, v = s, t = s^2,$$

where $s \in (-\infty, \infty)$. The complex solution set can also be represented as a smooth function:

$$u = -s^2, v = is, t = -s^2.$$

We now return to the general DAE (1.2) with a critical point as its initial value. As is suggested by Example 3.5, it is useful to introduce a new scalar parameter, s, in order to represent the solutions of the DAE (1.2) smoothly near a critical point. The parameter s is defined by a scalar constraint,

$$N(\mathbf{u}, \mathbf{v}, t, s) = 0. \tag{3.7}$$

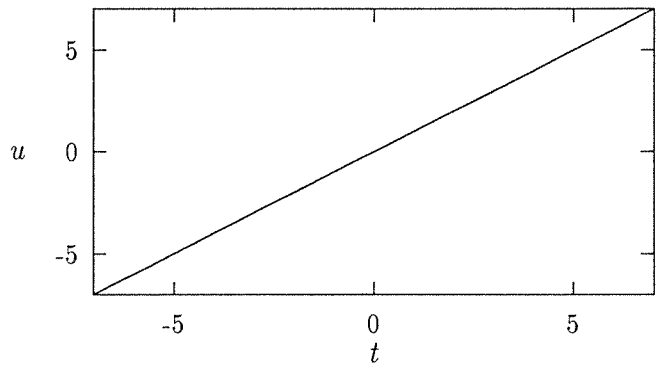

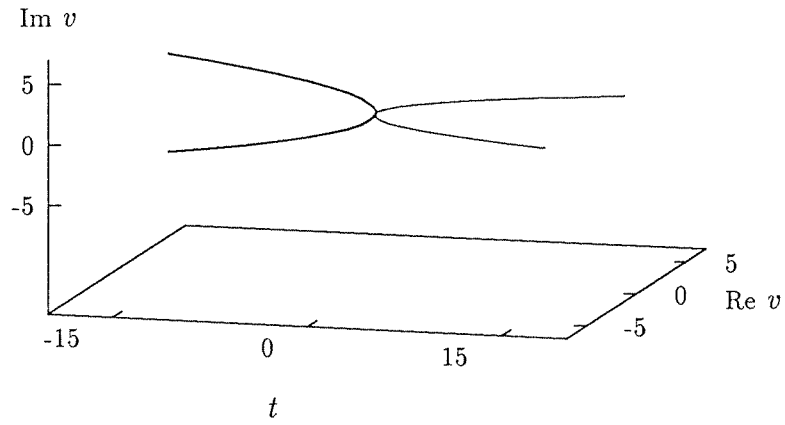

Figure 3.6: Solution set for Example 3.5. Both real and complex solutions are shown.

We do require that $N(\mathbf{0}, \mathbf{0}, 0, s^0) = 0$ for some $s^0 \in \mathbb{R}$, that $N(\mathbf{u}, \mathbf{v}, t, s)$ is at least twice continuously differentiable with respect to all its arguments, and that the partial derivative N_s satisfies

$$N_s \neq 0$$

for all values of its arguments. We further require that

$$N_{\mathbf{v}}^0 \Phi \neq \mathbf{0}.$$

The significance of this requirement will become evident later.

We now seek differentiable solutions of the form

$$\mathbf{x}(s) = \begin{pmatrix} \mathbf{u}(t(s)) \\ \mathbf{v}(t(s)) \\ t(s) \end{pmatrix}$$

which satisfy (1.2) and (3.7), given $\mathbf{u}(t(s^0)) = \mathbf{0}$, $\mathbf{v}(t(s^0)) = \mathbf{0}$, and $t(s^0) = 0$. Thus, we reformulate the problem as follows:

$$\frac{d\mathbf{u}}{dt} = \mathbf{f}(\mathbf{u}, \mathbf{v}), \tag{3.8a}$$

$$\mathbf{0} = \mathbf{g}(\mathbf{u}, \mathbf{v}), \tag{3.8b}$$

$$0 = N(\mathbf{u}, \mathbf{v}, t, s), \tag{3.8c}$$

$$\mathbf{u}(t(s^0)) = \mathbf{0}, \mathbf{v}(t(s^0)) = \mathbf{0}, t(s^0) = 0. \tag{3.8d}$$

We shall use a dot above any quantity to indicate that the quantity is differentiated with respect to s. For example, $\dot{\mathbf{u}} \equiv d\mathbf{u}/ds = (d\mathbf{u}/dt)\dot{t}$.

Example 3.9 *If we let*

$$N(\mathbf{u},\mathbf{v},t,s) \equiv (\dot{\mathbf{u}}^0)^T(\mathbf{u}-\mathbf{u}^0) + (\dot{\mathbf{v}}^0)^T(\mathbf{v}-\mathbf{v}^0) + \dot{t}^0(t-t^0) + (s-s^0)$$

then s *represents a "pseudo-arclength" parameter on a solution path* $\mathbf{x}(s)$ *satisfying* $\mathbf{u}(t(s^0)) = \mathbf{u}^0$, $\mathbf{v}(t(s^0)) = \mathbf{v}^0$, $t(s^0) = t^0$ *and* $\dot{\mathbf{u}}(t(s^0)) = \dot{\mathbf{u}}^0$, $\dot{\mathbf{v}}(t(s^0)) = \dot{\mathbf{v}}^0$, $\dot{t}(s^0) = \dot{t}^0$.

A question which naturally arises is precisely which trajectories can be parametrized smoothly by a specific variable s, or alternatively, which solutions of (1.2) we might miss by choosing a specific normalization (3.7). If a solution trajectory has a tangent vector $\dot{\mathbf{x}}^0 \equiv (\dot{\mathbf{u}}^0, \dot{\mathbf{v}}^0, \dot{t}^0)$ at $\mathbf{x} = 0$, then that tangent vector must satisfy

$$\left(\frac{dN}{ds}\right)^0 = N_{\mathbf{u}}^0\dot{\mathbf{u}}^0 + N_{\mathbf{v}}^0\dot{\mathbf{v}}^0 + N_t^0\dot{t}^0 + N_s^0 = 0. \tag{3.10}$$

In view of (3.10) and the requirement that $N_s^0 \neq 0$, we cannot parametrize solution trajectories with tangents $\dot{\mathbf{x}}^0$ satisfying

$$(N_{\mathbf{u}}^0, N_{\mathbf{v}}^0, N_t^0)\,\dot{\mathbf{x}}^0 = 0.$$

In other words, if a solution trajectory's tangent vector lies in the nullspace of the operator $(N_{\mathbf{u}}^0, N_{\mathbf{v}}^0, N_t^0)$, then that solution trajectory cannot be represented as a differentiable function of s. The nullspace of that operator is an $(n+m)$-dimensional subspace of $\mathbb{R}^{n+m+1}$. For instance, if we choose the parametrization

$$N(\mathbf{u},\mathbf{v},t,s) \equiv t - s, \tag{3.11}$$

we cannot smoothly represent solution trajectories which have a tangent perpendicular to the t-axis. Such trajectories would have to have a tangent satisfying $\dot{t}^0 = 0$, clearly violating (3.11), which dictates $\dot{t}^0 = 1$. It is for this reason that the solution set of Example 3.5 cannot be parametrized as a smooth function of t. Note that the set of tangent vectors $\dot{\mathbf{x}}^0$ with $\dot{t}^0 = 0$ spans an $(n+m)$-dimensional subset of $\mathbb{R}^{n+m+1}$.

The above leads to the conclusion that if we have k different normalizations (3.7), which are independent in the sense that their derivatives $(N_{\mathrm{u}}^0, N_{\mathrm{v}}^0, N_t^0)$ are all linearly independent, then we can parametrize all solution trajectories except ones with tangents in a subspace of $\mathbb{R}^{n+m+1}$ of dimension $n+m+1-k$. Thus there are at most $n+m+1$ independent normalizations. If we have $n+m+1$ independent normalizations, then every trajectory in $\mathbb{R}^{n+m+1}$ can be parametrized by at least one of the $n+m+1$ parameters defined by those normalizations. Furthermore, any distinct normalizations with the same nullspaces are equivalent in the sense that they yield the same trajectories, only with different parametrizations.

In the following, we shall assume that a specific normalization has been chosen.

3.4 Some Necessary Conditions

We now derive some necessary conditions for the existence of solutions of (3.8). In particular, we shall derive the *bifurcation equations*. We also introduce a "reduced" DAE which also represents a necessary condition. In

subsequent sections, we shall see that a sufficient condition for the existence of real solutions of (3.8) is that the bifurcation equations have a real, isolated root. The reduced DAE will aid in the proof of existence theorems.

A necessary condition for the existence of a differentiable solution path $\mathrm{x}(s)$ is

$$\dot{\mathrm{u}} = \frac{d\mathrm{u}}{dt}\frac{dt}{ds} = \mathrm{f}\dot{t}. \tag{3.12}$$

Any twice differentiable solution path must also satisfy

$$\ddot{\mathrm{u}} = \mathrm{f_u}\dot{\mathrm{u}}\dot{t} + \mathrm{f_v}\dot{\mathrm{v}}\dot{t} + \mathrm{f}\ddot{t} = \mathrm{f_u}\mathrm{f}(\dot{t})^2 + \mathrm{f_v}\dot{\mathrm{v}}\dot{t} + \mathrm{f}\ddot{t}. \tag{3.13}$$

Additional necessary conditions include

$$\frac{d^k}{ds^k}\mathrm{g}(\mathrm{u}(t(s)), \mathrm{v}(t(s))) = 0, \quad k = 0, 1, 2, \ldots \tag{3.14}$$

as well as

$$\frac{d^k}{ds^k}N(\mathrm{u}(t(s)), \mathrm{v}(t(s)), t(s), s) = 0, \quad k = 0, 1, 2, \ldots \tag{3.15}$$

Using (3.12) in the k=1 equation of (3.14), we obtain

$$\mathrm{g_u}\mathrm{f}\dot{t} + \mathrm{g_v}\dot{\mathrm{v}} = 0 \tag{3.16}$$

and the k=2 equation is

$$\mathrm{g_u}\mathrm{f}\ddot{t} + \mathrm{g_u}\mathrm{f_u}\mathrm{f}(\dot{t})^2 + \mathrm{g_u}\mathrm{f_v}\dot{\mathrm{v}}\dot{t} + \mathrm{g_{uu}}\mathrm{ff}(\dot{t})^2 + 2\mathrm{g_{vu}}\mathrm{f}\dot{\mathrm{v}}\dot{t} + \mathrm{g_{vv}}\dot{\mathrm{v}}\dot{\mathrm{v}} + \mathrm{g_v}\ddot{\mathrm{v}} = 0. \tag{3.17}$$

Here we have used the continuity of second derivatives to set $\mathrm{g_{uv}}\dot{\mathrm{v}}\mathrm{f} = \mathrm{g_{vu}}\mathrm{f}\dot{\mathrm{v}}$.

3.4.1 Fold Points versus Bifurcation Points

In particular, equations (3.14)-(3.17) must hold at the initial value, s^0. Using (3.1) in (3.16), evaluated at s^0, one obtains:

$$g_v^0 Z \dot{z}^0 = -g_u^0 f^0 \dot{t}^0. \tag{3.18}$$

The coefficient matrix of $\dot{z}^0$ is of order $m \times (m-r)$. If $g_u^0 f^0 \in \mathcal{R}(g_v^0)$, there are infinitely many combinations of $\dot{t}^0$ and $\dot{z}^0$ which satisfy (3.18). Since $g_v^0 Z$ has full rank, there exists a unique ζ such that

$$g_v^0 Z \zeta = -g_u^0 f^0.$$

All solutions of (3.18) are then given by:

$$\dot{z}^0 = \zeta \dot{t}^0. \tag{3.19}$$

If, on the other hand, $g_u^0 f^0 \notin \mathcal{R}(g_v^0)$, there is only one way that (3.18) can be satisfied: $\dot{t}^0 = 0$ and $\dot{z}^0 = \mathbf{0}$. This implies $\dot{u}^0 = \mathbf{0}$ by (3.12).

It is convenient at this point to divide critical points into two categories. If $g_u^0 f^0 \in \mathcal{R}(g_v^0)$, we call the initial value a *bifurcation point*; otherwise, if $g_u^0 f^0 \notin \mathcal{R}(g_v^0)$, the initial value is called a *fold point*:

Definition 3.20 *If* $x = 0$ *is a critical point, and* $g_u^0 f^0 \in \mathcal{R}(g_v^0)$, *then* $x = 0$ *is called a* bifurcation point.

Definition 3.21 *If* $x = 0$ *is a critical point, and* $g_u^0 f^0 \notin \mathcal{R}(g_v^0)$, *then* $x = 0$ *is called a* fold point.

Note that (3.19) holds for fold points, as well as for bifurcation points. For fold points, (3.19) holds for any choice of ζ. We shall define ζ=0 for fold points.

3.4.2 The Bifurcation Equations

If we evaluate (3.17) at s^0 and left multiply with Ψ^T, we obtain (using $\Psi^T \mathrm{g}_{\mathrm{v}}^0 = \mathbf{0}$):

$$\Psi^T \mathrm{g}_{\mathrm{u}}^0 \mathrm{f}^0 \ddot{t}^0 + \Psi^T \mathrm{g}_{\mathrm{u}}^0 \mathrm{f}_{\mathrm{u}}^0 \mathrm{f}^0 (\dot{t}^0)^2 + \Psi^T \mathrm{g}_{\mathrm{u}}^0 \mathrm{f}_{\mathrm{v}}^0 \dot{\mathrm{v}}^0 \dot{t}^0 + \Psi^T \mathrm{g}_{\mathrm{uu}}^0 \mathrm{f}^0 \mathrm{f}^0 (\dot{t}^0)^2 + 2\Psi^T \mathrm{g}_{\mathrm{vu}}^0 \mathrm{f}^0 \dot{\mathrm{v}}^0 \dot{t}^0 + \Psi^T \mathrm{g}_{\mathrm{vv}}^0 \dot{\mathrm{v}}^0 \dot{\mathrm{v}}^0 = \mathbf{0}. \tag{3.22}$$

By using equations (3.1) and (3.19) in (3.22), and adding the $k = 1$ equation of (3.15) evaluated at s^0, the *bifurcation equations* are derived:

$$\mathrm{h}(\dot{\mathrm{y}}^0, \dot{t}^0, \ddot{t}^0) \equiv \begin{pmatrix} \mathrm{h}_1(\dot{\mathrm{y}}^0, \dot{t}^0, \ddot{t}^0) \\ N_{\mathrm{v}}^0 \Phi \dot{\mathrm{y}}^0 + (N_{\mathrm{u}}^0 \mathrm{f}^0 + N_t^0 + N_{\mathrm{v}}^0 Z\zeta)\dot{t}^0 + N_s^0 \end{pmatrix} = 0 \tag{3.23}$$

where

$$\mathrm{h}_1(\dot{\mathrm{y}}^0, \dot{t}^0, \ddot{t}^0) \equiv \Psi^T \mathrm{g}_{\mathrm{u}}^0 \mathrm{f}^0 \ddot{t}^0 + \Psi^T \mathrm{g}_{\mathrm{vv}}^0 \Phi \dot{\mathrm{y}}^0 \Phi \dot{\mathrm{y}}^0 + A_1 \Phi \dot{\mathrm{y}}^0 \dot{t}^0 + A_0 (\dot{t}^0)^2 \tag{3.24}$$

with

$$A_1 \equiv \Psi^T \mathrm{g}_{\mathrm{u}}^0 \mathrm{f}_{\mathrm{v}}^0 + 2\Psi^T \mathrm{g}_{\mathrm{vu}}^0 \mathrm{f}^0 + 2\Psi^T \mathrm{g}_{\mathrm{vv}}^0 Z\zeta,$$

$$A_0 \equiv \Psi^T \mathrm{g}_{\mathrm{u}}^0 \mathrm{f}_{\mathrm{u}}^0 \mathrm{f}^0 + \Psi^T \mathrm{g}_{\mathrm{u}}^0 \mathrm{f}_{\mathrm{v}}^0 Z\zeta + \Psi^T \mathrm{g}_{\mathrm{uu}}^0 \mathrm{f}^0 \mathrm{f}^0 + 2\Psi^T \mathrm{g}_{\mathrm{vu}}^0 \mathrm{f}^0 Z\zeta + \Psi^T \mathrm{g}_{\mathrm{vv}}^0 Z\zeta Z\zeta.$$

The bifurcation equations represent a necessary condition for the existence of solution paths. We shall show that a sufficient condition for the existence

of a real solution path is that the bifucation equations have a real, isolated root $(\dot{\mathbf{y}}^0, \dot{t}^0, \ddot{t}^0)$. In fact, we shall show that for each such root, there exists a distinct real, differentiable solution path passing through the initial value.

3.4.3 A Reduced DAE

In view of Lemma 3.3 and equation (3.12), any differentiable solution of (3.8) is (locally) also a solution of the following reduced DAE in the $n+r+1$ variables $\mathbf{u}$, $\mathbf{y}$, and t (recall (3.4)):

$$\dot{\mathbf{u}} = \mathbf{f}(\mathbf{u}, \Phi\mathbf{y} + Z\mathbf{z}(\mathbf{u}, \mathbf{y}))\dot{t}; \tag{3.25a}$$

$$\mathbf{g}_3(\mathbf{u}, \mathbf{y}) = \mathbf{0}; \tag{3.25b}$$

$$N(\mathbf{u}, \Phi\mathbf{y} + Z\mathbf{z}(\mathbf{u}, \mathbf{y}), t, s) = 0; \tag{3.25c}$$

$$\mathbf{u} = \mathbf{0}, \mathbf{y} = \mathbf{0} \text{ and } t = 0 \text{ at } s = s^0. \tag{3.25d}$$

In order to demonstrate the existence of a solution of (3.8), we shall first prove the existence of a solution of (3.25). Then we shall show that this solution also satisfies (3.8) by using the following lemma:

Lemma 3.26 *Suppose* $\exists\, s_a < s^0, s_b > s^0$ *such that on* (s_a, s_b) *there exists a continuously differentiable solution* $\mathbf{u} = \mathbf{U}(s)$, $\mathbf{y} = \mathbf{y}(s)$, $t = t(s)$ *of (3.25). Furthermore, assume that this solution satisfies either*

(a) $\dot{t}^0 \neq 0$, *or*

(b) $t(s)$ *is twice continuously differentiable on* (s_a, s_b), *and* $\ddot{t}^0 \neq 0$.

Then

$$\mathbf{x}(s) = \begin{pmatrix} \mathbf{u}(t(s)) \\ \mathbf{v}(t(s)) \\ t(s) \end{pmatrix} = \begin{pmatrix} \mathbf{U}(s) \\ \Phi\mathbf{y}(s) + Z\mathbf{z}(\mathbf{U}(s), \mathbf{y}(s)) \\ t(s) \end{pmatrix}$$

is a solution of (3.8) and hence of (1.2) on some subinterval of (s_a, s_b) *containing* s^0.

Proof: From the Lyapunov-Schmidt reduction and Lemma 3.3, we know that (3.25b) is locally equivalent to $\mathbf{g}(\mathbf{u}, \mathbf{v}) = \mathbf{0}$, which is (3.8b). By (3.1), (3.25c) is the same as (3.8c). The initial condition (3.8d) is satisfied because in (3.25) we use $\mathbf{z}=\mathbf{z}(\mathbf{u},\mathbf{y})$ from Lemma 3.3, which guarantees

$$\mathbf{z}(\mathbf{u}(t(s^0)), \mathbf{v}(t(s^0))) = \mathbf{z}(\mathbf{0}, \mathbf{0}) = 0.$$

So we conclude that, at least locally, (3.8bcd) are satisfied. It remains to show that $\mathbf{x}(s)$ satisfies (3.8a).

Consider first the case when $\dot{t}^0 \neq 0$. Then $t = t(s)$ can be inverted, locally, to get a unique continuously differentiable function $s = S(t)$. Then

$$\mathbf{U}(s) = \mathbf{U}(S(t(s))) = \mathbf{u}(t(s)),$$

and

$$\frac{d\mathbf{u}}{dt} = \frac{d\mathbf{U}}{ds}\frac{dS}{dt} = \frac{\dot{\mathbf{u}}}{\dot{t}}$$

and (3.8a) is satisfied in some interval (s_c, s_d) containing s^0.

Now consider the case when $\dot{t}^0 = 0$, but $\ddot{t}^0 \neq 0$. Then the following expansions are valid for s near s^0:

$$\mathbf{u}(t(s)) = \mathbf{f}^0\ddot{t}^0\frac{(s - s^0)^2}{2} + O\left((s - s^0)^3\right)$$

$$t(s) = \ddot{t}^0 \frac{(s-s^0)^2}{2} + O\left((s-s^0)^3\right),$$
$$\dot{t}(s) = \ddot{t}^0 (s-s^0) + O\left((s-s^0)^2\right).$$

Then,

$$\frac{d\mathbf{u}}{dt}(t(s^0)) = \frac{\mathbf{f}^0 \ddot{t}^0}{\ddot{t}^0} = \mathbf{f}^0$$

so (3.8a) is satisfied at $s = s^0$. From the expansion of $\dot{t}(s)$, we may conclude that there exists an interval $I \subset (s_a, s_b)$ containing s^0 such that $\dot{t}(s) \neq 0$ for all $s \in J \equiv I \setminus \{s^0\}$. Then for all $s \in J$:

$$\frac{d\mathbf{u}}{dt}(t(s)) = \frac{\dot{\mathbf{u}}(t(s))}{\dot{t}(s)} = \frac{\mathbf{f}(\mathbf{u}(t(s)), \mathbf{v}(t(s)))\dot{t}(s)}{\dot{t}(s)} = \mathbf{f}(\mathbf{u}(t(s)), \mathbf{v}(t(s)))$$

and (3.8a) is satisfied for all $s \in I$. □

3.5 Existence of Real Solutions Near Fold Points

We are now ready to state some existence theorems. We first consider the case when the initial value is a fold point. That is,

$$\mathbf{g}_\mathbf{u}^0 \mathbf{f}^0 \notin \mathcal{R}(\mathbf{g}_\mathbf{v}^0),$$

which can also be written

$$\Psi^T \mathbf{g}_\mathbf{u}^0 \mathbf{f}^0 \neq \mathbf{0}.$$

We saw in Section 3.4.1 that all differentiable solutions passing through a fold point satisfy

$$\dot{t}^0 = 0,$$

$$\dot{\mathbf{u}}^0 = 0,$$

$$\dot{\mathbf{z}}^0 = 0.$$

This simplifies the bifurcation equations to:

$$\mathbf{h}_{fold}(\dot{\mathbf{y}}^0, \ddot{t}^0) \equiv \mathbf{h}(\dot{\mathbf{y}}^0, 0, \ddot{t}^0) = \begin{pmatrix} \Psi^T \mathbf{g}_{\mathbf{u}}^0 \mathbf{f}^0 \ddot{t}^0 + \Psi^T \mathbf{g}_{\mathbf{vv}}^0 \Phi \dot{\mathbf{y}}^0 \Phi \dot{\mathbf{y}}^0 \\ \\ N_{\mathbf{v}}^0 \Phi \dot{\mathbf{y}}^0 + N_s^0 \end{pmatrix} = \mathbf{0}. \quad (3.27)$$

Equation (3.27) is a set of $r+1$ equations in $r+1$ unknowns. The first r equations are quadratic in the components of $\dot{\mathbf{y}}^0$, and the last equation is linear. One of the quadratic equations can be used to solve for $\ddot{t}^0$ in terms of $\dot{\mathbf{y}}^0$. Then we are left with $r-1$ quadratic equations and one linear equation in $\dot{\mathbf{y}}^0$. Such a system can have at most 2^{r-1} isolated solutions, and the solutions are real or complex conjugate pairs.

Theorem 3.28 *Suppose* $\mathbf{x} = \mathbf{0}$ *is a fold point and Assumption 1.8 is satisfied. Then corresponding to each* real, isolated *root* $(\dot{\mathbf{y}}^0, \ddot{t}^0)$ *of (3.27), there exists a unique, real solution* $\mathbf{u} = \mathbf{U}(s)$, $\mathbf{y} = \mathbf{y}(s)$, $t = t(s)$ *of (3.25) on some interval* (s_a, s_b) *containing* s^0 *with:*

(a) $\mathbf{U}(s)$ *is twice continuously differentiable;*

(b) $\mathbf{y}(s)$ *is continuously differentiable;*

(c) $t(s)$ *is twice continuously differentiable.*

It has the form

$$\begin{aligned} \mathbf{U}(s) &= \frac{1}{2}\left(s - s^0\right)^2 \mathbf{f}^0 \ddot{t}^0 + O\left((s - s^0)^3\right), \\ \mathbf{y}(s) &= \left(s - s^0\right) \dot{\mathbf{y}}^0 + O\left((s - s^0)^2\right), \\ t(s) &= \frac{1}{2}\left(s - s^0\right)^2 \ddot{t}^0 + O\left((s - s^0)^3\right). \end{aligned}$$

Proof: We need only consider $s = s^0 + \epsilon$, where $|\epsilon| \ll 1$. We make the following rescaling:

$$\mathbf{y} = \epsilon\boldsymbol{\xi} \text{ and } t = \frac{\epsilon^2}{2}\tau.$$

Now define, recalling (3.4):

$$\mathbf{G}(\boldsymbol{\xi}, \tau, \epsilon, \mathbf{u}) \equiv \begin{cases} \begin{pmatrix} \frac{2}{\epsilon^2}\mathbf{g}_3(\mathbf{u}, \epsilon\boldsymbol{\xi}) \\ \frac{1}{\epsilon}N(\mathbf{u}, \Phi\epsilon\boldsymbol{\xi} + Z\mathbf{z}(\mathbf{u}, \epsilon\boldsymbol{\xi}), \frac{\epsilon^2}{2}\tau, s^0 + \epsilon) \end{pmatrix}, & \epsilon \neq 0; \\ \mathbf{h}_{fold}(\boldsymbol{\xi}, \tau), & \epsilon = 0. \end{cases}$$

When $\epsilon \neq 0$, the solutions of $\mathbf{G}(\boldsymbol{\xi}, \tau, \epsilon, \mathbf{u}) = \mathbf{0}$ are precisely the solutions of (3.25bc). Using Assumption 1.8 and L'Hôpital's rule, it is easily verified that $\mathbf{G}(\boldsymbol{\xi}, \tau, \epsilon, \mathbf{u})$ is a continuous function. Since we assumed that $(\dot{\mathbf{y}}^0, \ddot{t}^0)$ is an isolated real root of (3.27), one solution of $\mathbf{G}(\boldsymbol{\xi}, \tau, \epsilon, \mathbf{u}) = \mathbf{0}$ is

$$\boldsymbol{\xi} = \dot{\mathbf{y}}^0,$$

$$\tau = \ddot{t}^0,$$

$$\epsilon = 0,$$

$$\mathbf{u} = \mathbf{0}.$$

The Jacobian $\mathbf{G}_{\xi,\tau}(\dot{\mathbf{y}}^0, \ddot{t}^0, 0, 0)$ is nonsingular at any isolated root $(\dot{\mathbf{y}}^0, \ddot{t}^0)$; that is what we mean by an isolated root. Thus we can apply the Implicit Function Theorem to obtain, corresponding to each isolated root $(\dot{\mathbf{y}}^0, \ddot{t}^0)$, the existence of unique, continuous functions $\boldsymbol{\xi}(\mathbf{u}, \epsilon)$ and $\tau(\mathbf{u}, \epsilon)$ satisfying

(a) $\mathbf{G}(\boldsymbol{\xi}, \tau, \epsilon, \mathbf{u}) = \mathbf{0}$,

(b) $\boldsymbol{\xi}(\mathbf{0}, 0) = \dot{\mathbf{y}}^0$, and

(c) $\tau(\mathbf{0},0) = \ddot{t}^0$.

The existence and uniqueness of these functions is guaranteed in some sufficiently small neighborhood of $\mathbf{u} = \mathbf{0}$ and $\epsilon = 0$. Closer examination reveals that $\boldsymbol{\xi}(\mathbf{u},\epsilon)$ and $\tau(\mathbf{u},\epsilon)$ are actually twice continuously differentiable, except possibly when $\epsilon = 0$; this is because $\mathbf{G}(\boldsymbol{\xi},\tau,\epsilon,\mathbf{u})$ has two continuous derivatives for $\epsilon \neq 0$. Now, (3.25) is equivalent to

$$\frac{d\mathbf{u}}{ds} = \begin{cases} \mathbf{f}(\mathbf{u}, Z\mathbf{z}(\mathbf{u},\epsilon\boldsymbol{\xi}) + \Phi\epsilon\boldsymbol{\xi})\left(\epsilon\tau + \frac{\epsilon^2}{2}\tau_{\mathbf{u}}\frac{d\mathbf{u}}{ds} + \frac{\epsilon^2}{2}\tau_\epsilon\right), & \epsilon \neq 0; \\ \mathbf{0}, & \epsilon = 0; \end{cases}$$

$$\mathbf{u} = \mathbf{0} \text{ at } s = s^0;$$

where $\boldsymbol{\xi} = \boldsymbol{\xi}(\mathbf{u},\epsilon)$ and $\tau = \tau(\mathbf{u},\epsilon)$. This is an ODE initial value problem of the form:

$$\frac{d\mathbf{u}}{ds} = \mathbf{F}(\mathbf{u}, s),$$
$$\mathbf{u} = \mathbf{0} \text{ at } s = s^0,$$

where $\mathbf{F}(\mathbf{u},s)$ is at least once continuously differentiable for $\| \mathbf{u} \|$ and $\epsilon = s - s^0$ sufficiently small. Standard existence and uniqueness theory for non-autonomous ODEs then guarantees the existence of a unique function $\mathbf{u} = \mathbf{U}(s)$ satisfying (3.25) for s sufficiently close to s^0. That function has at least two continuous derivatives. Then $\mathbf{y}$ and t are uniquely given by:

$$\mathbf{y}(s) = (s - s^0)\,\boldsymbol{\xi}\left(\mathbf{U}(s), s - s^0\right).$$

$$t(s) = \frac{(s - s^0)^2}{2}\,\tau\left(\mathbf{U}(s), s - s^0\right).$$

A Taylor expansion of (3.13) and the above two equations in s about $s = s^0$ reveals the form of the solution given in the theorem. □

Theorem 3.29 *Suppose* $\mathbf{x} = \mathbf{0}$ *is a fold point and Assumption 1.8 is satisfied. Then corresponding to each* real, isolated *root* $(\dot{\mathbf{y}}^0, \ddot{t}^0)$ *of (3.27) with* $\ddot{t}^0 \neq 0$, *there exists a unique, real solution* $\mathbf{x}(s)$ *on some interval* s_c, s_d *containing* s^0, *satisfying (3.8) and hence (1.2), such that:*

(a) $\mathbf{u}(t(s))$ *is twice continuously differentiable;*

(b) $\mathbf{v}(t(s))$ *is continuously differentiable;*

(c) $t(s)$ *is twice continuously differentiable.*

It has the form

$$\begin{aligned} \mathbf{u}(t(s)) &= \frac{1}{2}\left(s - s^0\right)^2 \mathbf{f}^0 \ddot{t}^0 + O\left((s - s^0)^3\right), \\ \mathbf{v}(t(s)) &= \left(s - s^0\right) \Phi \dot{\mathbf{y}}^0 + O\left((s - s^0)^2\right), \\ t(s) &= \frac{1}{2}\left(s - s^0\right)^2 \ddot{t}^0 + O\left((s - s^0)^3\right). \end{aligned}$$

Proof: From Theorem 3.28 we know that for each isolated root of the bifurcation equations, (3.25) has a unique solution $\mathbf{u} = \mathbf{U}(s)$, $\mathbf{y} = \mathbf{y}(s)$, $t = t(s)$ for all s in some interval (s_a, s_b) containing s^0. Since we assume $\ddot{t}^0 \neq 0$, Lemma 3.26 guarantees that it corresponds to a unique solution satisfying (3.8) and hence (1.2) in some subinterval of (s_a, s_b) containing s^0.

The form of $\mathbf{u}(t(s))$ and $t(s)$ follows from Theorem 3.28. To get the form of $\mathbf{v}(t(s))$, recall (3.1) and consider that $\dot{\mathbf{z}}^0$ must be zero because of (3.18) and $\dot{t}^0 = 0$. The form of $\mathbf{v}(t(s))$ then follows from a Taylor expansion in s about $s = s^0$. □

Each solution branch $\mathbf{x}(s)$ with $\ddot{t}^0 > 0$ represents, locally, two solutions for $t > 0$ and no solutions for $t < 0$. Similarly, solution branches with $\ddot{t}^0 < 0$ locally have two solutions for $t < 0$, and none for $t > 0$. If all solution branches have $\ddot{t}^0 > 0$, then locally real solutions exist only for $t > 0$.

Likewise, if all solution branches have the $\ddot{t}^0 < 0$, then locally solutions exits only for $t < 0$. However, if some solution branches have $\ddot{t}^0 < 0$, and others $\ddot{t}^0 > 0$, then real solutions extend in both directions in t.

Example 3.30 *The problem in Example 3.5 on page 13 provides an example of a fold. In that example, $u = v = t = 0$ is a simple critical point. It qualifies as a fold point because $g_u^0 f^0 = 1$ and $g_v^0 = 0$, so $g_u^0 f^0 \notin \mathcal{R}(g_v^0)$. If we let*

$$N(u, v, t, s) = v - s,$$

then the bifurcation equations for this example are

$$\ddot{t}^0 - 2(\dot{y}^0)^2 = 0,$$

$$\dot{y}^0 - 1 = 0.$$

The bifurcation equations for this case have only one root, and it is $\dot{y}^0 = 1$, $\ddot{t}^0 = 2$. Since $\ddot{t}^0 \neq 0$, Theorem 3.29 applies. The solution corresponding to the only root of the bifurcation equations is $u(t(s)) = t(s) = s^2$, $v(t(s)) = s$. Two real solutions exist for $t > 0$, and no real solutions exist for $t < 0$. Note that there are also two complex solutions for $t < 0$. Complex solutions will be discussed in Chapter 4.

Example 3.31 *When $r > 1$, there may be up to 2^r real solution branches on one side of $t = 0$. Let $n = 1$, $m = 2$, and consider the DAE*

$$\frac{du}{dt} = f(u, v_1, v_2) \equiv 1,$$

$$0 = \mathrm{g}(u, v_1, v_2) \equiv \begin{pmatrix} u + v_1^2 \\ u + v_2^2 \end{pmatrix},$$

$$u = v_1 = v_2 = 0 \text{ at } t = 0.$$

Then $g_v^0 = 0$, *so* $r = \dim\{\mathcal{N}(g_v^0)\} = 2$. *There are four real solutions, all of which exist only for* $t \leq 0$ *(see Figure 3.32):*

(1) $u = t$, $v_1 = \sqrt{-t}$, $v_2 = \sqrt{-t}$;

(2) $u = t$, $v_1 = \sqrt{-t}$, $v_2 = -\sqrt{-t}$;

(3) $u = t$, $v_1 = -\sqrt{-t}$, $v_2 = \sqrt{-t}$;

(4) $u = t$, $v_1 = -\sqrt{-t}$, $v_2 = -\sqrt{-t}$.

If we set

$$N(u, v_1, v_2, t, s) = v_1 - s,$$

then the bifurcation equations are

$$\ddot{t}^0 + 2(\dot{v}_1^0)^2 = 0,$$

$$\ddot{t}^0 + 2(\dot{v}_2^0)^2 = 0,$$

$$\dot{v}_1^0 - 1 = 0.$$

There are two isolated roots: $\dot{v}_1^0 = 1$, $\dot{v}_2^0 = \pm 1$, $\ddot{t}^0 = -2$. *Thus, by Theorem 3.29, there are two solution paths. They are*

$u(t(s)) = t(s) = -s^2$,

$v_1(t(s)) = s$,

$v_2(t(s)) = \pm s$.

Notice that for both solution branches, $t(s) \leq 0$ *for all* $s \in (-\infty, \infty)$, *so real solutions exist only for* $t \leq 0$. *Note that if we allow complex solutions, there are also four solutions for* $t > 0$: *(1)* $u = t$, $v_1 = i\sqrt{t}$, $v_2 = i\sqrt{t}$;

(2) $u = t$, $v_1 = i\sqrt{t}$, $v_2 = -i\sqrt{t}$;

(3) $u = t$, $v_1 = -i\sqrt{t}$, $v_2 = i\sqrt{t}$;

(3) $u = t$, $v_1 = -i\sqrt{t}$, $v_2 = i\sqrt{t}$;

(4) $u = t$, $v_1 = -i\sqrt{t}$, $v_2 = -i\sqrt{t}$.

Here $i = \sqrt{-1}$. *If we let*

$$\hat{s} \equiv -iv_1,$$

we can write these four solutions as:

$u(t(\hat{s})) = t(\hat{s}) = \hat{s}^2$,

$v_1(t(\hat{s})) = i\hat{s}$,

$v_2(t(\hat{s})) = \pm i\hat{s}$,

where $\hat{s} \in (-\infty, \infty)$. *So if we include the complex solutions, there are four solutions for all* t, *and there are four differentiable solution paths passing through* $\mathbf{x} = \mathbf{0}$. *This phenomenon will be discussed in Chapter 4.*

Example 3.33 *If the bifurcation equations have no real roots, then no real solutions of the DAE exist. Let* $n = 1$, $m = 2$, *and consider the DAE*

$$\frac{du}{dt} = f(u, v_1, v_2) \equiv 1,$$

$$0 = \mathrm{g}(u, v_1, v_2) \equiv \begin{pmatrix} u - v_1^2 \\ u + v_2^2 \end{pmatrix},$$

$$u = v_1 = v_2 = 0 \text{ at } t = 0.$$

As in Example 3.31, $\mathrm{g}_{\mathrm{v}}^0 = 0$, *and* $r = \dim\{\mathcal{N}(\mathrm{g}_{\mathrm{v}}^0)\} = 2$. *But unlike Example 3.31, this DAE has no real solutions for either* $t > 0$ *or* $t < 0$. *Again we set*

$$N(u, v_1, v_2, t, s) = v_1 - s,$$

and the bifurcation equations for this example are

$$\ddot{t}^0 - 2(\dot{v}_1^0)^2 = 0,$$

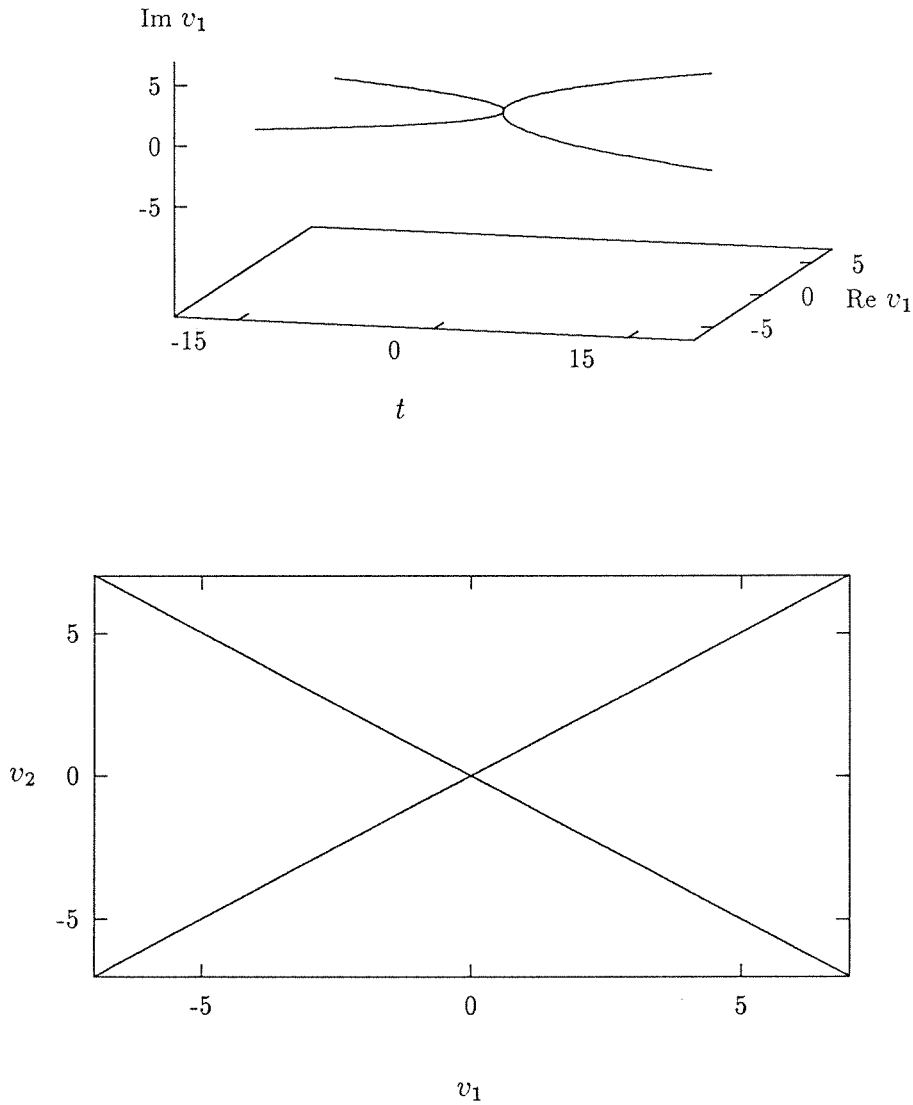

Figure 3.32: Solution set for Example 3.31. Both real and complex solutions are shown.

$$\ddot{t}^0 + 2(\dot{v}_2^0)^2 = 0,$$

$$\dot{v}_1^0 - 1 = 0.$$

The complex roots are $\dot{v}_1^0 = 1$, $\dot{v}_2^0 = \pm i$, $\ddot{t}^0 = 2$, *where* $i = \sqrt{-1}$. *The bifurcation equations have no real roots and the DAE has no real solutions. However, this DAE does have the four complex solutions*

$u = t, v_1 = \pm\sqrt{t}, v_2 = \pm\sqrt{-t}.$

Note that there are four complex solutions for $t < 0$ *and four for* $t > 0$. *If we let* $\hat{s} \in IR$, *then the solution set can be written as four differentiable functions of* $\hat{s}$:

(1) $u = \hat{s}^2$, $v_1 = \hat{s}$, $v_2 = i\hat{s}$;

(2) $u = \hat{s}^2$, $v_1 = \hat{s}$, $v_2 = -i\hat{s}$;

(3) $u = -\hat{s}^2$, $v_1 = i\hat{s}$, $v_2 = \hat{s}$;

(4) $u = -\hat{s}^2$, $v_1 = i\hat{s}$, $v_2 = -\hat{s}$.

It is no coincidence that the number of solutions for $t < 0$ *equals the number of solutions for* $t > 0$. *The theory for this will be discussed in Chapter 4.*

3.6 Existence of Real Solutions Near Bifurcation Points

We now consider the case when $\mathbf{x} = \mathbf{0}$ is a bifurcation point; that is,

$$\mathbf{g}_u^0 \mathbf{f}^0 \in \mathcal{R}(\mathbf{g}_v^0),$$

or equivalently,

$$\Psi^T \mathbf{g}_u^0 \mathbf{f}^0 = \mathbf{0}.$$

In this case, the first term of (3.24) vanishes and the bifurcation equations no longer contain the quantity $\ddot{t}^0$. The bifurcation equations become

$$\mathrm{h}_{bif}(\dot{\mathrm{y}}^0, \dot{t}^0) \equiv \begin{pmatrix} \Psi^T \mathrm{g}^0_{\mathrm{vv}} \Phi \dot{\mathrm{y}}^0 \Phi \dot{\mathrm{y}}^0 + A_1 \Phi \dot{\mathrm{y}}^0 \dot{t}^0 + A_0 (\dot{t}^0)^2 \\ N^0_{\mathrm{v}} \Phi \dot{\mathrm{y}}^0 + (N^0_{\mathrm{u}} \mathrm{f}^0 + N^0_t + N^0_{\mathrm{v}} Z\boldsymbol{\zeta}) \dot{t}^0 + N^0_s \end{pmatrix} = \mathbf{0}. \qquad (3.34)$$

As in the fold case, we have $r+1$ equations in $r+1$ unknowns; r of the equations are quadratic and one is linear, so there can be at most 2^r isolated roots. Since all coefficients are real, the roots must be real or complex conjugate pairs.

Theorem 3.35 *Suppose* $\mathrm{x} = \mathbf{0}$ *is a bifurcation point and Assumption 1.8 is satisfied. Then corresponding to each* real, isolated *solution* $(\dot{\mathrm{y}}^0, \dot{t}^0)$ *of (3.34), there exists a unique, real, continuously differentiable solution* $\mathrm{u} = \mathbf{U}(s)$, $\mathrm{y} = \mathrm{y}(s)$, $t = t(s)$ *satisfying (3.25) on some interval* (s_a, s_b) *containing* s^0. *It has the form*

$$\begin{aligned} \mathbf{U}(s) &= \left(s - s^0\right) \mathrm{f}^0 \dot{t}^0 + O\left((s-s^0)^2\right), \\ \mathrm{y}(s) &= \left(s - s^0\right) \dot{\mathrm{y}}^0 + O\left((s-s^0)^2\right), \\ t(s) &= \left(s - s^0\right) \dot{t}^0 + O\left((s-s^0)^2\right). \end{aligned}$$

Proof: The proof is similar to that of Theorem 3.28. As in the fold case, we only consider $s = s^0 + \epsilon$, where $|\epsilon| \ll 1$, and we make the rescaling:

$$\mathrm{y} = \epsilon \boldsymbol{\xi} \text{ and } t = \epsilon \tau.$$

Define

$$\mathbf{G}(\boldsymbol{\xi},\tau,\epsilon,\mathbf{u}) \equiv \begin{cases} \begin{pmatrix} \frac{2}{\epsilon^2}\mathbf{g}_3(\mathbf{u},\epsilon\boldsymbol{\xi}) \\ \frac{1}{\epsilon}N(\mathbf{u},\Phi\epsilon\boldsymbol{\xi}+Z\mathbf{z}(\mathbf{u},\epsilon\boldsymbol{\xi}),\epsilon\tau,s^0+\epsilon) \end{pmatrix}, & \epsilon\neq 0; \\ \mathbf{h}_{bif}(\boldsymbol{\xi},\tau), & \epsilon = 0. \end{cases}$$

When $\epsilon \neq 0$, the solutions of $\mathbf{G}(\boldsymbol{\xi},\tau,\epsilon,\mathbf{u}) = \mathbf{0}$ are exactly the solutions of (3.25bc). Using Assumption 1.8 and L'Hôpital's rule, it is easily verified that $\mathbf{G}(\boldsymbol{\xi},\tau,\epsilon,\mathbf{u})$ is a continuous function. Since we assumed that $(\dot{\mathbf{y}}^0, \dot{t}^0)$ is an isolated real root of (3.27), one solution of $\mathbf{G}(\boldsymbol{\xi},\tau,\epsilon,\mathbf{u}) = \mathbf{0}$ is

$$\boldsymbol{\xi} = \dot{\mathbf{y}}^0,$$

$$\tau = \dot{t}^0,$$

$$\epsilon = 0,$$

$$\mathbf{u} = \mathbf{0}.$$

Since this is an isolated root of (3.34), the Jacobian $\mathbf{G}_{\xi,\tau}(\dot{\mathbf{y}}^0, \dot{t}^0, 0, \mathbf{0})$ is non-singular. Thus we can apply the Implicit Function Theorem to obtain, corresponding to each isolated root $(\dot{\mathbf{y}}^0, \dot{t}^0)$, the existence of unique, continuous functions $\boldsymbol{\xi}(\mathbf{u},\epsilon)$ and $\tau(\mathbf{u},\epsilon)$ satisfying

(a) $\mathbf{G}(\boldsymbol{\xi},\tau,\epsilon,\mathbf{u}) = \mathbf{0}$,

(b) $\boldsymbol{\xi}(\mathbf{0},0) = \dot{\mathbf{y}}^0$, and

(c) $\tau(\mathbf{0},0) = \dot{t}^0$.

The existence and uniqueness of these functions is guaranteed in some sufficiently small neighborhood of $\mathbf{u} = \mathbf{0}$ and $\epsilon = 0$. As in the fold case, $\boldsymbol{\xi}(\mathbf{u},\epsilon)$

and $\tau(\mathbf{u}, \epsilon)$ are actually twice continuously differentiable, except possibly when $\epsilon = 0$; this is because $\mathbf{G}(\boldsymbol{\xi}, \tau, \epsilon, \mathbf{u})$ has two continuous derivatives for $\epsilon \neq 0$. Now, (3.25) is reduced to

$$\frac{d\mathbf{u}}{ds} = \begin{cases} \mathbf{f}(\mathbf{u}, Z\mathbf{z}(\mathbf{u}, \epsilon\boldsymbol{\xi}) + \Phi\epsilon\boldsymbol{\xi}) \left(\tau + \epsilon\tau_{\mathbf{u}} \frac{d\mathbf{u}}{ds} + \epsilon\tau_{\epsilon}\right), & \epsilon \neq 0; \\ \mathbf{f}(\mathbf{u}, Z\mathbf{z}(\mathbf{u}, 0))\,(\tau), & \epsilon = 0; \end{cases}$$

$$\mathbf{u} = \mathbf{0} \text{ at } s = s^0;$$

where $\boldsymbol{\xi} = \boldsymbol{\xi}(\mathbf{u}, \epsilon)$ and $\tau = \tau(\mathbf{u}, \epsilon)$. This is an ODE initial value problem of the form

$$\frac{d\mathbf{u}}{ds} = \mathbf{F}(\mathbf{u}, s),$$

$$\mathbf{u} = \mathbf{0} \text{ at } s = s^0,$$

and it can be shown that $\mathbf{F}(\mathbf{u}, s)$ is Lipschitz continuous in a neighborhood of $\mathbf{x} = \mathbf{0}$ and $\epsilon = s - s^0 = 0$. Standard existence and uniqueness theory for non-autonomous ODEs then guarantees the existence of a unique function $\mathbf{u} = \mathbf{U}(s)$ satisfying (3.25) for s sufficiently close to s^0. That function has at least one continuous derivative. Then $\mathbf{y}$ and t are uniquely given by:

$$\mathbf{y}(s) = (s - s^0)\,\boldsymbol{\xi}\left(\mathbf{U}(s), s - s^0\right),$$

$$t(s) = (s - s^0)\,\tau\left(\mathbf{U}(s), s - s^0\right).$$

The form of the solution given in the theorem is obtained by a Taylor expansion of the above two equations and (3.12) in s about $s = s^0$. □

Theorem 3.36 *Suppose* $\mathbf{x} = \mathbf{0}$ *is a bifurcation point and Assumption 1.8 is satisfied. Then corresponding to each* real, isolated *solution* $(\dot{\mathbf{y}}^0, i^0)$ *of (3.34)*

with $\dot{t}^0 \neq 0$, *there exists a unique, real, continuously differentiable solution* $\mathbf{x}(s)$ *satisfying (3.8) and hence (1.2) on some interval* (s_c, s_d) *containing* s^0. *It has the form*

$$\begin{aligned} \mathbf{u}(t(s)) &= \left(s - s^0\right) \mathbf{f}^0 \dot{t}^0 + O\left((s - s^0)^2\right), \\ \mathbf{v}(t(s)) &= \left(s - s^0\right) \left(\Phi \dot{\mathbf{y}}^0 + Z\zeta \dot{t}^0\right) + O\left((s - s^0)^2\right), \\ t(s) &= \left(s - s^0\right) \dot{t}^0 + O\left((s - s^0)^2\right). \end{aligned}$$

Proof: From Theorem 3.35 we know that for each isolated root of the bifurcation equations, (3.25) has a unique solution $\mathbf{x}(s)$ for all s in some interval (s_a, s_b) containing s^0. Since we assume $\dot{t}^0 \neq 0$, Lemma 3.26 guarantees that it corresponds to a unique solution satisfying (3.8) and hence (1.2) on (s_c, s_d) for some $s_c < s^0$ and $s_d > s^0$. The form of the solution is obtained from Theorem 3.35 and from a Taylor expansion of $\mathbf{v}(t(s))$ in s about $s = s^0$, making use of (3.18). □

Example 3.37 *Let* $n = m = 1$ *and consider the DAE*

$$\frac{du}{dt} = f(u, v) \equiv 1,$$

$$0 = g(u, v) \equiv u^2 - v^2,$$

$$u = v = 0 \text{ at } t = 0.$$

Here: $g_v^0 = -2v|_{v=0} = 0$, *so the initial value is a critical point. Also:* $g_u^0 = 2u|_{u=0} = 0$, *so* $g_u^0 f^0 \in \mathcal{R}(g_v^0)$ *and the initial value is a bifurcation point. There are two solutions, both valid for all* t, *and they are given by* $u = t$ *and* $v = \pm t$ *(see Figure 3.38). If we let*

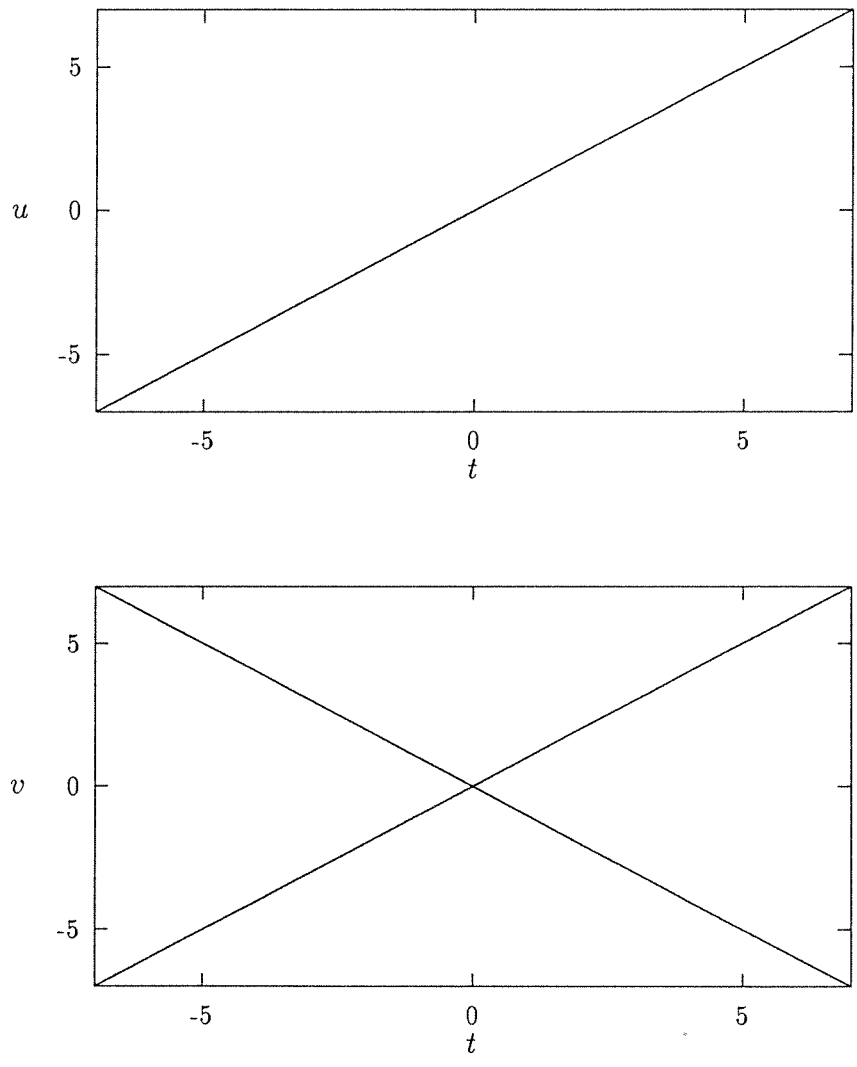

Figure 3.38: Solution set for Example 3.37

$$N(u, v, t, s) = v - s,$$

then the bifurcation equations are

$$-2(\dot{v}^0)^2 + 2(\dot{t}^0)^2 = 0,$$

$$\dot{v}^0 - 1 = 0.$$

The bifurcation equations have two isolated solutions, $\dot{v}^0 = 1$ *and* $\dot{t}^0 = \pm 1$. *Theorem 3.36 applies to each root, since both satisfy* $\dot{t}^0 \neq 0$. *Therefore, there are two solution paths. One is given by* $u(t(s) = v(t(s)) = t(s) = s$ *and the other by* $u(t(s)) = t(s) = s$, $v(t(s)) = -s$.

Example 3.39 *When* $r > 1$, *there may be up to* 2^r *solution branches. Let* $n = 1$, $m = 2$, *and consider the DAE*

$$\frac{du}{dt} = f(u, v_1, v_2) \equiv 1,$$

$$0 = \mathrm{g}(u, v_1, v_2) = \begin{pmatrix} u^2 - 2v_1v_2 \\ 9u^2 - 4(v_1 + v_2)^2 \end{pmatrix},$$

$$u = v_1 = v_2 = 0 \ \textit{at}\ t = 0.$$

Then $\mathrm{g}_{\mathrm{v}}^0 = 0$, *so* $r = \dim\{\mathcal{N}(\mathrm{g}_{\mathrm{v}}^0)\} = 2$. *Since* $\mathrm{g}_{\mathrm{u}}^0 = 0$, *the initial value is a bifurcation point. There are four solutions, all of which are valid for all* t *(see Figure 3.40):*

(1) $u = t$, $v_1 = t$, $v_2 = t/2$;

(2) $u = t$, $v_1 = -t$, $v_2 = -t/2$;

(3) $u = t$, $v_1 = t/2$, $v_2 = t$;

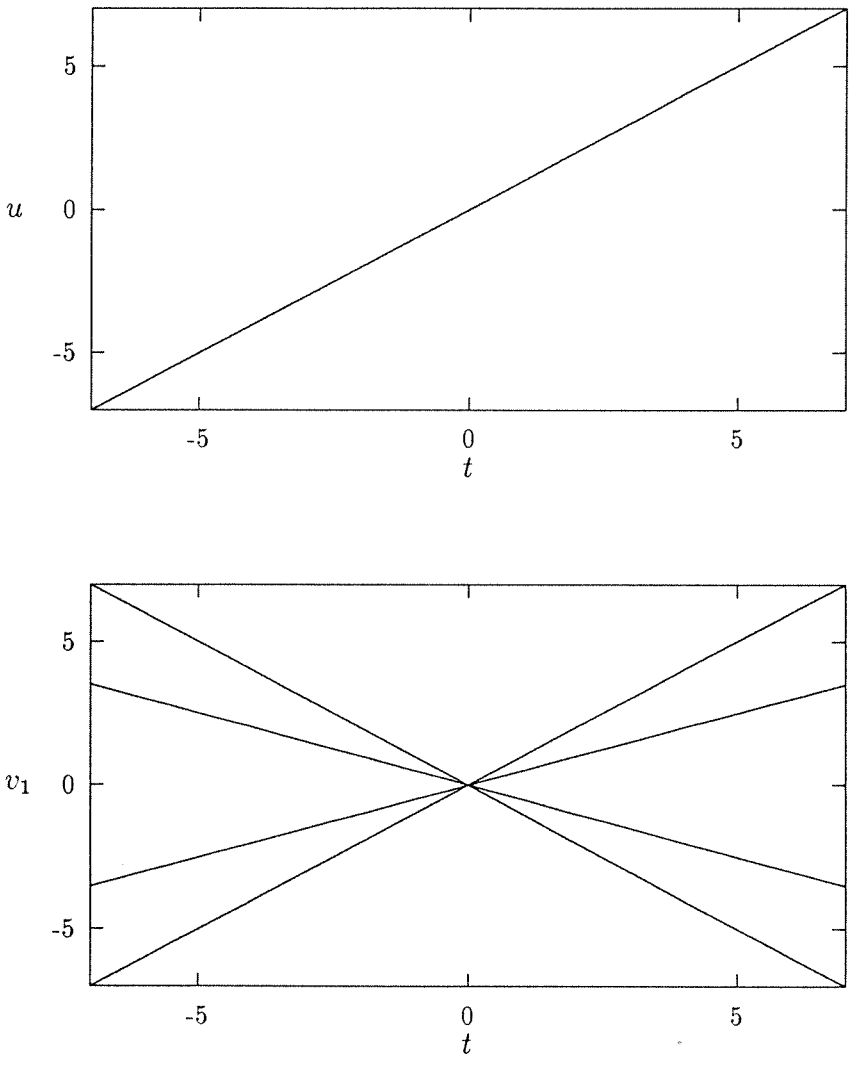

Figure 3.40: Solution set for Example 3.39

(4) $u = t$, $v_1 = -t/2$, $v_2 = -t$.

If we set

$$N(u, v_1, v_2, t, s) = v_1 - s,$$

then the bifurcation equations are

$$2(\dot{t}^0)^2 - 4\dot{v}_1^0\dot{v}_2^0 = 0,$$

$$18(\dot{t}^0)^2 - 8(\dot{v}_1^0 + \dot{v}_2^0)^2 = 0,$$

$$\dot{v}_1^0 - 1 = 0.$$

There are four isolated real roots:

(1) $\dot{t}^0 = 2$, $\dot{v}_1^0 = 1$, $\dot{v}_2^0 = 2$;

(2) $\dot{t}^0 = -2$, $\dot{v}_1^0 = 1$, $\dot{v}_2^0 = 2$;

(3) $\dot{t}^0 = 1$, $\dot{v}_1^0 = 1$, $\dot{v}_2^0 = 1/2$;

(4) $\dot{t}^0 = -1$, $\dot{v}_1^0 = 1$, $\dot{v}_2^0 = 1/2$;

none of these roots have $\dot{t}^0 = 0$, *so Theorem 3.36 applies to each of them, and there are four solution paths, given by:*

(1) $u(t(s)) = t(s) = v_1(t(s)) = s$, $v_2(t(s)) = s/2$;

(2) $u(t(s)) = t(s) = -s$, $v_1(t(s)) = s$, $v_2(t(s)) = s/2$;

(3) $u(t(s)) = t(s) = 2s$, $v_1(t(s)) = s$, $v_2(t(s)) = 2s$;

(4) $u(t(s)) = t(s) = -2s$, $v_1(t(s)) = s$, $v_2(t(s)) = 2s$.

Example 3.41 *The proof of Theorem 3.36 relies on the assumption that the bifurcation equations have a real, isolated root. If the root is not isolated there may not be any real solution path passing through* $\mathbf{x} = \mathbf{0}$. *Consider the following DAE with* $n = m = 1$*:*

$$\frac{du}{dt} = f(u, v) \equiv 1,$$

$$0 = g(u, v) \equiv v^2 + u^4,$$

$$u = v = 0 \text{ at } t = 0.$$

The initial value is a bifurcation point, but the only solutions of this DAE are $u = t$, $v = \pm it^2$, *where* $i = \sqrt{-1}$. *Neither of the two solution paths is real except at* $t = 0$. *If we let*

$$N(u, v, t, s) = v + t - s,$$

then the bifurcation equations are

$$2(\dot{v}^0)^2 = 0,$$

$$\dot{v}^0 + \dot{t}^0 - 1 = 0.$$

There is one double root and it is $\dot{v}^0 = 0$, $\dot{t}^0 = 1$. *Since the root is not isolated, Theorem 3.36 does not apply, and in fact there are no real solutions of the DAE.*

3.7 Pitchfork Bifurcation

A special case of bifurcation arises when several solution paths cross and one or more of those paths lies entirely on one side of $t = 0$. We call this a *pitchfork bifurcation.* One sign of a pitchfork bifurcation is that $\dot{t}^0 = 0$ is a root of the bifurcation equations (3.34). That case is not covered in Theorem 3.36. In order to establish the existence and uniqueness of a solution branch corresponding to a root with $\dot{t}^0 = 0$, we make some additional

assumptions which guarantee $\ddot{t}^0 \neq 0$. Then we can simply apply Theorem 3.35 and Lemma 3.26 to obtain an existence and uniqueness theorem.

Definition 3.42 *Let*

$$A(\dot{\mathbf{y}}^0) \equiv \begin{pmatrix} 3\Psi^T \mathrm{g}^0_{\mathrm{vv}} \Phi \dot{\mathbf{y}}^0 \Phi \\ N^0_{\mathrm{v}} \Phi \end{pmatrix},$$

$$B(\dot{\mathbf{y}}^0) \equiv \begin{pmatrix} 3\Psi^T \mathrm{g}^0_{\mathrm{uv}} \Phi \dot{\mathbf{y}}^0 \mathrm{f}^0 + 3\Psi^T \mathrm{g}^0_{\mathrm{vv}} \Phi \dot{\mathbf{y}}^0 Z\zeta \\ N^0_{\mathrm{u}} \mathrm{f}^0 + N^0_t + N^0_{\mathrm{v}} Z\zeta \end{pmatrix},$$

$$\mathrm{d}(\dot{\mathbf{y}}^0) \equiv \begin{pmatrix} -\Psi^T \mathrm{g}^0_{\mathrm{vvv}} \Phi \dot{\mathbf{y}}^0 \Phi \dot{\mathbf{y}}^0 \Phi \dot{\mathbf{y}}^0 \\ -N^0_{ss} - 2N^0_{\mathrm{v}s} \Phi \dot{\mathbf{y}}^0 - N^0_{\mathrm{vv}} \Phi \dot{\mathbf{y}}^0 \Phi \dot{\mathbf{y}}^0 \end{pmatrix}.$$

Theorem 3.43 *Suppose* $\mathbf{x} = \mathbf{0}$ *is a bifurcation point and Assumptions 1.8 and 1.9 are satisfied. Then corresponding to each* isolated, real *root* $(\dot{\mathbf{y}}^0, \dot{t}^0)$ *of (3.34) with*

(a) $\dot{t}^0 = 0$, *and*

(b) $\mathrm{d}(\dot{\mathbf{y}}^0) \notin \mathcal{R}(A(\dot{\mathbf{y}}^0))$,

there exists a unique, real solution $\mathbf{x}(s)$ *satisfying (3.8) and hence(1.2) in some interval* (s_a, s_b) *containing* s^0 *such that*

(a) $\mathbf{x}(s)$ *is twice continuously differentiable;*

(b) $\ddot{t}^0 \neq 0$.

It has the form

$$\begin{aligned} \mathbf{u}(t(s)) &= \frac{1}{2}\left(s - s^0\right)^2 \mathrm{f}^0 \ddot{t}^0 + O\left((s - s^0)^3\right), \\ \mathbf{v}(t(s)) &= \left(s - s^0\right) \Phi \dot{\mathbf{y}}^0 + O\left((s - s^0)^2\right), \\ t(s) &= \frac{1}{2}\left(s - s^0\right)^2 \ddot{t}^0 + O\left((s - s^0)^3\right). \end{aligned}$$

Proof: From Theorem 3.35, we know that for each isolated root of the bifurcation equations, (3.25) has a unique solution $\mathbf{x}(s)$ for all s in some interval (s_a, s_b) containing s^0. Since we have assumed the additional differentiability Assumption 1.9, that solution is twice continuously differentiable. We shall show that, under the assumptions of a pitchfork bifurcation point, this solution has $\ddot{t}^0 \neq 0$. The existence and uniqueness result then follows from a straightforward application of Lemma 3.26.

We shall first prove that under the assumptions of Theorem 3.43, $\ddot{t}^0 \neq 0$. Firstly, if $\dot{t}^0 = 0$, it follows immediately from (3.34) that

$$\Psi^T \mathrm{g}^0_{\mathrm{vv}} \Phi \dot{\mathrm{y}}^0 \Phi \dot{\mathrm{y}}^0 = 0. \tag{3.44}$$

Secondly, by using $\dot{t}^0 = 0$ in (3.19), (3.12) and (3.13), we have

$$\dot{\mathrm{z}}^0 = \zeta \dot{t}^0 = 0, \tag{3.45a}$$

$$\dot{\mathrm{u}}^0 = \mathrm{f}^0 \dot{t}^0 = 0, \tag{3.45b}$$

$$\ddot{\mathrm{u}}^0 = \mathrm{f}^0 \ddot{t}^0. \tag{3.45c}$$

Due to (3.44) and (3.45), the k=2 equation of (3.14), evaluated at s^0, simplifies to:

$$\mathrm{g}^0_{\mathrm{v}} \ddot{\mathrm{z}}^0 + \mathrm{g}^0_{\mathrm{u}} \mathrm{f}^0 \ddot{t}^0 = 0. \tag{3.46}$$

Equation (3.46) is similar to (3.18). The solutions are related by:

$$\ddot{\mathrm{z}}^0 = \zeta \ddot{t}^0. \tag{3.47}$$

In order to get an expression for the unknown quantities $\ddot{\mathrm{y}}^0$ and $\ddot{t}^0$, we consider the system of equations made up of

(a) the k=3 equation of (3.14), left multiplied with Ψ^T and evaluated at s^0, and

(b) the k=2 equation of (3.15), evaluated at s^0.

Using (3.45) and (3.47), this is simply the linear system:

$$A(\dot{\mathbf{y}}^0)\ddot{\mathbf{y}}^0 + B(\dot{\mathbf{y}}^0)\ddot{t}^0 = \mathbf{d}(\dot{\mathbf{y}}^0), \tag{3.48}$$

where $A(\dot{\mathbf{y}}^0)$, $B(\dot{\mathbf{y}}^0)$, and $\mathbf{d}(\dot{\mathbf{y}}^0)$ are as in Definition 3.42 above. Since we assumed $\mathbf{d}(\dot{\mathbf{y}}^0) \notin \mathcal{R}(A(\dot{\mathbf{y}}^0))$, (3.48) cannot have a solution with $\ddot{t}^0 = 0$.

Since $\ddot{t}^0 \neq 0$, lemma 3.26 applies, and the existence and uniqueness result of the theorem follows immediately. The form of the solution is simply obtained by a Taylor expansion in s about $s = s^0$. □

Example 3.49 *A simple example of a pitchfork bifurcation occurs if we let* $n = m = 1$ *and consider the DAE*

$$\frac{du}{dt} = f(u,v) \equiv 1,$$

$$0 = g(u,v) \equiv v(u - v^2),$$

$$u = v = 0 \text{ at } t = 0.$$

Then $g_v^0 = 0$ *and* $g_u^0 = 0$ *so the initial value is a bifurcation point. The solutions, plotted in Figure 3.50, are*

(1) $u = t$, $v = 0$;

(2) $u = t$, $v = \sqrt{t}$;

(3) $u = t$, $v = -\sqrt{t}$.

If we set

$$N(u,v,t,s) = v - v^2 + t - s,$$

then the bifurcation equations are

$$2\dot{v}^0\dot{t}^0 = 0,$$

$$(1-2v)\dot{v}^0 + \dot{t}^0 - 1 = 0.$$

The roots are $(\dot{v}^0 = 0, \dot{t}^0 = 1)$ *and* $(\dot{v}^0 = 1, \dot{t}^0 = 0)$. *The first root corresponds to the solution* $v = 0$ *and the existence of that solution is given by Theorem 3.36. The second root has* $\dot{t}^0 = 0$ *and theorem 3.43 applies because*

$$A(\dot{v}^0) = A(1) = \begin{pmatrix} 0 \\ 1 \end{pmatrix}, \text{ and}$$

$$\mathrm{d}(\dot{v}^0) = \mathrm{d}(1) = \begin{pmatrix} 6 \\ 0 \end{pmatrix},$$

so $\mathrm{d}(\dot{v}^0) \notin \mathcal{R}(A(\dot{v}^0))$. *The two solutions corresponding to the two roots of the bifurcation equations are*

(1) $u(t(s)) = s$, $v(t(s)) = 0$, $t(s) = s$;

(2) $u(t(s)) = s^2$, $v(t(s)) = s$, $t(s) = s^2$.

Notice that this DAE has one real solution for $t < 0$ *and three real solutions for* $t > 0$. *However, if we allow complex solutions, this DAE has two more solutions for* $t < 0$, *namely* $u = t$ *and* $v = \pm i\sqrt{-t}$. *If we let* $\hat{s} \in I\!R$, *then the two complex solutions for* $t < 0$ *can be written as a single differentiable solution path* $u(t(\hat{s})) = t(\hat{s}) = -\hat{s}^2$, $v(t(\hat{s})) = i\hat{s}$. *So if we include complex solutions, the DAE actually has three solutions for* $t < 0$ *and three for* $t > 0$. *The theory for this phenomenon will be presented in Chapter 4.*

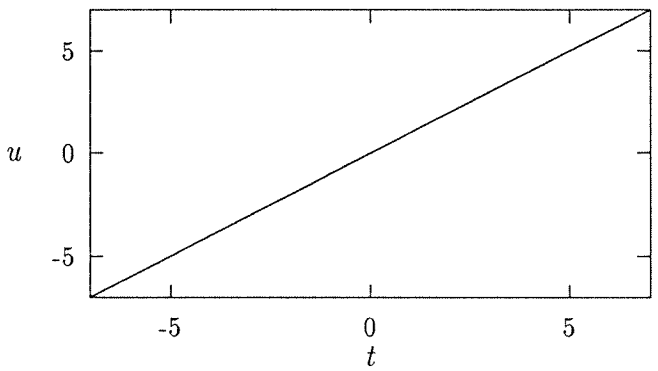

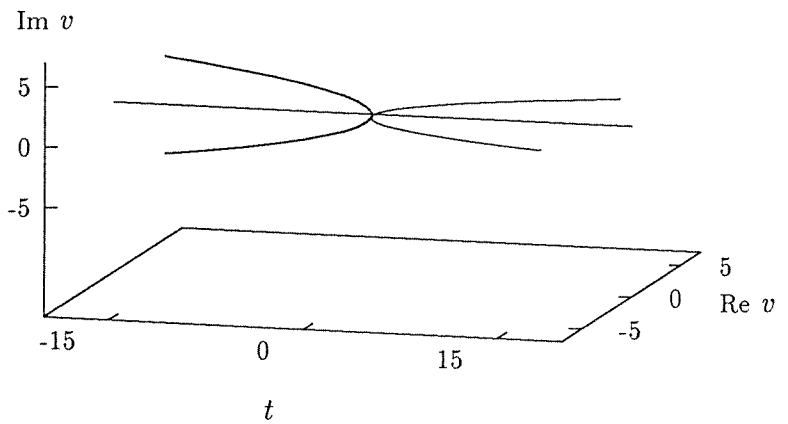

Figure 3.50: Solution set for Example 3.49. Both real and complex solutions are shown.

Chapter 4

Complex Solutions Near Critical Points

In the previous chapter, we sought real solution trajectories of the DAE (1.2). In this chapter, we shall define a complex extension of (1.2) and show that this extension may have complex solution trajectories near $\mathbf{x} = \mathbf{0}$. The complex solutions will correspond to complex roots of the bifurcation equations.

The theory of this chapter is an extension of the work of Henderson and Keller in [11] and [12]. Henderson and Keller examined complex bifurcation in algebraic nonlinear equations. Here we extend their theory to cover DAEs of the form (1.2).

4.1 The Complex Extension of a Real DAE

Assuming that Assumption 1.7 holds, the real functions $\mathbf{f}$ and $\mathbf{g}$ are continuously differentiable in a neighborhood, call it Ω, of $\mathbf{x} = \mathbf{0}$. Then there are unique analytic mappings $\mathbf{f}_{co} : \mathbb{C}^n \times \mathbb{C}^m \to \mathbb{C}^n$ and $\mathbf{g}_{co} : \mathbb{C}^n \times \mathbb{C}^m \to \mathbb{C}^m$ which coincide with $\mathbf{f}$ and $\mathbf{g}$ in Ω. The complex extension of (1.2) is then

$$\frac{d\mathbf{u}_{co}}{dt} = \mathbf{f}_{co}(\mathbf{u}_{co}, \mathbf{v}_{co}), \tag{4.1a}$$

$$\mathbf{0} = \mathbf{g}_{co}(\mathbf{u}_{co}, \mathbf{v}_{co}), \tag{4.1b}$$

$$\mathbf{u}_{co} = \mathbf{0} \text{ and } \mathbf{v}_{co} = \mathbf{0} \text{ at } t = 0, \tag{4.1c}$$

where $\mathbf{u}_{co} \equiv \mathbf{u}_{re} + i\mathbf{u}_{im} \in \mathbb{C}^n$, $\mathbf{v}_{co} \equiv \mathbf{v}_{re} + i\mathbf{v}_{im} \in \mathbb{C}^m$ and we retain $t \in \mathbb{R}$. The real vectors $\mathbf{u}_{re}$ and $\mathbf{u}_{im}$ stand for the real and imaginary parts of $\mathbf{u}_{co}$, respectively. Similarly, $\mathbf{v}_{re}$ and $\mathbf{v}_{im}$ are the real and imaginary parts of $\mathbf{v}_{co}$. We shall use the notation $\mathbf{x}_{co} \equiv (\mathbf{u}_{co}, \mathbf{v}_{co}, t)^T$. We can also split $\mathbf{f}_{co}$ and $\mathbf{g}_{co}$ into their respective real and imaginary parts by defining $\mathbf{f}_{re}$, $\mathbf{f}_{im}$, $\mathbf{g}_{re}$ and $\mathbf{g}_{im}$, all of which map $\mathbb{R}^n \times \mathbb{R}^n \times \mathbb{R}^m \times \mathbb{R}^m \to \mathbb{R}^n$, such that

$$\begin{aligned}
\mathbf{f}_{co}(\mathbf{u}_{re} + i\mathbf{u}_{im}, \mathbf{v}_{re} + i\mathbf{v}_{im}) &= \mathbf{f}_{re}(\mathbf{u}_{re}, \mathbf{u}_{im}, \mathbf{v}_{re}, \mathbf{v}_{im}) + \\
&\quad i\mathbf{f}_{im}(\mathbf{u}_{re}, \mathbf{u}_{im}, \mathbf{v}_{re}, \mathbf{v}_{im}), \\
\mathbf{g}_{co}(\mathbf{u}_{re} + i\mathbf{u}_{im}, \mathbf{v}_{re} + i\mathbf{v}_{im}) &= \mathbf{g}_{re}(\mathbf{u}_{re}, \mathbf{u}_{im}, \mathbf{v}_{re}, \mathbf{v}_{im}) + \\
&\quad i\mathbf{g}_{im}(\mathbf{u}_{re}, \mathbf{u}_{im}, \mathbf{v}_{re}, \mathbf{v}_{im}).
\end{aligned}$$

Since the complexified problem must locally reduce to the real one, we have, for all $\mathbf{u}$ and $\mathbf{v}$ in Ω:

$$\mathbf{f}_{co}(\mathbf{u} + i\mathbf{0}, \mathbf{v} + i\mathbf{0}) = \mathbf{f}(\mathbf{u}, \mathbf{v}), \tag{4.2a}$$

$$\mathbf{g}_{co}(\mathbf{u}+i\mathbf{0},\mathbf{v}+i\mathbf{0})=\mathbf{g}(\mathbf{u},\mathbf{v}). \tag{4.2b}$$

Because we chose $\mathbf{f}_{co}$ and $\mathbf{g}_{co}$ to be analytic everywhere, the Cauchy-Riemann equations hold for both functions and for all $\mathbf{u}_{co}\in\mathbb{C}^n$ and $\mathbf{v}_{co}\in\mathbb{C}^m$:

$$\frac{\partial \mathbf{f}_{re}}{\partial \mathbf{u}_{re}}=\frac{\partial \mathbf{f}_{im}}{\partial \mathbf{u}_{im}}, \tag{4.3a}$$

$$\frac{\partial \mathbf{f}_{re}}{\partial \mathbf{v}_{re}}=\frac{\partial \mathbf{f}_{im}}{\partial \mathbf{v}_{im}}, \tag{4.3b}$$

$$\frac{\partial \mathbf{f}_{re}}{\partial \mathbf{u}_{im}}=-\frac{\partial \mathbf{f}_{im}}{\partial \mathbf{u}_{re}}, \tag{4.3c}$$

$$\frac{\partial \mathbf{f}_{re}}{\partial \mathbf{v}_{im}}=-\frac{\partial \mathbf{f}_{im}}{\partial \mathbf{v}_{re}}, \tag{4.3d}$$

$$\frac{\partial \mathbf{g}_{re}}{\partial \mathbf{u}_{re}}=\frac{\partial \mathbf{g}_{im}}{\partial \mathbf{u}_{im}}, \tag{4.3e}$$

$$\frac{\partial \mathbf{g}_{re}}{\partial \mathbf{v}_{re}}=\frac{\partial \mathbf{g}_{im}}{\partial \mathbf{v}_{im}}, \tag{4.3f}$$

$$\frac{\partial \mathbf{g}_{re}}{\partial \mathbf{u}_{im}}=-\frac{\partial \mathbf{g}_{im}}{\partial \mathbf{u}_{re}}, \tag{4.3g}$$

$$\frac{\partial \mathbf{g}_{re}}{\partial \mathbf{v}_{im}}=-\frac{\partial \mathbf{g}_{im}}{\partial \mathbf{v}_{re}}. \tag{4.3h}$$

There are two ways to study the solutions of the complexified DAE. One is to perform the entire analysis in the complex space. The Lyapunov-Schmidt reduction, the Implicit Function Theorem, and the existence theory for ODEs can all be applied in the complex case, just as we did for the real case in Chapter 3. The other way is to rewrite the complexified DAE (4.1) as a real problem of size $2n+2m$:

$$\frac{d\mathbf{u}_{re}}{dt}=\mathbf{f}_{re}(\mathbf{u}_{re},\mathbf{u}_{im},\mathbf{v}_{re},\mathbf{v}_{im}), \tag{4.4a}$$

$$\frac{d\mathbf{u}_{im}}{dt} = \mathbf{f}_{im}(\mathbf{u}_{re}, \mathbf{u}_{im}, \mathbf{v}_{re}, \mathbf{v}_{im}), \tag{4.4b}$$

$$\mathbf{0} = \mathbf{g}_{re}(\mathbf{u}_{re}, \mathbf{u}_{im}, \mathbf{v}_{re}, \mathbf{v}_{im}), \tag{4.4c}$$

$$\mathbf{0} = \mathbf{g}_{im}(\mathbf{u}_{re}, \mathbf{u}_{im}, \mathbf{v}_{re}, \mathbf{v}_{im}), \tag{4.4d}$$

$$\mathbf{u}_{re} = \mathbf{0}, \mathbf{u}_{im} = \mathbf{0}, \mathbf{v}_{re} = \mathbf{0}, \mathbf{v}_{im} = \mathbf{0} \text{ at } t = 0. \tag{4.4e}$$

Now define

$$\hat{\mathbf{f}}(\hat{\mathbf{u}}, \hat{\mathbf{v}}) \equiv \begin{pmatrix} \mathbf{f}_{re}(\mathbf{u}_{re}, \mathbf{u}_{im}, \mathbf{v}_{re}, \mathbf{v}_{im}) \\ \\ \mathbf{f}_{im}(\mathbf{u}_{re}, \mathbf{u}_{im}, \mathbf{v}_{re}, \mathbf{v}_{im}) \end{pmatrix}$$

and

$$\hat{\mathbf{g}}(\hat{\mathbf{u}}, \hat{\mathbf{v}}) \equiv \begin{pmatrix} \mathbf{g}_{re}(\mathbf{u}_{re}, \mathbf{u}_{im}, \mathbf{v}_{re}, \mathbf{v}_{im}) \\ \\ \mathbf{g}_{im}(\mathbf{u}_{re}, \mathbf{u}_{im}, \mathbf{v}_{re}, \mathbf{v}_{im}) \end{pmatrix}$$

with $\hat{\mathbf{u}} \equiv (\mathbf{u}_{re}, \mathbf{u}_{im})^T$ and $\hat{\mathbf{v}} \equiv (\mathbf{v}_{re}, \mathbf{v}_{im})^T$. Then (4.4) can be written in the form (1.2):

$$\frac{d\hat{\mathbf{u}}}{dt} = \hat{\mathbf{f}}(\hat{\mathbf{u}}, \hat{\mathbf{v}}), \tag{4.5a}$$

$$\mathbf{0} = \hat{\mathbf{g}}(\hat{\mathbf{u}}, \hat{\mathbf{v}}), \tag{4.5b}$$

$$\hat{\mathbf{u}} = \mathbf{0} \text{ and } \hat{\mathbf{v}} = \mathbf{0} \text{ at } t = 0. \tag{4.5c}$$

The system (4.5) is a real DAE, exactly in the form specified in (1.2). All the results of Chapter 3 can be applied to find real solutions of (4.5). Real solutions of (4.4) with nonzero $\mathbf{u}_{im}$ or $\mathbf{v}_{im}$ correspond to complex solutions of (4.1). Note that since the initial value is real, the Jacobian of $\hat{\mathbf{g}}$ with respect to $\hat{\mathbf{v}}$ evaluated at the initial value is

$$\hat{\mathbf{g}}^0_{\hat{\mathbf{v}}} = \begin{pmatrix} \left(\frac{\partial \mathbf{g}_{re}}{\partial \mathbf{v}_{re}}\right)^0 & \left(\frac{\partial \mathbf{g}_{re}}{\partial \mathbf{v}_{im}}\right)^0 \\ \left(\frac{\partial \mathbf{g}_{im}}{\partial \mathbf{v}_{re}}\right)^0 & \left(\frac{\partial \mathbf{g}_{im}}{\partial \mathbf{v}_{im}}\right)^0 \end{pmatrix} = \begin{pmatrix} \mathbf{g}^0_{\mathbf{v}} & 0 \\ 0 & \mathbf{g}^0_{\mathbf{v}} \end{pmatrix}. \tag{4.6}$$

Here we have made use of (4.2) and the Cauchy-Riemann equations (4.3). Clearly, $\hat{\mathrm{g}}^0_{\hat{\mathrm{v}}}$ is nonsingular if and only if $\mathrm{g}^0_{\mathrm{v}}$ is nonsingular. So regular points of the complexified DAE correspond to regular points of the original real DAE. Also note that if $\mathrm{g}^0_{\mathrm{v}}$ has a nullspace of dimension r, then the nullspace of $\hat{\mathrm{g}}^0_{\hat{\mathrm{v}}}$ has dimension $2r$. If Φ and Ψ are bases for the right and left nullspaces of $\mathrm{g}^0_{\mathrm{v}}$, then

$$\hat{\Phi} \equiv \begin{pmatrix} \Phi & 0 \\ 0 & \Phi \end{pmatrix} \text{ and } \hat{\Psi} \equiv \begin{pmatrix} \Psi & 0 \\ 0 & \Psi \end{pmatrix}$$

are bases for the right and left nullspaces of $\hat{\mathrm{g}}^0_{\hat{\mathrm{v}}}$.

We can now apply the theory of Chapter 3 to (4.4). In accordance with that theory, we define

$$\hat{\mathrm{y}} \equiv \begin{pmatrix} \mathrm{y}_{re} \\ \mathrm{y}_{im} \end{pmatrix} \equiv \hat{\Phi}^T \hat{\mathrm{v}} = \begin{pmatrix} \Phi^T \mathrm{v}_{re} \\ \Phi^T \mathrm{v}_{im} \end{pmatrix},$$

where $\mathrm{y}_{re} \in \mathbb{R}^r$ and $\mathrm{y}_{im} \in \mathbb{R}^r$. We introduce a real scalar constraint,

$$\hat{N}(\hat{\mathrm{u}}, \hat{\mathrm{v}}, t, \hat{s}) = 0, \tag{4.7}$$

which defines a real parameter $\hat{s}$ to be used to parametrize solution trajectories of (4.4). We choose the constraint (4.7) to satisfy $\hat{N}(\mathbf{0}, \mathbf{0}, 0, \hat{s}^0) = 0$ for some $\hat{s}^0 \in \mathbb{R}$, and

$$\hat{N}^0_{\hat{\mathrm{v}}} = \left(N^0_{\mathrm{v}}, N^0_{\mathrm{v}}\right), \tag{4.8a}$$

$$\hat{N}^0_{\hat{\mathrm{u}}} = \left(N^0_{\mathrm{u}}, N^0_{\mathrm{u}}\right), \tag{4.8b}$$

$$\hat{N}^0_t = N^0_t, \tag{4.8c}$$

$$\hat{N}^0_{\hat{s}} = N^0_s, \tag{4.8d}$$

$$\hat{N}^0_{\hat{s}\hat{s}} = N^0_{ss}, \tag{4.8e}$$

$$\hat{N}^0_{\hat{\mathrm{v}}s} = \left(N^0_{\mathrm{v}s}, -N^0_{\mathrm{v}s}\right), \tag{4.8f}$$

$$\hat{N}^0_{\hat{\mathrm{v}}\hat{\mathrm{v}}} \begin{pmatrix} \mathrm{x}_1 \\ \mathrm{x}_2 \end{pmatrix} = (N^0_{\mathrm{vv}}\mathrm{x}_1, -N^0_{\mathrm{vv}}\mathrm{x}_2), \tag{4.8g}$$

for all $\mathrm{x}_1, \mathrm{x}_2 \in \mathbb{R}^m$. By assuming (4.8), we equate scales in the two constraints (3.7) and (4.7), which helps ease the notation below.

4.2 Complex Solutions Near Fold Points

We first look for solutions of the complexified system near a fold point of the original DAE. So we assume

$$\Psi^T \mathrm{g}^0_{\mathrm{u}} \mathrm{f}^0 \neq \mathbf{0}.$$

By making use of (4.2), (4.3) and (4.8), the bifurcation equations (3.27) for (4.4) at a fold point can be written

$$\Psi^T \mathrm{g}^0_{\mathrm{u}} \mathrm{f}^0 \ddot{t}^0 + \Psi^T \mathrm{g}^0_{\mathrm{vv}} (\Phi \dot{\mathrm{y}}^0_{re} \Phi \dot{\mathrm{y}}^0_{re} - \Phi \dot{\mathrm{y}}^0_{im} \Phi \dot{\mathrm{y}}^0_{im}) = \mathbf{0}, \tag{4.9a}$$

$$\Psi^T \mathrm{g}^0_{\mathrm{vv}} \Phi \dot{\mathrm{y}}^0_{re} \Phi \dot{\mathrm{y}}^0_{im} = \mathbf{0}, \tag{4.9b}$$

$$N^0_{\mathrm{v}} \Phi (\dot{\mathrm{y}}^0_{re} + \dot{\mathrm{y}}^0_{im}) + N^0_s = 0. \tag{4.9c}$$

Now suppose that $(\dot{\mathrm{y}}^0, \ddot{t}^0)$ is an isolated root of (3.27) with $\ddot{t}^0 \neq 0$ and $\ddot{t}^0 \in \mathbb{R}$. Then it corresponds to two real, isolated roots $(\dot{\mathrm{y}}^0_{re}, \dot{\mathrm{y}}^0_{im}, \ddot{t}^0)$ of (4.9): one with $\dot{\mathrm{y}}^0_{re} = \mathrm{Re}\ \dot{\mathrm{y}}^0$ and $\dot{\mathrm{y}}^0_{im} = \mathrm{Im}\ \dot{\mathrm{y}}^0$, and the other with $\dot{\mathrm{y}}^0_{re} = \mathrm{Im}\ \dot{\mathrm{y}}^0$, $\dot{\mathrm{y}}^0_{im} = \mathrm{Re}\ \dot{\mathrm{y}}^0$ and the sign of $\ddot{t}^0$ reversed. Each of these roots in turn yields a unique, real solution trajectory of (4.4) and a complex solution trajectory

satisfying the complexified DAE (4.1). The existence of those solutions is given by Theorem 3.29.

So we see that solutions near a fold point occur in pairs. Each member of a pair lies on only one side of $t = 0$, and the other member lies on the opposite side. In particular, a real isolated root of (3.27) leads not only to the real solution found in Theorem 3.29, but also to a complex solution which has a purely imaginary tangent, on the opposite side of $t = 0$. The following theorem states this result in precise form:

Theorem 4.10 *Suppose* $\mathbf{x} = \mathbf{0}$ *is a fold point and Assumption 1.8 is satisfied. Then corresponding to each isolated root* $(\dot{\mathbf{y}}^0, \ddot{t}^0)$ *of (3.27) with* $\ddot{t}^0 \neq 0$ *and* $\ddot{t}^0 \in I\!R$, *there exist exactly two complex solutions* $\mathbf{x}_{co}(\hat{s})$ *on some interval* $(\hat{s}_a, \hat{s}_b)$ *containing* $\hat{s}^0$, *satisfying the complexified DAE (4.1), such that:*

(a) $\mathbf{u}_{co}(t(\hat{s}))$ *is twice continuously differentiable;*

(b) $\mathbf{v}_{co}(t(\hat{s}))$ *is continuously differentiable;*

(c) $t(\hat{s})$ *is twice continuously differentiable.*

Each of the solutions locally exists on only one side of $t = 0$, *and the two solutions lie on opposite sides of* $t = 0$.

The proof of Theorem 4.10 is a straightforward application of Theorem 3.29 to the DAE (4.4). For examples of complex solutions near fold points, we refer the reader to Example 3.5 on page 13 (discussed also in Example 3.30 on page 29), Example 3.31 on page 29, and Example 3.33 on page 31.

4.3 Complex Solutions Near Bifurcation Points

In Chapter 3 we showed that near bifurcation points, there exists a real solution trajectory of (1.2) corresponding to each real, isolated root of the bifurcation equations (3.34). But we also mentioned that (3.34) may have complex, isolated roots which would have to occur as complex conjugate pairs. Clearly, these roots will not lead to real solutions of (1.2), but each of the isolated complex roots corresponds to a complex solution of the complexified DAE (4.1).

The bifurcation equations for the extended system at a bifurcation point are:

$$\Psi^T \mathrm{g}^0_{\mathrm{vv}}(\Phi\dot{\mathrm{y}}^0_{re}\Phi\dot{\mathrm{y}}^0_{re} - \Phi\dot{\mathrm{y}}^0_{im}\Phi\dot{\mathrm{y}}^0_{im}) + A_1\Phi\dot{\mathrm{y}}^0_{re}\dot{t}^0 + A_0(\dot{t}^0)^2 = 0, \tag{4.11a}$$

$$2\Psi^T \mathrm{g}^0_{\mathrm{vv}}\Phi\dot{\mathrm{y}}^0_{re}\Phi\dot{\mathrm{y}}^0_{im} + A_1\Phi\dot{\mathrm{y}}^0_{im}\dot{t}^0 = 0, \tag{4.11b}$$

$$N^0_{\mathrm{v}}\Phi(\dot{\mathrm{y}}^0_{re} + \dot{\mathrm{y}}^0_{im}) + (N^0_{\mathrm{u}}\mathrm{f}^0 + N^0_t + N^0_{\mathrm{v}}Z\zeta)\dot{t}^0 + N^0_s = 0. \tag{4.11c}$$

Here we have made use of (4.2), (4.3) and (4.8). Now suppose that $(\dot{\mathrm{y}}^0, \dot{t}^0)$ is an isolated complex root of the bifurcation equations (3.34) of the original, real DAE. Also assume that the root satisfies $\dot{t}^0 \in \mathbb{R}$, since we want to look for solutions with t real. Note that since the last equation of (3.34) is satisfied, and all coefficients in that equation are real, the root must satsify

$$N^0_{\mathrm{v}}\Phi(\mathrm{Im}\ \dot{\mathrm{y}}^0) = 0. \tag{4.12}$$

Since $(\dot{\mathrm{y}}^0, \dot{t}^0)$ is an isolated root of (3.34), $(\dot{\mathrm{y}}^0_{re}, \dot{\mathrm{y}}^0_{im}, \dot{t}^0)$ with $\dot{\mathrm{y}}^0_{re} = \mathrm{Re}\ \dot{\mathrm{y}}^0$ and $\dot{\mathrm{y}}^0_{im} = \mathrm{Im}\ \dot{\mathrm{y}}^0$ is a real isolated root of (4.11). It is also evident from (4.11) that the complex conjugate of $(\dot{\mathrm{y}}^0, \dot{t}^0)$ must also be a root of (3.34).

Theorem 4.13 *Suppose* $\mathrm{x} = 0$ *is a bifurcation point and Assumption 1.8 is satisfied. Then corresponding to each (real or complex) isolated root* $(\dot{\mathrm{y}}^0, \dot{t}^0)$ *of (3.34) with* $\dot{t}^0 \neq 0$, *there exists a unique, continuously differentiable solution* $\mathrm{x}_{co}(\hat{s})$ *satisfying the complexified DAE (4.1) on some interval* $(\hat{s}_a, \hat{s}_b)$ *containing* $\hat{s}^0$.

The proof is a simple application of Theorem 3.36 to the extended system (4.4).

Example 4.14 *Let* $n = m = 1$ *and consider the DAE*

$$\frac{du}{dt} = f(u, v_1, v_2) \equiv 1,$$

$$0 = \mathrm{g}(u, v) = u^2 + v^2,$$

$$u = v = 0 \ \textit{at}\ t = 0.$$

Then $\mathrm{g}^0_{\mathrm{v}} = 0$, *so* $r = \dim\{\mathcal{N}(\mathrm{g}^0_{\mathrm{v}})\} = 1$. *Since* $\mathrm{g}^0_{\mathrm{u}} = 0$, *the initial value is a bifurcation point. This DAE has two complex solutions (shown in Figure 4.15), given by* $u = t$ *and* $v = \pm it$. *If we set*

$$N(u, v, t, s) = t - s,$$

then the bifurcation equations are

$$2(\dot{t}^0)^2 + 2(\dot{v}^0)^2 = 0,$$

$$\dot{t}^0 - 1 = 0.$$

There are two isolated complex roots, $\dot{t}^0 = 1$ and $\dot{v}^0 = \pm i$. Theorem 4.13 applies to both roots, and there is a complex solution path corresponding to each of them.

We must devote special attention to pitchfork bifurcation points. Suppose the bifurcation equations (3.34) have a real, isolated root $(\dot{\mathbf{y}}^0, \dot{t}^0)$ with $\dot{t}^0 = 0$. Suppose also that this root satisfies

$$\mathbf{d}(\dot{\mathbf{y}}^0) \notin \mathcal{R}(A(\dot{\mathbf{y}}^0)),$$

and that the solution of (3.48) satisfies $\ddot{t}^0 \in \mathbb{R}$. Then the bifurcation equations (4.11) for the extended system have at least two real, isolated roots:

$$(\dot{\mathbf{y}}^0_{re}, \dot{\mathbf{y}}^0_{im}, \dot{t}^0) = (\text{Re } \dot{\mathbf{y}}^0, \mathbf{0}, 0) \text{ and} \tag{4.16a}$$

$$(\dot{\mathbf{y}}^0_{re}, \dot{\mathbf{y}}^0_{im}, \dot{t}^0) = (\mathbf{0}, \text{Re } \dot{\mathbf{y}}^0, 0). \tag{4.16b}$$

In order to establish the existence of solutions corresponding to these two roots, we apply the theory of Section 3.7. Thus we apply Definition 3.42 to obtain $\hat{A}(\dot{\mathbf{y}}^0_{re}, \dot{\mathbf{y}}^0_{im})$, $\hat{B}(\dot{\mathbf{y}}^0_{re}, \dot{\mathbf{y}}^0_{im})$ and $\hat{\mathbf{d}}(\dot{\mathbf{y}}^0_{re}, \dot{\mathbf{y}}^0_{im})$, the equivalents of $A(\dot{\mathbf{y}}^0)$, $B(\dot{\mathbf{y}}^0)$ and $\mathbf{d}(\dot{\mathbf{y}}^0)$ for the extended system (4.4):

Definition 4.17 *Let*

$$\hat{A}(\dot{\mathbf{y}}^0_{re}, \dot{\mathbf{y}}^0_{im}) \equiv \begin{pmatrix} 3\Psi^T \mathrm{g}^0_{\mathrm{vv}} \Phi \dot{\mathbf{y}}^0_{re} \Phi & -3\Psi^T \mathrm{g}^0_{\mathrm{vv}} \Phi \dot{\mathbf{y}}^0_{im} \Phi \\ 3\Psi^T \mathrm{g}^0_{\mathrm{vv}} \Phi \dot{\mathbf{y}}^0_{im} \Phi & 3\Psi^T \mathrm{g}^0_{\mathrm{vv}} \Phi \dot{\mathbf{y}}^0_{re} \Phi \\ N^0_{\mathrm{v}} \Phi & N^0_{\mathrm{v}} \Phi \end{pmatrix},$$

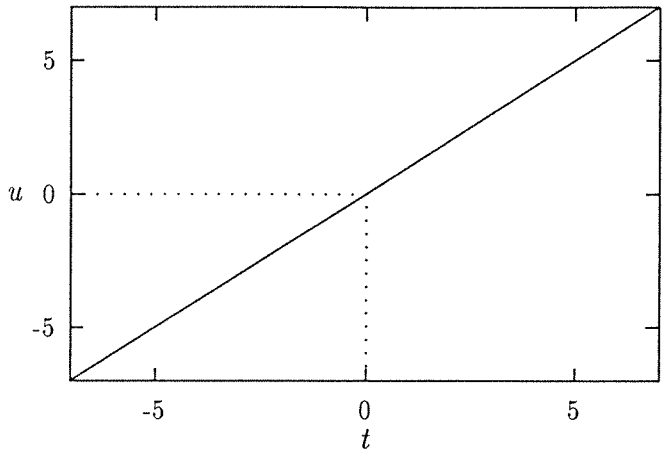

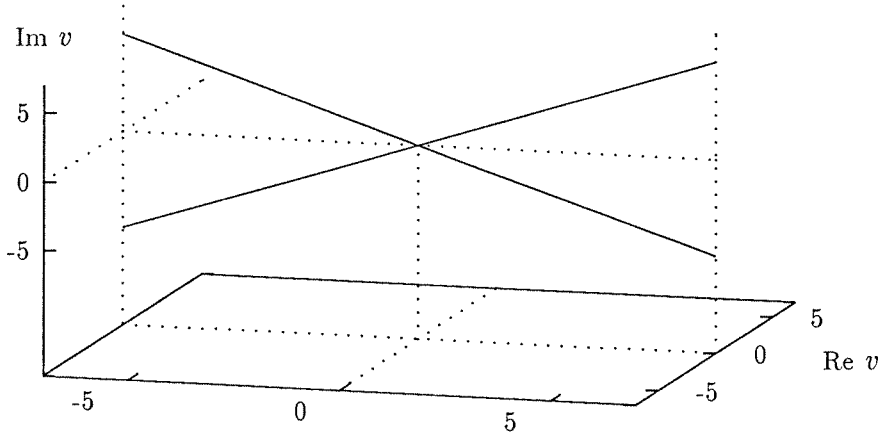

Figure 4.15: Solution set for Example 4.14. Both solutions are complex except at $t = 0$.

$$\hat{B}(\dot{y}^0_{re}, \dot{y}^0_{im}) \equiv \begin{pmatrix} 3\Psi^T g^0_{uv} \Phi \dot{y}^0_{re} f^0 + 3\Psi^T g^0_{vv} \Phi \dot{y}^0_{re} Z\zeta \\ 3\Psi^T g^0_{uv} \Phi \dot{y}^0_{im} f^0 + 3\Psi^T g^0_{vv} \Phi \dot{y}^0_{im} Z\zeta \\ N^0_u f^0 + N^0_t + N^0_v Z\zeta \end{pmatrix},$$

$$\hat{d}(\dot{y}^0_{re}, \dot{y}^0_{im}) \equiv \begin{pmatrix} -\Psi^T g^0_{vvv}(\Phi \dot{y}^0_{re} \Phi \dot{y}^0_{re} \Phi \dot{y}^0_{re} - 3\Phi \dot{y}^0_{re} \Phi \dot{y}^0_{im} \Phi \dot{y}^0_{im}) \\ -\Psi^T g^0_{vvv}(3\Phi \dot{y}^0_{re} \Phi \dot{y}^0_{re} \Phi \dot{y}^0_{im} - \Phi \dot{y}^0_{im} \Phi \dot{y}^0_{im} \Phi \dot{y}^0_{im}) \\ -\hat{N}^0_{ss} - \hat{N}^0_{vs} \Phi(\dot{y}^0_{re} - \dot{y}^0_{im}) - N^0_{vv} \Phi(\dot{y}^0_{re} \Phi \dot{y}^0_{re} - \dot{y}^0_{im} \Phi \dot{y}^0_{im}) \end{pmatrix}$$

The equivalent of (3.48) for the extended system is then

$$\hat{A}(\dot{y}^0_{re}, \dot{y}^0_{im}) \begin{pmatrix} \ddot{y}^0_{re} \\ \ddot{y}^0_{im} \end{pmatrix} + \hat{B}(\dot{y}^0_{re}, \dot{y}^0_{im}) \ddot{t}^0 = \hat{d}(\dot{y}^0_{re}, \dot{y}^0_{im}). \tag{4.18}$$

For simplicity, assume that we choose (as we always can) a constraint (3.7) which satisfies $N^0_{ss} = 0$. Now if we use the first root (4.16a) in (4.18), then the only solution $(\ddot{y}^0_{re}, \ddot{y}^0_{im}, \ddot{t}^0)$ of (4.18) is $(\ddot{y}^0, 0, \ddot{t}^0)$, the solution of (3.48). If we use the second root (4.16b) instead, then the solution of (4.18) will be $(-\ddot{y}^0, 0, -\ddot{t}^0)$. Thus we see that in addition to each solution branch given by Theorem 3.43, the complexified DAE (4.1) has a complex solution branch on the opposite side of $t = 0$. The complex branch has a purely imaginary tangent at $t = 0$. The following theorem summarizes this result:

Theorem 4.19 *Suppose* $\mathbf{x} = \mathbf{0}$ *is a bifurcation point and Assumptions 1.8 and 1.9 are satisfied. Then corresponding to each* isolated, real *root* $(\dot{y}^0, \dot{t}^0)$ *of (3.34) with*

(a) $\dot{t}^0 = 0$, *and*

(b) $\mathrm{d}(\dot{y}^0) \notin \mathcal{R}(A(\dot{y}^0))$,

there exist exactly two solutions $\mathbf{x}_{co}(\hat{s})$ *satisfying (4.1) in some interval* $(\hat{s}_a, \hat{s}_b)$ *containing* $\hat{s}^0$ *such that*

(a) $\mathbf{x}_{co}(\hat{s})$ *is twice continuously differentiable;*

(b) $\ddot{i}^0 \neq 0$.

One of these solutions is real and lies entirely on one side of $t = 0$. *The other has a purely imaginary tangent at* $t = 0$ *and it lies on the opposite side of* $t = 0$.

Theorem 4.19 is proved by applying Theorem 3.29 to the extended DAE (4.4). An example of this phenomenon is provided by Example 3.49 on page 45.

Chapter 5

Simple Critical Points

A special case of critical points arises when the dimension of the nullspace of g_V^0 is one. In this case, the bifurcation equations (3.23) are only two equations, one of which is quadratic and the other of which is linear. Due to the simplified nature of the problem, we can make much stronger statements about the existence of solutions near simple critical points than we can about solutions near general critical points.

5.1 The Nullspaces

At simple critical points, g_V^0 has a one-dimensional nullspace. Therefore, there is only one choice for the bases Φ and Ψ. If ϕ and ψ are the normalized right and left nullvectors of g_V^0, then:

$$\Phi = \phi,$$

$$\Psi = \psi.$$

We shall use the small letters ϕ and ψ instead of Φ and Ψ to emphasize that, for simple critical points, these quantities are vectors, not matrices. Also, for simple critical points, the vector $\mathbf{y}$ has only one component, which we shall call η.

5.2 Simple Fold Points

Definition 5.1 *If* $\mathbf{x} = \mathbf{0}$ *is a simple critical point, and* $\mathrm{g}_{\mathrm{u}}^0 \mathrm{f}^0 \notin \mathcal{R}(\mathrm{g}_{\mathrm{v}}^0)$, *then* $\mathbf{x} = \mathbf{0}$ *is called a* simple fold point.

For simple fold points, the bifurcation equations (3.27) reduce to

$$\psi^T \mathrm{g}_{\mathrm{u}}^0 \mathrm{f}^0 \ddot{t}^0 + \psi^T \mathrm{g}_{\mathrm{vv}}^0 \phi\phi (\dot{\eta}^0)^2 = 0, \tag{5.2a}$$

$$N_{\mathrm{v}}^0 \phi \dot{\eta}^0 + N_s^0 = 0. \tag{5.2b}$$

The only solution of (5.2) is:

$$\dot{\eta}^0 = -\frac{N_s^0}{N_{\mathrm{v}}^0 \phi}, \tag{5.3a}$$

$$\ddot{t}^0 = -\left(\frac{N_s^0}{N_{\mathrm{v}}^0 \phi}\right)^2 \left(\frac{\psi^T \mathrm{g}_{\mathrm{vv}}^0 \phi\phi}{\psi^T \mathrm{g}_{\mathrm{u}}^0 \mathrm{f}^0}\right). \tag{5.3b}$$

Recall that we assumed $N_{\mathrm{v}}^0 \phi \neq 0$ when we defined N, and that the range condition for a fold point can be expressed $\psi^T \mathrm{g}_{\mathrm{u}}^0 \mathrm{f}^0 \neq 0$. Therefore, the right-hand sides of (5.3) are well defined.

Theorem 5.4 *Suppose* $\mathbf{x} = \mathbf{0}$ *is a simple fold point, Assumption 1.8 is satisfied, and* $\psi^T \mathrm{g}^0_{\mathrm{vv}} \phi\phi \neq 0$. *Then there exists a unique solution* $\mathbf{x}(s)$ *of (3.8) and hence of (1.2) on some interval* (s_a, s_b) *containing* s^0 *such that:*

(a) $\mathbf{u}(t(s))$ *is twice continuously differentiable;*

(b) $\mathbf{v}(t(s))$ *is continuously differentiable;*

(c) $t(s)$ *is twice continuously differentiable.*

It has the form

$$\begin{aligned} \mathbf{u}(t(s)) &= \frac{1}{2}\left(s - s^0\right)^2 \mathrm{f}^0 \ddot{t}^0 + O\left((s - s^0)^3\right), \\ \mathbf{v}(t(s)) &= \left(s - s^0\right) \phi \dot{\eta}^0 + O\left((s - s^0)^2\right), \\ t(s) &= \frac{1}{2}\left(s - s^0\right)^2 \ddot{t}^0 + O\left((s - s^0)^3\right). \end{aligned}$$

Proof: The unique real solution of (3.27) is given in (5.3) and the assumptions of Theorem 3.29 are satisfied. A direct application of Theorem 3.29 yields the desired result. □

If $(\psi^T \mathrm{g}^0_{\mathrm{vv}} \phi\phi)/(\psi^T \mathrm{g}^0_{\mathrm{u}} \mathrm{f}^0) < 0$, then, locally, there are two solutions for $t > 0$ and no solutions for $t < 0$. Similarly, if $(\psi^T \mathrm{g}^0_{\mathrm{vv}} \phi\phi)/(\psi^T \mathrm{g}^0_{\mathrm{u}} \mathrm{f}^0) > 0$, then locally there are two real solutions for $t < 0$ and no real solutions for $t > 0$. Note that this result corresponds to that for "impasse points" in [24].

Now consider the complexified DAE (4.1) at a simple fold point. According to the theory of Chapter 4, particularly Theorem 4.10, the complexified problem has another solution branch. It lies on the opposite side of $t = 0$ from the real one, and its tangent is purely imaginary.

Theorem 5.5 *Suppose* $\mathbf{x} = \mathbf{0}$ *is a simple fold point, Assumption 1.8 is satisfied, and* $\psi^T \mathrm{g}^0_{\mathrm{vv}} \phi\phi \neq 0$. *Then there exist exactly two solutions* $\mathbf{x}_{co}(\hat{s})$ *of the*

complexified DAE (4.1) on some interval $(\hat{s}_a, \hat{s}_b)$ *containing* $\hat{s}^0$ *such that:*

(a) $\mathbf{u}(t(\hat{s}))$ *is twice continuously differentiable;*

(b) $\mathbf{v}(t(\hat{s}))$ *is continuously differentiable;*

(c) $t(\hat{s})$ *is twice continuously differentiable.*

If the real *root of the bifurcation equations is denoted* $(\dot{\eta}^0, \ddot{t}^0)$*, then one solution is given in Theorem 5.4, and the other has the form*

$$\begin{aligned} \mathbf{u}(t(\hat{s})) &= -\frac{1}{2}\left(\hat{s}-\hat{s}^0\right)^2 \mathbf{f}^0 \ddot{t}^0 + O\left((\hat{s}-\hat{s}^0)^3\right), \\ \mathbf{v}(t(\hat{s})) &= i\left(\hat{s}-\hat{s}^0\right)\phi\dot{\eta}^0 + O\left((\hat{s}-\hat{s}^0)^2\right), \\ t(\hat{s}) &= -\frac{1}{2}\left(\hat{s}-\hat{s}^0\right)^2 \ddot{t}^0 + O\left((\hat{s}-\hat{s}^0)^3\right), \end{aligned}$$

where $i = \sqrt{-1}$*. In a neighborhood of* $\mathbf{x} = \mathbf{0}$*, each solution lies entirely on one side of* $t = 0$ *and the two solutions lie on opposite sides of* $t = 0$*. One solution is real and the other has a purely imaginary tangent at* $\mathbf{x} = 0$*.*

The proof is a simple application of Theorem 4.10. We see that near a simple fold point, the complexified problem has two solutions for $t < 0$ and two solutions for $t > 0$.

Example 3.5 on page 13 provides an example of a simple fold. A discussion of this example is found in Example 3.30 on page 29.

5.3 Simple Bifurcation Points

Definition 5.6 *If* $\mathbf{x} = \mathbf{0}$ *is a simple critical point, and* $\mathrm{g}_{\mathrm{u}}^0 \mathbf{f}^0 \in \mathcal{R}(\mathrm{g}_{\mathrm{v}}^0)$*, then* $\mathbf{x} = \mathbf{0}$ *is called a* simple bifurcation point.

For simple bifurcation points, the bifurcation equations (3.34) reduce to

$$a_2(\dot{\eta}^0)^2 + a_1\dot{\eta}^0\dot{t}^0 + a_0(\dot{t}^0)^2 = 0 \tag{5.7a}$$

$$b_1\dot{\eta}^0 + b_2\dot{t}^0 + b_3 = 0 \tag{5.7b}$$

where

$$a_2 \equiv \psi^T \mathrm{g}^0_{\mathrm{vv}}\phi\phi,$$

$$a_1 \equiv \psi^T \mathrm{g}^0_{\mathrm{u}}\mathrm{f}^0_{\mathrm{v}}\phi + 2\psi^T \mathrm{g}^0_{\mathrm{vu}}\mathrm{f}^0\phi + 2\psi^T \mathrm{g}^0_{\mathrm{vv}}Z\zeta\phi,$$

$$a_0 \equiv \psi^T \mathrm{g}^0_{\mathrm{u}}\mathrm{f}^0_{\mathrm{u}}\mathrm{f}^0 + \psi^T \mathrm{g}^0_{\mathrm{u}}\mathrm{f}^0_{\mathrm{v}}Z\zeta + \psi^T \mathrm{g}^0_{\mathrm{uu}}\mathrm{f}^0\mathrm{f}^0 + 2\psi^T \mathrm{g}^0_{\mathrm{vu}}\mathrm{f}^0 Z\zeta + \psi^T \mathrm{g}^0_{\mathrm{vv}}Z\zeta Z\zeta,$$

$$b_1 \equiv N^0_{\mathrm{v}}\phi,$$

$$b_2 \equiv N^0_{\mathrm{u}}\mathrm{f}^0 + N^0_{\mathrm{v}}Z\zeta + N^0_t,$$

$$b_3 \equiv N^0_s.$$

In order to describe the solution set of (5.7), it is useful to define the discriminant

$$\Delta \equiv a_1^2 - 4a_0a_2.$$

The two roots of (5.7) are given by

$$\dot{\eta}^0 = \frac{-b_3R}{2a_2b_2 + b_1R},$$

$$\dot{t}^0 = \frac{-2b_3a_2}{2a_2b_2 + b_1R},$$

with

$$R \equiv -a_1 \pm \sqrt{\Delta}.$$

Clearly, the normalization N can be chosen so that the denominator $2a_2b_2 + b_1R$ is nonzero. The sign of Δ determines the character of thr roots. If $\Delta > 0$,

then there are two distinct, isolated, real roots. If $\Delta < 0$, then neither root is real and the two roots are a complex conjugate pair. If $\Delta = 0$, then there is one real double root. If $\Delta > 0$ and $a_2 = 0$, then $a_1 \neq 0$ and one of the two (real, isolated) roots has $\dot{t}^0 = 0$, leading us to expect a pitchfork bifurcation.

The theory of Chapters 3 and 4 applies when $\Delta \neq 0$ because the roots are isolated in this case. Thus we shall see that if $\Delta > 0$, two real solutions pass through the initial value $\mathbf{x} = \mathbf{0}$. If $\Delta < 0$, two complex solutions pass through $\mathbf{x} = \mathbf{0}$, and $\mathbf{x} = \mathbf{0}$ is an isolated solution of the original real problem. When $\Delta = 0$, the DAE may or may not have real solutions which pass through $\mathbf{x} = \mathbf{0}$. Any (real or complex) differentiable solution trajectories must have a real tangent at such a point, but one cannot conclude that the solution trajectories are real in a neighborhood of $\mathbf{x} = \mathbf{0}$. This is demonstrated by Example 3.41.

5.3.1 Simple Transcritical Bifurcation

Definition 5.8 *Suppose* $\mathbf{x} = \mathbf{0}$ *is a simple bifurcation point and* $a_2 \neq 0$. *Then if* $\Delta > 0$, $\mathbf{x} = \mathbf{0}$ *is called a* simple transcritical bifurcation point. *If* $\Delta < 0$, *then* $\mathbf{x} = \mathbf{0}$ *is called a* simple complex bifurcation point.

Theorem 5.9 *Suppose* $\mathbf{x} = \mathbf{0}$ *is a simple transcritical bifurcation point and Assumption 1.8 is satisfied. Then there exist exactly two continuously differentiable solutions* $\mathrm{x}(s)$ *satisfying (3.8) and hence (1.2) for all* s *in some interval* (s_a, s_b) *containing* s^0. *Each has the form*

$$\mathrm{u}(t(s)) \;=\; \left(s - s^0\right) \mathrm{f}^0 \dot{t}^0 + O\left((s - s^0)^2\right),$$

$$\begin{aligned} \mathbf{v}(t(s)) &= \left(s - s^0\right)\left(\Phi\dot{\eta}^0 + Z\zeta\dot{t}^0\right) + O\left((s-s^0)^2\right), \\ t(s) &= \left(s - s^0\right)\dot{t}^0 + O\left((s-s^0)^2\right), \end{aligned}$$

where $(\dot{\eta}^0, \dot{t}^0)$ *is one of the two real roots of the bifurcation equations.*

Proof: Since $\Delta > 0$ and $a_2 \neq 0$, there are two isolated real solutions of the bifurcation equation, and neither has $\dot{t}^0 = 0$. Theorem 3.36 guarantees that, corresponding to each of the two solutions, there exists a unique differentiable solution path satsifying (3.8) and hence (1.2) in some neighborhood of s^0. □

A simple transcritical bifurcation point is a point at which two solution paths cross. Near such a point, there are two solutions for $t > 0$ and two solutions for $t < 0$. For an example of simple transcritical bifurcation, see Example 3.37 on page 37.

Theorem 5.10 *Suppose* $\mathbf{x} = \mathbf{0}$ *is a simple complex bifurcation point and Assumption 1.8 is satisfied. Then there exist exactly two continuously differentiable solutions* $\mathbf{x}_{co}(\hat{s})$ *satisfying (3.8) and hence (1.2) for all* $\hat{s}$ *in some interval* $(\hat{s}_a, \hat{s}_b)$ *containing* $\hat{s}^0$*. Each has the form*

$$\begin{aligned} \mathbf{u}(t(\hat{s})) &= \left(\hat{s} - \hat{s}^0\right)\mathbf{f}^0\dot{t}^0 + O\left((\hat{s} - \hat{s}^0)^2\right), \\ \mathbf{v}(t(\hat{s})) &= \left(\hat{s} - \hat{s}^0\right)\left(\Phi\dot{\eta}^0 + Z\zeta\dot{t}^0\right) + O\left((\hat{s} - \hat{s}^0)^2\right), \\ t(\hat{s}) &= \left(\hat{s} - \hat{s}^0\right)\dot{t}^0 + O\left((\hat{s} - \hat{s}^0)^2\right), \end{aligned}$$

where $(\dot{\eta}^0, \dot{t}^0)$ *is one of the two complex roots of the bifurcation equations.*

Proof: At simple complex bifurcation points, $\Delta < 0$. This means that the bifurcation equations have two complex conjugate roots. We can apply

Theorem 4.13 to each of them to prove the existence of a solution trajectory corresponding to each root. □

We see that as long as $\Delta \neq 0$, the complexified DAE has two solutions for $t < 0$ and two solutions for $t > 0$.

5.3.2 Simple Pitchfork Bifurcation

Definition 5.11 *Suppose* $\mathbf{x} = \mathbf{0}$ *is a simple bifurcation point, and Assumptions 1.8 and 1.9 are satisfied. If*

(a) $a_2 = 0$, *and*

(b) $a_1 \neq 0$, *and*

(c) $\psi^T \mathrm{g}^0_{\mathrm{vvv}} \phi\phi\phi \neq 0$, *and*

(d) $N^0_{\mathrm{v}} \phi a_0 - \left(N^0_{\mathrm{u}} \mathrm{f}^0 + N^0_{\mathrm{v}} Z\zeta + N^0_t\right) a_1 \neq 0$,

then $\mathbf{x} = \mathbf{0}$ *is called a* simple pitchfork bifurcation point.

Lemma 5.12 *Suppose* $\mathbf{x} = \mathbf{0}$ *is a simple pitchfork bifurcation point and Assumptions 1.8 and 1.9 are satisfied. Then the bifurcation equations have two isolated roots, one of which satisfies* $i^0 \neq 0$ *and the other of which satisfies*

(a) $i^0 = 0$, *and*

(b) $\mathbf{d}(\dot{\eta}^0) \notin \mathcal{R}(A(\dot{\eta}^0))$,

where $\mathbf{d}(\dot{\eta}^0)$ *and* $A(\dot{\eta}^0)$ *are as in definition 3.42 on page 43.*

Proof: For simple pitchfork bifurcation points, the bifurcation equations are

$$\left(a_1 \dot{\eta}^0 + a_0 i^0\right) i^0 = 0, \tag{5.13a}$$

$$N^0_{\mathrm{v}} \phi \dot{\eta}^0 + \left(N^0_{\mathrm{u}} \mathrm{f}^0 + N^0_{\mathrm{v}} Z\zeta + N^0_t\right) i^0 + N^0_s = 0. \tag{5.13b}$$

The system (5.13) has two roots,

$$\dot{t}^0 = \frac{N_s^0 a_1}{N_{\rm v}^0 \phi a_0 - \left(N_{\rm u}^0 {\rm f}^0 + N_{\rm v}^0 Z\zeta + N_t^0\right) a_1} \text{ and } \dot{\eta}^0 = -\frac{a_0}{a_1}\dot{t}^0;$$

$$\dot{t}^0 = 0 \text{ and } \dot{\eta}^0 = -\frac{N_s^0}{N_{\rm v}^0 \phi}.$$

The first of these roots satisfies $\dot{t}^0 \neq 0$ because we assumed $a_1 \neq 0$. The second root satisfies $\dot{t}^0 = 0$ and ${\rm d}(\dot{\eta}^0) \notin \mathcal{R}(A(\dot{\eta}^0))$, since, by definition 3.42,

$$A(\dot{\eta}^0) = \begin{pmatrix} 3a_2\dot{\eta}^0 \\ N_{\rm v}^0 \phi \end{pmatrix} = \begin{pmatrix} 0 \\ N_{\rm v}^0 \phi \end{pmatrix},$$

$${\rm d}(\dot{\eta}^0) = \begin{pmatrix} -\psi^T {\rm g}_{\rm vvv}^0 \phi\phi\phi(\dot{\eta}^0)^3 \\ -N_{ss}^0 - N_{{\rm v}s}^0 \phi\dot{\eta}^0 - N_{\rm vv}^0 \phi\phi(\dot{\eta}^0)^2 \end{pmatrix}.$$

Because $\dot{\eta}^0 \neq 0$ when $\dot{t}^0 = 0$, and because we assumed $\psi^T {\rm g}_{\rm vvv}^0 \phi\phi\phi \neq 0$, it follows that ${\rm d}(\dot{\eta}^0) \notin \mathcal{R}(A(\dot{\eta}^0))$. □

Theorem 5.14 *Suppose* $\mathbf{x} = \mathbf{0}$ *is a simple pitchfork bifurcation point, and Assumptions 1.8 and 1.9 are satisfied. Then there exist exactly two twice continuously differentiable solutions* $\mathbf{x}(s)$ *satisfying (3.8) and hence (1.2) for all* s *in some interval* (s_a, s_b) *containing* s^0. *One corresponds to a root* $(\dot{\eta}^0, \dot{t}^0)$ *with* $\dot{t}^0 = 0$ *and it has the form*

$$\begin{aligned} \mathbf{u}(t(s)) &= \frac{1}{2}\left(s - s^0\right)^2 {\rm f}^0 \ddot{t}^0 + O\left((s - s^0)^3\right), \\ \mathbf{v}(t(s)) &= \left(s - s^0\right) \Phi\dot{\eta}^0 + O\left((s - s^0)^2\right), \\ t(s) &= \frac{1}{2}\left(s - s^0\right)^2 \ddot{t}^0 + O\left((s - s^0)^3\right). \end{aligned}$$

The other corresponds to a root $(\dot{\eta}^0, \dot{t}^0)$ *with* $\dot{t}^0 \neq 0$ *and it has the form*

$$\begin{aligned} \mathbf{u}(t(s)) &= \left(s - s^0\right) \mathrm{f}^0 \dot{t}^0 + O\left((s - s^0)^2\right), \\ \mathbf{v}(t(s)) &= \left(s - s^0\right) \left(\Phi \dot{\eta}^0 + Z\zeta \dot{t}^0\right) + O\left((s - s^0)^2\right), \\ t(s) &= \left(s - s^0\right) \dot{t}^0 + O\left((s - s^0)^2\right). \end{aligned}$$

Proof: By Lemma 5.12, the bifurcation equations for a simple pitchfork bifurcation point have two isolated roots, exactly one of which has $\dot{t}^0 = 0$. Theorem 3.43 guarantees the existence and uniqueness of a solution $\mathbf{x}(s)$ in a neighborhood of s^0 corresponding to the root with $\dot{t}^0 = 0$. Similarly, Theorem 3.36 guarantees the existence and uniqueness of a solution $\mathbf{x}(s)$ in a neighborhood of s^0 corresponding to the root with $\dot{t}^0 \neq 0$. □

Note that we can solve for the second derivative $\ddot{t}^0$ belonging to the real solution with $\dot{t}^0 = 0$. From (3.48), one obtains

$$\ddot{t}^0 = -\frac{\psi^T \mathrm{g}^0_{\mathrm{vvv}} \phi\phi\phi (N_s^0)^2}{(3\psi^T \mathrm{g}^0_{\mathrm{uv}} \phi \mathrm{f}^0 + 3\psi^T \mathrm{g}^0_{\mathrm{vv}} \phi Z\zeta)(N_{\mathrm{v}}^0 \phi)^2}.$$

If this quantity is positive, then (1.2) has three real solutions for $t > 0$ and one real solution for $t < 0$. If it is negative, (1.2) has one real solution for $t > 0$ and three real solutions for $t < 0$.

Now consider the complexified DAE (4.1) near a simple pitchfork bifurcation point. By applying the theory of Chapter 4, we find that the bifurcation equations corresponding to the complexified problem actually have three isolated roots. Two of them are the same as for the real DAE, and the third is complex. The complex root satisfies $\dot{t}^0 = 0$. Each root will lead to a solution of the complexified DAE:

Theorem 5.15 *Suppose* $\mathbf{x} = \mathbf{0}$ *is a simple pitchfork bifurcation point, and Assumptions 1.8 and 1.9 are satisfied. Then there exist exactly three twice continuously differentiable solutions* $\mathbf{x}_{co}(\hat{s})$ *satisfying (3.8) and hence (1.2) for all* $\hat{s}$ *in some interval* $(\hat{s}_a, \hat{s}_b)$ *containing* $\hat{s}^0$.

The proof is a simple application of Theorem 4.19. The new complex root leads to a solution which lies on the opposite side of $t = 0$ from the real root with $\dot{t}^0 = 0$. Thus the complexified DAE has three solutions for $t < 0$ and three solutions for $t > 0$.

Example 3.49 on page 45 is an example of simple pitchfork bifurcation. In that example, $\ddot{t}^0 = 2$ for the branch with $\dot{t}^0 = 0$, so there are three real solutions for $t > 0$ and one real solution for $t < 0$. As predicted by Theorem 5.15, there are three complex solutions for all $t \neq 0$.

Chapter 6

Applications and Physical Examples

DAEs occur naturally in many practical applications, and many contain fold or bifurcation points. Here, we present a few simple examples.

6.1 A Hydrodynamic Semiconductor Model

In [1], Ascher *et al.* study transonic solutions of the steady-state one-dimensional unipolar hydrodynamic model for semiconductors in the isoentropic phase. The model used is the following DAE:

$$F_x = nE - \alpha J, \tag{6.1a}$$

$$E_x = n - 1, \tag{6.1b}$$

$$F = \frac{J^2}{n} + n. \tag{6.1c}$$

Here, n is the electron density and E the electric field; J and α are assumed to be known positive constants. The DAE is subject to the boundary conditions

$$n(0) = n(\beta) = \bar{n}, \tag{6.2}$$

where β and $\bar{n}$ are also known positive constants. In ananlyzing this problem, Ascher *et al.* first study the initial value problem with the initial condition

$$n(0) = n_0, \tag{6.3a}$$

$$E(0) = E_0. \tag{6.3b}$$

To make the initial value consistent, we must have

$$F(0) = J^2/n_0 + n_0.$$

Critical points clearly occur when $n_0 = J$. Ascher *et al.* recognize that at such points the solution trajectory of the initial value problem is not unique. By a phase plane analysis, they find that if $E_0 = \alpha$, there are two distinct solutions which cross the initial value. One solution represents a transition from the subsonic to the supersonic region, and the other from the supersonic to the subsonic region. If $E_0 \neq \alpha$, Ascher *et al.* find that $|n_x|$ is infinite. If $E_0 < \alpha$, they find that two solution trajectories "end" at the initial value, so that (real) solutions exist only for $t < 0$. If $E_0 > \alpha$, then two trajectories begin at the initial value, so (real) solutions exist only for $t > 0$.

The initial value problem (6.1) with (6.3) clearly is of the form (1.2). We can thus apply our theory to find fold and bifurcation points. We find that

the initial value is a simple bifurcation point if $n_0 = J$ and $E_0 = \alpha$. It is a simple fold point if $n_0 = J$ and $E_0 \neq \alpha$. All other points are regular points. Clearly, Ascher *et al.*'s results follow from our theory in Chapter 5.

6.2 Nonlinear Circuit Problems

One of the most common applications of DAEs is the modeling of electrical circuits. If an electrical circuit has any nonlinear elements (such as a nonlinear resistor), then the nonlinear DAE which models it may have solutions which pass through critical points. Often the solution of a nonlinear circuit problem cannot be continued beyond some finite time. In the elctrical engineering language, points at which solutions cannot be continued into the future are called *forward impasse points.* Sometimes solutions can be continued into the future but not the past, and such points are called *backward impasse points.* Clearly, impasse points are closely related to fold points, as defined in Definition 3.21. In fact, Rabier and Rheinboldt's definition of a *standard* impasse point in [25] is equivalent to that of our simple fold point.

Impasse points are of great importance because they occur naturally in models of circuits which exhibit a so-called *jump phenomenon* (see [3]). In these cases, the model is considered defective, as its solution does not approximate the behavior of the physical circuit. Fortunately, it is possible to augment the circuit with a small "parasitic" series inductor so that the resulting circuit agrees well with the physical observations (see [4] for more details). In order to obtain a meaningful solution of a circuit exhibiting the

jump phenomenon, it is important to locate the impasse points in the model so that they can be treated appropriately.

As an example, consider a simple circuit with a nonlinear resistor, linear capacitor, and linear inductor in parallel. The characteristic of the resistor is given by $u = \gamma + i^2$, where i and u denote the corresponding branch current and voltage drop, respectively, and γ is a constant. This example has been considered in several articles, including [25]. It is modeled by the DAE

$$x_3' = x_4, \tag{6.4a}$$

$$x_4' = x_2, \tag{6.4b}$$

$$0 = x_1 + x_2 + x_3, \tag{6.4c}$$

$$0 = x_4 - \gamma - x_1^2, \tag{6.4d}$$

where $x_j = i_j, j = 1, 2, 3$ are the currents in the three branches and $x_4 = u$ is the voltage drop. The differentiation is with respect to the time t. For simplicity, the capacitance and inductance were normalized to one.

Critical points of the DAE (6.4) occur when $x_1 = 0$. Points with $x_1 = x_2 = 0$ are simple bifurcation points; critical points with $x_2 \neq 0$ are simple fold points. All other points are regular points. Rabier and Rheinboldt find in [25] that points with $x_1 = 0, x_2 \neq 0$ are standard impasse points, equivalent to our simple fold points. When $x_1 = x_2 = 0$, Rabier and Rheinboldt call the point a "higher singularity" with different character depending on the value of γ. They separate the qualitative behavior into the four cases (i) $\gamma > 1/8$, (ii) $0 < \gamma \leq 1/8$, (iii) $\gamma = 0$, (iv) $\gamma < 0$. Neither the theory nor the numerical method they use was designed to handle the point $x_1 = x_2 = 0$, as it is not

what they call a "standard impasse point." However, Rabier and Rheinboldt speculate that there are no C^1 solutions passing through $x_1 = x_2 = x_3 = 0$, $x_4 = \gamma = -1$ and that the t-derivative of all solutions is infinite at that point.

Our theory is capable of handling the point $x_1 = x_2 = 0$, as it is a simple bifurcation point. We need simply apply the theory for simple bifurcation points in Chapter 5. The bifurcation equation is, in this case:

$$-2(x_1')^2 - x_1' - \gamma = 0, \tag{6.5}$$

where the differentiation is with respect to t. Equation (6.5) has the roots

$$x_1' = -\frac{1}{4}(1 \pm \sqrt{\Delta}), \tag{6.6}$$

where $\Delta = 1 - 8\gamma$ is the discriminant. The derivative x_2' is then given by

$$x_2' = -x_1' - \gamma.$$

In case (i), where $\gamma > 1/8$, the discriminant is negative, so that there are no real solutions to the DAE. When $\gamma < 1/8$, there are exactly two solutions in both directions in time. This is in contradiction to Rabier and Rheinboldt's conjecture that there are no C^1 solutions through $x_1 = x_2 = x_3 = 0$, $x_4 = -1$. We predict *two* C^1 solutions with finite derivatives corresponding to the two roots (6.6).

We implemented a numerical procedure to compute solution trajectories of the DAE (6.4). In order to pass through folds in the solutions, we employed a pseudo-arclength parametrization. Given an initial value $(x_1^{(0)},x_2^{(0)},x_3^{(0)},x_4^{(0)})$ which satisfies (6.4cd) and represents the state of the system at $t = t^{(0)} = 0$,

the algorithm computes a sequence

$$(x_1^{(k)}, x_2^{(k)}, x_3^{(k)}, x_4^{(k)}, t^{(k)}),\ k = 1, 2, 3, \ldots$$

such that

$$x_3^{(k)} - x_3^{(k-1)} = \frac{x_4^{(k)} + x_4^{(k-1)}}{2}\left(t^{(k)} - t^{(k-1)}\right), \tag{6.7a}$$

$$x_4^{(k)} - x_4^{(k-1)} = \frac{x_2^{(k)} + x_2^{(k-1)}}{2}\left(t^{(k)} - t^{(k-1)}\right), \tag{6.7b}$$

$$0 = x_1^{(k)} + x_2^{(k)} + x_3^{(k)}, \tag{6.7c}$$

$$0 = x_4^{(k)} - \gamma - (x_1^{(k)})^2, \tag{6.7d}$$

$$0 = \sum_{j=1}^{4}\left[\dot{x}_j^{(k-1)}(x_1^{(k)} - x_1^{(k-1)})\right] + \dot{t}^{(k-1)}(t^{(k)} - t^{(k-1)}) - \Delta s. \tag{6.7e}$$

Equation (6.7e) is a standard pseudo-arclength constraint which allows us to pass through folds. The scalar Δs is a given pseudo-arclenth step size, and the derivatives $\dot{x}_j^{(k-1)}$ are taken to be

$$\dot{x}_j^{(k-1)} = \frac{x_j^{(k-1)} - x_j^{(k-2)}}{\Delta s},\ j = 1, 2, 3, 4.$$

The first step, $k = 1$, is handled as a special case. Euler-Newton continuation is applied to obtain the solution trajectory. Note that the discretization (6.7) of (6.4) is accurate to $O((\Delta s)^2)$.

We applied this method to compute solutions for various initial conditions. Figure 6.9 shows a representative set of computed solutions of (6.4) with $\gamma = -1$. The points A-I are critical points, as are all points with $x_1 = 0$. All these points are fold points, except point E, which is a bifurcation point. This graph should be compared to Figure 3 in [25]. We note that there is a discrepancy in the direction of the arrows in [25] and the direction of our

	Solution trajectory I		Solution trajectory II	
Δs	numerical x_1'	error from -1	numerical x_1'	error from $\frac{1}{2}$
0.1	-0.99958339	-4.166e-04	0.49981488	1.851e-04
0.01	-0.99999583	-4.167e-06	0.49999815	1.852e-06
0.001	-0.99999996	-4.167e-08	0.49999998	1.852e-08
0.0001	-1.00000000	-4.167e-10	0.50000000	1.852e-10
0.00001	-1.00000000	-3.986e-12	0.50000000	1.852e-12

Table 6.8: Convergence of x_1' at the bifurcation point $x_1 = x_2 = 0$ as $\Delta s \to 0$ with $\gamma = -1$. The theoretical values are -1 for solution trajectory I and $\frac{1}{2}$ for solution trajectory II.

arrows in Figure 6.9. A linear stability analysis of the two stationary points $x_1 = \pm 1$, $x_2 = 0$ shows that the point with $x_1 = -1$ is unstable, whereas the point with $x_1 = 1$ is stable. This confirms that the direction of the arrows in our graph is in the direction of increasing t.

In Figure 6.10 we plot solutions passing through the two fold points B and H of Figure 6.9. Figure 6.11 shows the two solutions at point E of Figure 6.9. the bifurcation point $x_1 = x_2 = x_3 = 0$, $x_4 = \gamma = -1$. Note that, as predicted, there are two continuously differentiable solution trajectories passing through that point. Moreover, as $\Delta s \to 0$, the derivatives x_1' at $t = 0$ for the two trajectories converge to -1 and $\frac{1}{2}$, exactly the roots (6.6). We used the centered difference

$$\frac{x_1^{(1)} - x_1^{(-1)}}{t^{(1)} - t^{(-1)}}$$

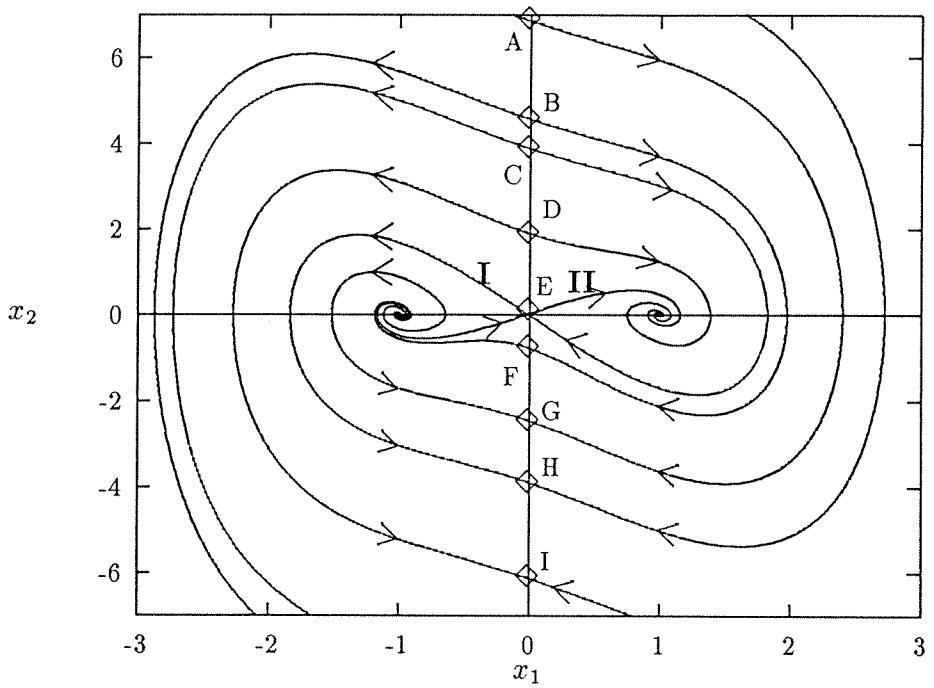

Figure 6.9: Solutions of the nonlinear circuit problem with $\gamma = -1$. The points A-I are critical points, as are all points with $x_1 = 0$. All these points are fold points, except point E, which is a bifurcation point. The trajectories I and II, both of which pass through the bifurcation point E, are shown in detail in Figure 6.11.

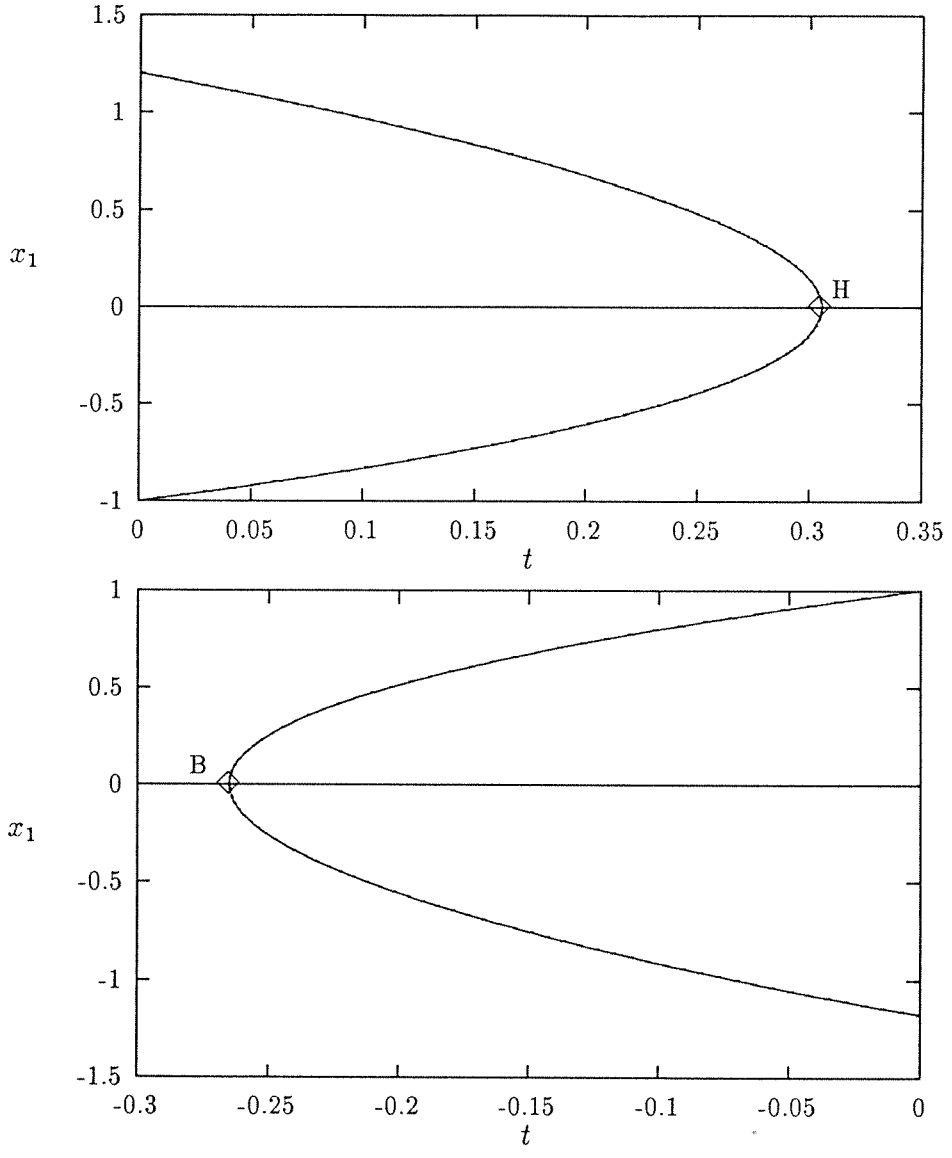

Figure 6.10: Solutions with $\gamma = -1$ containing fold points. The fold points B and H correspond to the points B and H in Figure 6.9.

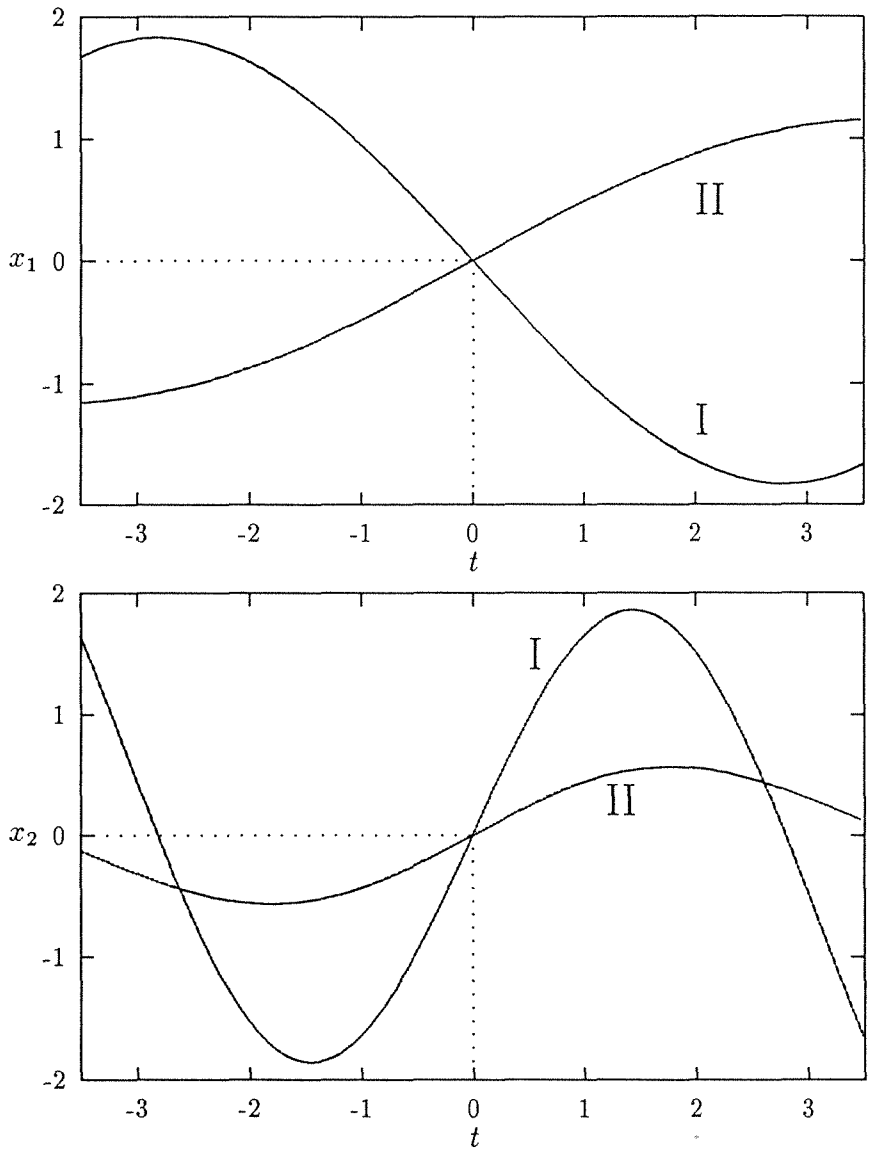

Figure 6.11: Solution trajectories I and II passing through the bifurcation point $x_1 = x_2 = 0$ with $\gamma = -1$.

to estimate the derivative x_1' at $x_1^{(0)} = x_2^{(0)} = 0$ with $\gamma = -1$. Table 6.8 shows the convergence of the derivative x_1' as $\Delta s \to 0$. This table also confirms the $O((\Delta s)^2)$ accuracy of the discretization.

6.3 Folds and Bifurcations in Ordinary Differential Equations

Our DAE theory can be useful in the analysis of ODEs of the form

$$\frac{d\mathbf{u}}{dt} = \mathbf{F}(\mathbf{u}) \tag{6.12}$$

when the function $\mathbf{F}(\mathbf{u})$ is just continuous or even discontinuous. The standard existence and uniqueness theory for ODEs, which requires Lipschitz continuity, does not apply in these cases. The Peano existence theory gives the existence but not uniqueness of a solution when $\mathbf{F}(\mathbf{u})$ is continuous. But that theory fails at discontinuities of $\mathbf{F}(\mathbf{u})$ and it can never give the number of solutions even if $\mathbf{F}(\mathbf{u})$ is continuous. When it is possible to rewrite the ODE (6.12) as a DAE of the form (1.2) with smooth functions $\mathbf{f}$ and $\mathbf{g}$, our theory can be applied to find the solutions. This includes many cases not covered by the standard theories.

As an example, consider the ODE initial value problem

$$\frac{du}{dt} = \sqrt{u}, \tag{6.13a}$$

$$u = 0 \text{ at } t = 0, \tag{6.13b}$$

where u is a real scalar. The initial value problem (6.13) has infintely many solution trajectories. There is a trivial solution, $u(t) = 0$ for all t. The other solutions are given by

$$u = 0, t \leq T \tag{6.14a}$$

$$u = \frac{1}{4}(t - T)^2, t \geq T \tag{6.14b}$$

for all $T \geq 0$.

Now consider the related DAE intial value problem

$$\frac{du}{dt} = v, \tag{6.15a}$$

$$0 = v^2 - u, \tag{6.15b}$$

$$u = v = 0 \text{ at } t = 0. \tag{6.15c}$$

Here, u and v are real scalars. The solution set of the ODE problem (6.13) is a subset of the solution set of the DAE (6.15): the solutions of (6.15) with $v \geq 0$ are the solutions of (6.13). So one way to find the solutions of (6.13) is to find the solutions of the DAE (6.15) and then discard any solutions with $v < 0$.

We find that the point $u = v = 0$ is a simple bifurcation point of the DAE (6.15). The theory of Chapter 5 thus predicts two C^1 solutions. Because of (6.15a), these correspond to C^2 solutions of (6.13). Using

$$N(u, v, t, s) = t - s,$$

we obtain the tangents $\dot{v}^0 = 0$ and $\dot{v}^0 = \frac{1}{2}$. The first tangent corresponds to the trivial solution $u = 0$ for all t. The second tangent corresponds to a

solution with $\dot{u}^0 = 0$ and $\ddot{u}^0 = \dot{v}^0 = \frac{1}{2}$. This second solution thus has the form

$$u = \frac{1}{4}t^2 + O(t^3), \tag{6.16a}$$

$$v = \frac{1}{2}t + O(t^2) \tag{6.16b}$$

for $t \to 0$. We see that $v < 0$ for $t < 0$ so that only the $t \geq 0$ half-trajectory is a solution of the ODE (6.13). For $t \geq 0$, the form (6.16) of the solution matches the nontrivial solution (6.14) of the ODE with $T = 0$.

So our theory gives us only the two C^2 solutions (which correspond to C^1 solutions of the DAE), but not the rest which have discontinuous derivatives. These other solutions occur because every point on the trivial ($u = 0$) solution trajectory is a bifurcation point. Unfortunately, our theory cannot predict this, and this phenomenon would be an interesting subject of future investigation.

As a second example, take the initial value problem

$$\frac{du}{dt} = \frac{1}{u}, \tag{6.17a}$$

$$u = 0 \text{ at } t = 0. \tag{6.17b}$$

Again, u is a scalar. If we multiply both sides of (6.17a) with u and introduce a new variable $v = u^2$, then we obtain the following DAE initial value problem:

$$\frac{dv}{dt} = 2, \tag{6.18a}$$

$$0 = u^2 - v, \tag{6.18b}$$

$$u = v = 0 \text{ at } t = 0. \tag{6.18c}$$

The solution set of the DAE (6.18) is the same as that of the original ODE

(6.17). Using the theory of Chapter 5, we find that $u = v = 0$ is a simple fold point of the DAE (6.18). We introduce the normalization

$$N(u, v, t, s) = u - s, \tag{6.19}$$

and obtain the bifurcation equations

$$2\ddot{t}^0 - 2\left(\dot{u}^0\right)^2 = 0, \tag{6.20a}$$

$$\dot{u}^0 - 1 = 0. \tag{6.20b}$$

The only root of (6.20) is $\dot{u}^0 = \ddot{t}^0 = 1$. Since $\ddot{t}^0 > 0$, the theory predicts two real solutions for $t > 0$ and none for $t < 0$. We also predict two complex solutions for $t < 0$. The form of the solutions for $s \to 0$ is

$$u = s + O(s^2),$$

$$t = \frac{1}{2}s^2 + O(s^3),$$

so near the intial value we expect solutions of the form

$$u = \pm\sqrt{2t} + O(t^{3/4}).$$

In fact, it is easily seen that the exact solutions of (6.18) are given by $v = 2t$ and $u = \pm\sqrt{2t}$. Note that, as predicted by the theory of Chapter 4, there are also two complex solutions for $t < 0$, namely

$$u = \pm i\sqrt{-2t}.$$

Chapter 7

Numerical Implementation

The theory developed in the previous chapters can be used to compute solutions of DAEs which pass through critical points. There are many good methods for solving DAEs of the form (1.2) as long as the solution contains only regular points ([2] is a good reference). However, these methods generally fail when the solution encounters a critical point. In this chapter, we shall show how a numerical method for (1.2) can be modified to handle critical points.

7.1 Detection of Critical Points

As long as g_v remains nonsingular on the solution trajectory, we can use any of the known methods for solving the DAE without modification. When we approach a critical point, we can modify the method so that it will not fail when the critical point is reached.

There are many ways to detect the approach of a critical point. If we assume that $\mathbf{g}$ is at least once continuously differentiable, so that the entries of $\mathbf{g}_\mathbf{v}$ are continuous functions of $\mathbf{u}$ and $\mathbf{v}$, then the eigenvalues of $\mathbf{g}_\mathbf{v}$ must also be continuous functions of $\mathbf{u}$ and $\mathbf{v}$. At a critical point, at least one of the eigenvalues of $\mathbf{g}_\mathbf{v}$ is zero, and so as we pass a critical point, we expect at least one eigenvalue to change in sign. Note that the number of zero eigenvalues at a critical point need not be equal to the dimension of the nullspace, r.

Since it is expensive to monitor the eigenvalues of $\mathbf{g}_\mathbf{v}$, particularly if m is large, it is not practical to compute the eigenvalues of $\mathbf{g}_\mathbf{v}$ at every step in order to detect critical points. A related and more practical check is to monitor the determinant of $\mathbf{g}_\mathbf{v}$. That determinant must be zero at a critical point, and it is also a continuous function of the matrix entries of $\mathbf{g}_\mathbf{v}$. All methods to solve (1.2) must solve a system of the form

$$\mathbf{g}_\mathbf{v}\boldsymbol{\xi} = \mathbf{b} \tag{7.1}$$

in order to determine $\mathbf{v}$ at the next time step. If LU-decomposition is used to solve (7.1), then the determinant is trivially computed. So we can detect critical points by watching for a change of sign in the determinant.

Finally, for large problems an iterative solver such as Newton's method is often employed to solve for $\mathbf{v}$ at the new time step. As we approach a critical point and $\mathbf{g}_\mathbf{v}$ becomes close to singular, the convergence rate of such methods deteriorates drastically. This is perhaps the most robust test for a critical point when m is large.

7.2 Classifying Critical Points

Suppose now that, during the computation of a solution trajectory, we detect a critical point by one of the means discussed in Section 7.1. In order to treat the point appropriately, we must determine what type of critical point it is.

One important feature of fold points is that the tangent of the solution trajectory is normal to the t-axis. This means that, as we approach a fold point, the (always non-negative) ratio

$$\theta \equiv \frac{\mid t^{n+1} - t^n \mid}{\| \mathbf{x}^{n+1} - \mathbf{x}^n \|} \rightarrow 0. \tag{7.2}$$

Here, t^n and $\mathbf{x}^n$ represent the computed values of t and the solution $(\mathbf{u}, \mathbf{v}, t)^T$ at the n^{th} time step, respectively. By itself, (7.2) does not imply that the critical point in question is a fold because the same phenomenon occurs at pitchfork bifurcation points. If (7.2) does not hold as we approach a critical point, we know that the point must be a bifurcation point.

7.3 Computing Past Fold Points

If we find that (7.2) holds as we approach a critical point, we know that we are on a solution trajectory whose t-derivative becomes infinite as we approach the critical point. If the critical point is a fold point, the DAE may have no solution for values of t beyond the fold. Conventional solution methods will fail as a result.

We point out that Rabier and Rheinboldt [25] have developed a method which handles simple fold points. We wish to present a more general approach which can adapt almost any DAE solution method to handle folds as well as bifurcations.

Whether the critical point in question is a fold point or pitchfork bifurcation point, we know that all solution trajectories can be represented smoothly near the critical point if we introduce a proper parametrization. Thus, instead of solving (1.2) directly, we propose introducing a new parametrization (3.7), such as a pseudo-arclength constraint. This is done whenever the ratio θ falls below a certain cut-off value, θ_c. Then we solve the augmented DAE

$$\frac{d\mathbf{u}}{ds} = \mathbf{f}(\mathbf{u},\mathbf{v})\tau, \tag{7.3a}$$

$$\frac{dt}{ds} = \tau, \tag{7.3b}$$

$$\mathbf{0} = \mathbf{g}(\mathbf{u},\mathbf{v}), \tag{7.3c}$$

$$0 = N(\mathbf{u},\mathbf{v},t,s). \tag{7.3d}$$

The DAE (7.3) is equivalent to the reduced DAE (3.25) via the Lyapunov-Schmidt reduction (3.4). The scalar τ has been introduced to obtain a DAE of the form (1.2). If we differentiate (7.3cd) once with respect to s and substitute (7.3ab), we obtain the following linear system relating the derivative $\dot{\mathbf{v}}$ and the scalar τ:

$$\begin{pmatrix} \mathbf{g}_\mathbf{v} & \mathbf{g}_\mathbf{u}\mathbf{f} \\ N_\mathbf{v} & N_\mathbf{u}\mathbf{f} + N_t \end{pmatrix} \begin{pmatrix} \dot{\mathbf{v}} \\ \tau \end{pmatrix} = \begin{pmatrix} \mathbf{0} \\ -N_s \end{pmatrix}.$$

As we saw in Section 3.4.1, at fold points we must have

$$\dot{t} = \tau = 0.$$

So as we pass through a fold, we expect the value of τ to change sign.

If the value of θ increases back to above θ_c, the solution can once again be represented as a smooth function of t and we can "turn off" the augmentation and return to solving the original DAE.

We note that for simple fold points, the DAE (7.3) has a unique, smooth solution (see Chapter 5). So any method we use to solve (7.3) should have no trouble passing through a simple fold. If a fold is non-simple or we are at a pitchfork bifurcation point, then the critical point in question is also a critical point of the augmented system so that the corresponding Jacobian

$$\begin{pmatrix} \mathrm{g_v} & \mathrm{g_u f} \\ N_{\mathrm{v}} & N_{\mathrm{u}}\mathbf{f} + N_t \end{pmatrix},$$

which is nonsingular at simple folds, will be singular at the critical point.

For non-simple folds, one must locate the fold by finding the zero of τ. Then the bifurcation equations (3.27) can be solved to find the tangents of all solution trajectories which pass through the fold point. We will discuss how this is done in Section 7.5. Knowing all tangents, we can follow each individual trajectory separately. The existence of those trajectories is ensured by Theorem 3.29.

Of course the value of τ also passes through zero at pitchfork bifurcation points along branches with $\dot{t} = 0$. In order to differentiate between pitchfork bifurcations and folds, we must determine whether or not the vector $\mathrm{g_u f}$ is in the range of $\mathrm{g_v}$. The classification of the critical point is then given by Definitions 3.20 and 3.21: if $\mathrm{g_u f} \in \mathcal{R}(\mathrm{g_v})$, we are at a pitchfork bifurcation point, otherwise we are at a fold point. At pitchfork bifurcation points, we

must solve the bifurcation equations (3.34) in order to find the tangents of all solution trajectories (see Section 7.5). Then each trajectory can be followed individually.

7.4 Computing Past Bifurcation Points

If the determinant of g_v has a zero on a solution trajectory, but the value of τ does not pass through zero, then the trajectory must contain a bifurcation point. In order to find all trajectories through a bifurcation point, one should solve the bifurcation equations (3.34) for the tangents of all trajectories (see Section 7.5 below). Each trajectory can then be computed individually. In the case of pitchfork bifurcation, a suitable pseudo-arclength or other parametrization must be used, just as in the case of folds. The existence of solution trajectories is given by Theorems 3.36 and 3.43.

7.5 Solving the Bifurcation Equations

The bifurcation equations are a set of quadratic and linear equations. Given the coefficients of all terms, there is no difficulty in solving them. However, the coefficients involve orthonormal bases for the left and right nullspaces of g_v at the critical point. We shall now describe how these bases can be computed so that the coefficients of the bifurcation equations can be evaluated.

7.5.1 Determining the Dimension of the Nullspace

The first step in computing bases for the nullspaces of $\mathbf{g_v}$ will be to find the dimension of those spaces. We mentioned that any DAE solver of (1.2) must be able to solve systems of the form (7.1). This is typically done by LU-decomposition. If a complete pivoting strategy is used and there is no round-off, then the LU-decompsition procedure will reveal the rank of $\mathbf{g_v}$ and hence the dimension r of the nullspace of $\mathbf{g_v}$. (We will later take into account round-off error and almost singular $\mathbf{g_v}$.) After $m - r$ steps of the LU-decomposition have been completed, the algorithm terminates with a factorization of the form

$$P\mathbf{g_v}Q = LU = \begin{pmatrix} L_{11} & 0 \\ L_{21} & I_r \end{pmatrix} \begin{pmatrix} U_{11} & U_{12} \\ 0 & 0 \end{pmatrix}. \tag{7.4}$$

Here L is lower triangular has 1 for each diagonal entry, U is upper triangular, L_{11} and U_{11} are $(m-r)$-by-$(m-r)$, L_{21} and U_{12}^T are r-by-$(m-r)$, and P and Q are m-by-m permutation matrices.

7.5.2 Computing the Right Nullspace

We can use the LU-decomposition (7.4) to obtain bases for the left and right nullspaces of $\mathbf{g_v}$. Let us first concentrate on the right nullspace, Φ. In order to find a single nullvector ϕ of $\mathbf{g_v}$ we must find a solution of $\mathbf{g_v}\phi = \mathbf{0}$. Since P and Q are nonsingular permutation matrices, we can equivalently solve

$$P\mathbf{g_v}\phi = P\mathbf{g_v}Q(Q^{-1}\phi) = LU\tilde{\phi} = \mathbf{0}. \tag{7.5}$$

Here we have introduced the m-dimensional vector

$$\tilde{\phi} = \begin{pmatrix} \tilde{\phi}_1 \\ \tilde{\phi}_2 \end{pmatrix},$$

where $\tilde{\phi}_1 \in \mathbb{R}^{m-r}$ and $\tilde{\phi}_2 \in \mathbb{R}^r$. It is related to ϕ via

$$Q\tilde{\phi} = \phi,$$

so $\tilde{\phi}$ is just a permuted version of the nullvector ϕ. In fact, since L is nonsingular, (7.5) can be further simplified to

$$U\tilde{\phi} = \begin{pmatrix} U_{11}\tilde{\phi}_1 + U_{12}\tilde{\phi}_2 \\ 0 \end{pmatrix} = 0. \tag{7.6}$$

To obtain a scrambled nullvector $\tilde{\phi}$, we pick some value for $\tilde{\phi}_2$ and solve for $\tilde{\phi}_1$ using (7.6). This requires only half of a backsolve, i.e., the solution of an upper triangular linear system. By picking r linearly independent vectors $\tilde{\phi}_2$, such as the r unit vectors in $\mathbb{R}^r$, we obtain r linearly independent scrambled nullvectors $\tilde{\phi}$, which can be unscrambled to obtain a basis $\tilde{\Phi}$ for the right nullspace of g_v.

We can obtain an orthonormal basis Φ by computing a QR factorization of $\tilde{\Phi}$. Several algorithms exist for this purpose. The QR factorization can be computed directly by the Gram-Schmidt process. A more stable but also more expensive procedure is to use Householder orthogonalization.

7.5.3 Computing the Left Nullspace

The left nullspace of g_v can be obtained in a similar manner as the right

nullspace with minimal additional effort. If the LU-decomposition of $\mathrm{g_v}$ is given by (7.4), then

$$Q^T \mathrm{g_v}^T P^T = U^T L^T.$$

We now wish to find a single left nullvector $\boldsymbol{\psi}$ of $\mathrm{g_v}$, which is a right nullvector of $\mathrm{g_v}^T$. So we want to solve

$$Q^T \mathrm{g_v}^T P^T \left((P^T)^{-1} \boldsymbol{\psi} \right) = U^T L^T P \boldsymbol{\psi} = U^T \tilde{\boldsymbol{\psi}} = \mathbf{0}.$$

The above follows from the fact that the transpose of a permutation matrix is equal to its inverse. We have introduced the vector $\tilde{\boldsymbol{\psi}} \in \mathbb{R}^m$, which is related to $\boldsymbol{\psi}$ via

$$L^T P \boldsymbol{\psi} = \tilde{\boldsymbol{\psi}}. \tag{7.7}$$

From the form of U, we deduce that the first $m - r$ components of $\tilde{\boldsymbol{\psi}}$ are zero and the last r are arbitrary. In order to obtain r linearly independent nullvectors, we pick r linearly independent vectors for the last r components of $\tilde{\boldsymbol{\psi}}$. For each, we solve the upper triangular linear system (7.7) for the scrambled nullvector $P\boldsymbol{\psi}$. The nullvector can be obtained by unscrambling the entries. Just as for the right nullspace, we obtain an orthonormal basis, Ψ, for the left nullspace by computing the QR factorization of the r linearly independent nullvectors.

7.5.4 Almost Singular Jacobian

In practice we never have the exact values of $\mathbf{u}$ and $\mathbf{v}$ at the critical point, and there will be round-off error in evaluating the Jacobian $\mathrm{g_v}$. Even

if we have $\mathbf{g}_v$ exactly, round-off error will be introduced during the LU-decomposition procedure. So $\mathbf{g}_v$ is most likely not singular, but almost singular and the LU-decomposition procedure will rarely encounter a zero pivot. Thus, the above method appears to fail to yield the desired nullspace bases Φ and Ψ.

We remedy this problem by declaring $\mathbf{g}_v$ singular not only if a pivot is zero, but if a pivot is "small" compared to the diagonal entries of U_{11}. We then proceed as outlined above, setting the lower right r-by-r submatrix of U to zero. In this way, we obtain approximations of the nullspaces at the (nearby) critical point. They are also approximations to the least dominant r-dimensional left and right invariant subspaces of $\mathbf{g}_v$. The quality of these invariant subspaces can be improved by inverse iteration. This involves only tools which we have already used: solving linear systems of the form (7.1) and QR factorization.

7.6 Numerical Examples

The computations of Section 6.2 provide an example of the numerical method described above. In that computation, the time derivatives were discretized using a centered Euler approximation. Without the pseudo-arclength parametrization defined by (6.7e), the method fails at fold points. But by introducing the pseudo-arclength parametrization, we can easily compute past fold points. We used pseudo-arclength continuation when θ fell below the cut-off value $\theta_c = 0.1$. Near the bifurcation point $x_1 = x_2 = 0$, the

convergence of Newton's method slowed drastically. By computing the roots of the bifurcation equations, we were able to continue past the bifurcation point.

As a second example, we once again compute the solutions of the circuit problem of Section 6.2. This time we discretize the time derivatives using the second order BDF (backward differencing) formula. BDF is a popular method for solving initial value problems in DAEs. For instance, Petzold's code DASSL [20] is based on BDF methods. BDF is an implicit linear multistep method; in the k-step, BDF method, time derivatives are replaced by one sided approximations of the derivatives which involve the solution at the new time and at k previous time steps. Thus the k-step BDF method is of accuracy order k. In the second order constant stepsize BDF method, the approximation

$$\frac{d\mathbf{u}^{(n)}}{dt} \doteq \frac{3\mathbf{u}^{(n)} - 4\mathbf{u}^{(n-1)} + \mathbf{u}^{(n-2)}}{2\Delta t}$$

is used. Here, Δt is the stepsize, and $\mathbf{u}^{(n)}$ is the computed solution at the n^{th} time step.

Using, the second order BDF method, we obtained the same qualitative results as with the centered Euler approximation. Just as the centered Euler method, BDF achieved second order accuracy. The accuracy was slightly better for the centered Euler method. We monitored the value of the determinant of $\mathbf{g}_\mathbf{v}$ during computations and it proved an excellent tool in locating critical points. Figure 7.8 shows the value of the determinant as solutions pass through a fold point (top graph) and a bifurcation point (bottom graph). The critical points occur at the zeroes of the determinant of the unaugmented

system, when $x_1 = 0$. The determinant of the augmented system changes sign at the bifurcation point, but not at the simple fold point.

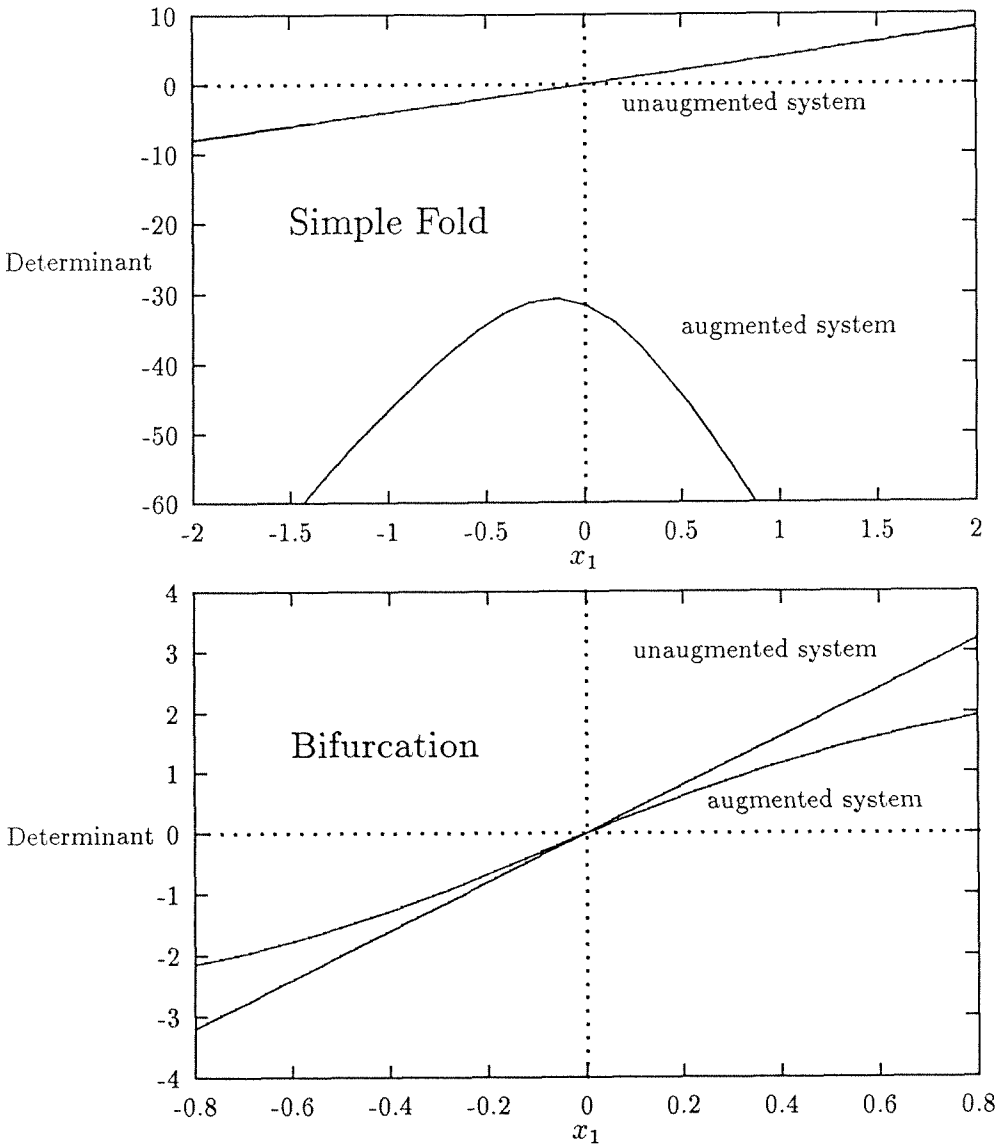

Figure 7.8: Determinants of the Jacobians of the unaugmented and augmented DAEs as solutions of the nonlinear circuit problem ($\gamma = -1$) pass through a simple fold point and a bifurcation point.

Chapter 8

Conclusions and Future Directions

We have introduced a new bifurcation theory for the solutions of semi-explicit DAEs. This theory covers the phenomena of folds, bifurcation, and complex bifurcation. In addition, we have presented a numerical method which can be used to compute solutions near critical points. Using this method, we were able to solve a nonlinear circuit problem which was not solvable using previously known methods.

Although our theory has proven useful in many problems, not all DAEs can be written in the semi-explicit form (1.2). As an extension of this work, we hope to obtain analogous theories for more general forms of DAEs. These include the semi-implicit form

$$\mathbf{F}_1(\mathrm{x}, \dot{\mathrm{x}}, t) = \mathbf{0}, \tag{8.1a}$$

$$\mathbf{F}_2(\mathbf{x}, t) = \mathbf{0}, \tag{8.1b}$$

and the fully implicit form (1.1).

Another extension of great interest lies in the area of higher index DAEs. Often DAEs (1.2) have the property that $\mathbf{g}_\mathbf{v}^0$ is always singular with some maximum rank less than m. The index of the DAE is then said to be higher than one. In these degenerate cases, a unique solution may exist even if $\mathbf{g}_\mathbf{v}^0$ is singular. For example, the so-called index-2 semi-explicit Hessenberg form is

$$\frac{d\mathbf{u}}{dt} = \mathbf{f}(\mathbf{u}, \mathbf{v}), \tag{8.2a}$$

$$\mathbf{0} = \mathbf{g}(\mathbf{u}). \tag{8.2b}$$

It is well known that, as long as the m-by-m matrix $\mathbf{g}_\mathbf{u}\mathbf{f}_\mathbf{v}$ remains nonsingular, such DAEs have a unique solution. This is consistent with our theory. We would consider every point a critical point, and the corresponding bifurcation equations (using the parametrization $t = s$) would be

$$\mathbf{g}_\mathbf{u}^0\mathbf{f}_\mathbf{v}^0\dot{\mathbf{v}}^0 + \mathbf{g}_{\mathbf{uu}}^0\mathbf{f}^0\mathbf{f}^0 + \mathbf{g}_\mathbf{u}^0\mathbf{f}_\mathbf{u}^0\mathbf{f}^0 = \mathbf{0}.$$

This is a set of m linear equations. Therefore, if $\mathbf{g}_\mathbf{u}^0\mathbf{f}_\mathbf{v}^0$ is nonsingular, the bifurcation equations have only one root, corresponding to a unique solution trajectory. Bifurcations and folds presumably occur when the matrix $\mathbf{g}_\mathbf{u}^0\mathbf{f}_\mathbf{v}^0$ becomes singular. A treatment of this special degenerate case would be a useful extension of our theory.

Finally, our theory has important applications in the analysis of ordinary differential equations. We have only scratched the surface of this area in Section 6.3. A subject of future investigation will be to create a bifurcation theory for ODEs by using the approach of Section 6.3.

Part II

The Recursive Projection Method Applied to Differential-Algebraic Equations and Incompressible Fluid Mechanics

Chapter 9

Introduction

In the study of incompressible fluid mechanics, we are often interested in numerically computing branches of steady state solutions which depend on one or more parameters. Here, we present a method for this purpose.

Incompressible, viscous fluid flows are governed by the Navier-Stokes equations. We assume that the method of lines (MOL) has been applied to these equations. That is, the equations have been discretized in all spatial dimensions by finite differences, finite elements, spectral methods, some other technique, or a combination of methods. We are thus left with a differential-algebraic equation (DAE) of the form

$$\frac{d\mathbf{u}}{dt} = \mathbf{f}(\mathbf{u}, \mathbf{p}; \lambda), \tag{9.1a}$$

$$\mathbf{0} = \mathbf{g}(\mathbf{u}). \tag{9.1b}$$

Here, $\mathbf{u} \in \mathbb{R}^n$ contains a discretization of the velocity of the fluid, and $\mathbf{p} \in \mathbb{R}^m$ a discretization of the pressure. The scalar λ is a parameter which may,

for example, represent a Reynolds number or some geometric feature of the problem. The operators $\mathbf{f} : \mathbb{R}^n \times \mathbb{R}^m \to \mathbb{R}^n$, $\mathbf{g} : \mathbb{R}^n \to \mathbb{R}^m$ are smooth. Note that boundary conditions and other constraints may be incorporated into (9.1b). Also, the vector $\mathbf{p}$ may contain, in addition to a representation of the pressure, Lagrange multipliers used to satisfy those additional boundary conditions and constraints.

The DAE (9.1) is an approximation to the Navier-Stokes equations, and the accuracy of that approximation is determined by the discretization that was used to obtain (9.1). In this work, we address only the issue of solving the approximate equations (9.1). Thus when we speak of a "solution," we mean a solution of the approximate equations (9.1), not of the original problem.

If we are interested in steady state solutions, we want to solve the $n + m$ nonlinear parameter-dependent algebraic equations obtained by setting the time derivative in (9.1) to zero. An excellent method for solving such parameter-dependent equations is Keller's continuation algorithm [14]. This is a predictor-corrector scheme. Knowing a solution at some parameter value λ_0, one changes the value of the parameter slightly. The predictor is then used to estimate the solution at the new parameter value, and the corrector is typically an iterative method which is used to converge to the new solution. For example, in Euler-Newton continuation, the predictor estimates the new solution by using the tangent (or an approximation of the tangent) of the old solution; then Newton's method is used as the corrector.

Euler-Newton continuation is a robust method, but Newton's method requires the solution of linear systems at each step. If the number of equations is large, the solution of these linear systems may be quite expensive. This

may limit the size of the problem we can solve in reasonable time, and hence the accuracy of the approximation (9.1) we can achieve.

The Recursive Projection Method (RPM) [16] provides an alternative to Newton's method as the corrector. We assume that the reader is familiar with RPM as presented in [16]. For convenience, the results of [16] relevant to our work are summarized in Appendix A. RPM is a stabilization method for fixed point iterations. When a fixed point iteration is not contracting, RPM provides a way to obtain a modified hybrid iteration which is contracting. One application of this is "RPM continuation" (see [16] and Appendix A). In this case, the fixed point iteration may represent a numerical time integration over some small time interval of a parameter-dependent ordinary differential equation (ODE)

$$\frac{d\mathbf{v}}{dt} = \mathbf{F}(\mathbf{v}, \lambda). \tag{9.2}$$

Such a time integration may or may not converge to a steady state

$$\mathbf{F}(\mathbf{v}, \lambda) = \mathbf{0}.$$

The time integration may diverge for a variety of reasons, but most commonly because the steady state is unstable or because the time step size is too large. RPM can be used to restore convergence, and also to accelerate convergence when the original time integration converges. The resulting hybrid iteration is used as the continuation corrector instead of Newton's method.

For many problems, RPM continuation performs better than the Euler-Newton method. However, the continuation method as presented in [16] is restricted to dynamical systems in the ODE form (9.2). In order to use RPM

to solve (9.1), we reformulate the DAE (9.1) as an ODE (9.2), to which RPM can be applied.

The resulting method applies to all DAEs of the form (9.1), but we will give special consideration to MOL-discretizations of the incompressible Navier-Stokes equations. In that special case, the algebraic constraint (9.1b) is linear, and the vector $\mathbf{p}$ enters into (9.1a) only linearly. We shall take advantage of this property to specialize the method for MOL-discretizations of the Navier-Stokes equations.

Finally, we employ our new method to compute steady state and solutions of the incompressible flow between two concentric, rotating cylinders. Our implementation is also capable of computing branches of travelling wave solutions. We compare our results to past investigations and show that RPM is an efficient procedure for computing solutions of such problems.

Chapter 10

Applying RPM to DAEs

In order to apply RPM to solve a DAE (9.1), we would like to reformulate the problem as an ODE.

10.1 Nonsingularity of DAEs

Not all DAEs (9.1) can be reformulated as ODEs (9.2). To ensure that this reformulation is possible, we assume that the DAE (9.1) is "nonsingular." That is, we assume that the m-by-m matrix $\mathbf{g_u}(\mathbf{u}^0)\mathbf{f_p}(\mathbf{u}^0, \mathbf{p}^0; \lambda^0)$ is nonsingular for any "consistent" initial value $(\mathbf{u}^0, \mathbf{p}^0; \lambda^0)$. We say that an initial condition $(\mathbf{u}^0, \mathbf{p}^0; \lambda^0)$ is consistent if

$$\mathbf{g}(\mathbf{u}^0) = \mathbf{0}, \tag{10.1a}$$

$$\mathbf{g}_\mathbf{u}^0\mathbf{f}^0 = \mathbf{0}. \tag{10.1b}$$

Here, superscript "0" represents evaluation at the initial value. The first

condition (10.1a) just states that u^0 is a solution of the algebraic equations (9.1b). The second condition (10.1b) is required to ensure the existence of a differentiable solution trajectory $(\mathrm{u}(t), \mathrm{p}(t))$ near the parameter value $\lambda = \lambda^0$ through the initial condition, since any such trajectory must satisfy, for all t:

$$0 = \frac{d\mathrm{g}(\mathrm{u}(t))}{dt} = \mathrm{g_u}(\mathrm{u}(t))\frac{d\mathrm{u}(t)}{dt} = \mathrm{g_u}(\mathrm{u}(t))\mathrm{f}(\mathrm{u}(t), \mathrm{p}(t); \lambda^0). \tag{10.2}$$

Now consider the initial value problem composed of (9.1) and a consistent initial condition

$$\mathrm{u} = \mathrm{u}^0 \text{ and } \mathrm{p} = \mathrm{p}^0 \text{ at } t = t^0, \tag{10.3}$$

with $\lambda = \lambda^0$ fixed. It is a well known result that, if the DAE (9.1) is nonsingular according to the above assumption, a unique differentiable solution trajectory $(\mathrm{u}(t), \mathrm{p}(t))$ exists for the initial value problem (9.1),(10.3) [19].

From here on, we assume that the DAE (9.1) we intend to solve is nonsingular.

10.2 From DAEs to ODEs

Each point on a solution trajectory of a nonsingular DAE (9.1) must be a consistent initial value, and therefore satisfy the conditions (10.1). So we need not look for solutions which are arbitrary vectors $(\mathbf{u}, \mathrm{p})^T \in \mathbb{R}^{n+m}$. Rather, only vectors satisfying

$$\mathrm{g}(\mathrm{u}) = 0, \tag{10.4a}$$

$$\mathrm{g_u(u)f(u,p;\lambda)} = \mathbf{0}, \tag{10.4b}$$

are potential solutions. The system (10.4) is a set of $2m$ independent equations, in the sense that the Jacobian

$$J(\mathrm{u,p};\lambda) \equiv \begin{pmatrix} \mathrm{g_u} & 0 \\ \mathrm{g_{uu}f} + \mathrm{g_u f_u} & \mathrm{g_u f_p} \end{pmatrix}$$

always has full rank by the assumption that the DAE is nonsingular. Thus we expect that solution vectors $(\mathbf{u},\mathbf{p})^T$ must lie in a subspace of $\mathbb{R}^{n+m}$ of dimension $n+m-2m = n-m$.

Suppose we are given a consistent initial value (10.3). We can apply the implicit function theorem to solve (10.4b) for $\mathbf{p} = \mathbf{P}(\mathbf{u};\lambda)$ in a neighborhood of that initial value. An interpretation of this is that the vector $\mathbf{p}$ acts purely as a Langrange multiplier. While $\mathbf{u}$ changes according to the differential equation (9.1a), $\mathbf{p}$ takes on whatever value it must in order to keep the constraint (9.1b) satisfied.

With $\mathbf{p} = \mathbf{P}(\mathbf{u};\lambda)$, the constraint (9.1b) will always be satisfied, and an equivalent formulation of (9.1) is the following ODE in n variables:

$$\frac{d\mathbf{u}}{dt} = \mathbf{f}(\mathbf{u},\mathbf{P}(\mathbf{u};\lambda);\lambda). \tag{10.5}$$

However, we note that a further reduction is possible. The constraint (9.1b) defines, locally, an $(n-m)$-dimensional subspace of $\mathbb{R}^n$. All vectors $\mathbf{u}$ in that $(n-m)$-dimensional subspace can be parametrized by $n-m$ parameters, $\boldsymbol{\alpha} \in \mathbb{R}^{n-m}$. Having introduced $n-m$ new variables, we may introduce $n-m$ new equations which serve to define the new vector $\boldsymbol{\alpha}$:

$$\mathbf{N}(\mathbf{u},\boldsymbol{\alpha}) = \mathbf{0}. \tag{10.6}$$

We assume that (10.6) is chosen such that the following assumptions are satisfied:

- $\mathbf{N}(\mathbf{u}^0, \boldsymbol{\alpha}^0) = \mathbf{0}$ for some $\boldsymbol{\alpha}^0 \in \mathbb{R}^{n-m}$;
- $\mathbf{N}_{\boldsymbol{\alpha}}^0 \in \mathbb{R}^{(n-m)\times(n-m)}$ is nonsingular;
- $\begin{pmatrix} \mathbf{g}_{\mathrm{u}}^0 \\ \mathbf{N}_{\mathrm{u}}^0 \end{pmatrix} \in \mathbb{R}^{n\times n}$ is nonsingular.

Now consider the system of n equations composed of (9.1b) and (10.6). By the implicit function theorem, there exists a unique function $\mathbf{u} = \mathbf{U}(\boldsymbol{\alpha})$ such that $\mathbf{u}^0 = \mathbf{U}(\boldsymbol{\alpha}^0)$ and both (9.1b) and (10.6) are satisfied. This representation is valid in a neighborhood of the initial value.

Since $\mathbf{p} = \mathbf{P}(\mathbf{u}; \lambda) = \mathbf{P}(\mathbf{U}(\boldsymbol{\alpha}); \lambda)$, all solutions of the DAE initial value problem (9.1),(10.3) can be parametrized by the $n - m$ parameters $\boldsymbol{\alpha}$, in a neighborhood of the initial value. The vector $\boldsymbol{\alpha}$ satisfies the differential equation obtained by differentiating (10.6) with respect to t:

$$\mathbf{N}_{\mathrm{u}} \frac{d\mathbf{u}}{dt} + \mathbf{N}_{\boldsymbol{\alpha}} \frac{d\boldsymbol{\alpha}}{dt} = \mathbf{0}. \tag{10.7}$$

By substituting (10.5) and $\mathbf{u} = \mathbf{U}(\boldsymbol{\alpha})$, we obtain an ordinary differential equation for $\boldsymbol{\alpha}$:

$$\mathbf{N}_{\boldsymbol{\alpha}} \frac{d\boldsymbol{\alpha}}{dt} = -\mathbf{N}_{\mathrm{u}} \mathbf{f}(\mathbf{U}(\boldsymbol{\alpha}), \mathbf{P}(\mathbf{U}(\boldsymbol{\alpha}); \lambda); \lambda), \tag{10.8}$$

which is equivalent to

$$\frac{d\boldsymbol{\alpha}}{dt} = -\mathbf{N}_{\boldsymbol{\alpha}}^{-1} \mathbf{N}_{\mathrm{u}} \mathbf{f}(\mathbf{U}(\boldsymbol{\alpha}), \mathbf{P}(\mathbf{U}(\boldsymbol{\alpha}); \lambda); \lambda) \equiv \mathbf{F}(\boldsymbol{\alpha}, \lambda) \tag{10.9}$$

as long as $\mathbf{N}_{\boldsymbol{\alpha}}$ remains nonsingular.

Now, in a neighborhood of an initial value, $\boldsymbol{\alpha}(t)$ is a solution of (10.9) if and only if $\mathbf{u} = \mathbf{U}(\boldsymbol{\alpha}(t)), \mathbf{p} = \mathbf{P}(\mathbf{U}(\boldsymbol{\alpha}(t)))$ is a solution of (9.1). In particular, steady state solutions of (10.9) correspond to steady state solutions of (9.1).

10.3 Applying RPM Continuation

We are now in a position to use RPM to find the steady state solutions of (9.1) we seek. We simply apply the method to find steady states of the ODE (10.9). Thus our continuation corrector will be a time integration of (10.9), accelerated by RPM.

10.3.1 Choosing a Time Integration Method

In order to make the method most efficient, an explicit time integration method, such as Runge-Kutta, should be used. Implicit methods require the solution of large linear systems, which is precisely what we want to avoid. The best choice of time integration method depends, of course, on the application.

A major disadvantage of explicit time integration methods is that, if the ODE (10.9) is stiff, a small step size may be necessary to avoid numerical instability. For example, when the DAE (9.1) represents a discretization of a partial differential equation, the step size may be limited by a Courant condition. However, RPM can remedy this problem. If we take time steps which are too large and violate a numerical stability condition, then one or a

few of the most negative eigenvalues of $\mathbf{F}_{\boldsymbol{\alpha}}$ will cause the time iteration to be unstable. RPM will treat this numerical instability just as if it were a "real" one caused by the underlying problem, and stabilize it. Of course, if the number of offending eigenvalues is too large, then the method will no longer be efficient. But it *is* possible to take time steps bigger than allowed by the Courant condition and still converge to the steady state, because RPM can treat numerical instabilities as well as real ones.

10.3.2 Choosing a Parametrization

There are many allowable choices for the parameters $\boldsymbol{\alpha}$ and the constraint (10.6) which we introduce. This choice should be made to make the evaluation of the right hand side $\mathbf{F}(\boldsymbol{\alpha}, \lambda)$ as inexpensive as possible.

One possible choice is to relate $\mathbf{u}$ to a basis for the nullspace of $\mathrm{g}_{\mathrm{u}}^0$. Suppose we have a matrix $Q \in \mathbb{R}^{n\times(n-m)}$ whose columns span the nullspace of $\mathrm{g}_{\mathrm{u}}^0$. Then an allowable constraint (10.6) is

$$\mathbf{N}(\mathbf{u}, \boldsymbol{\alpha}) \equiv \boldsymbol{\alpha} - Q^T\mathbf{u} = \mathbf{0}. \tag{10.10}$$

In the special case that the nullspace of g_{u} is constant and if Q is orthogonal, we obtain

$$\mathrm{u} = \mathbf{U}(\boldsymbol{\alpha}) = Q\boldsymbol{\alpha} + \mathrm{k},$$

where $\mathrm{k} \in \mathbb{R}^n$ is the projection of u^0 onto $\mathbb{R}^n \backslash \mathcal{N}(\mathrm{g}_{\mathrm{u}}^0)$ and is given by

$$\mathrm{k} = (I - QQ^T)\mathrm{u}^0.$$

Another approach is to choose for the parameters $\boldsymbol{\alpha}$ a subset of the components of $\mathbf{u}$. If we know $n - m$ independent components of $\mathbf{u}$, we can determine the rest from (9.1b). In this case, we use a constraint (10.6) of the form

$$\mathrm{N}(\mathbf{u}, \boldsymbol{\alpha}) \equiv \boldsymbol{\alpha} - (I_{n-m}, 0_m)\, P\mathbf{u} = \mathbf{0}, \tag{10.11}$$

where $P \in \mathbb{R}^{n\times n}$ is a permutation matrix. Clearly, P can be chosen so that (10.11) satisfies the required assumptions.

We emphasize that the validity of any specific parametrization defined by (10.6) is only local, to the extent of the validity of the implicit function theorem. If, during the course of time integration or continuation, we leave the domain of validity of the parametrization, we may need to update the definition of our parameters.

10.4 Application to Incompressible Fluid Mechanics

We are especially concerned with DAEs (9.1) which are discrete (MOL) approximations of the incompressible Navier-Stokes equations. Such DAEs have the special form

$$\frac{d\mathbf{u}}{dt} = \mathrm{f}(\mathbf{u}, \mathrm{p}; \lambda) = \mathrm{h}(\mathbf{u}; \lambda) - G\mathrm{p}, \tag{10.12a}$$

$$\mathbf{0} = \mathrm{g}(\mathbf{u}) = D\mathbf{u}, \tag{10.12b}$$

where $G \in \mathbb{R}^{n\times m}$ and $D \in \mathbb{R}^{m\times n}$ are related to discrete versions of the gradient and divergence operators, respectively.

We assume that both D and G have full rank. That is, any redundant equations and variables have been eliminated. In practice, this means that:

- The indeterminacy of the pressure has been eliminated. That is, for example, an equation has been added to fix the pressure at one point, or the average of the pressure.
- One equation of the discretization of the continuity equation has been eliminated. Discretizations of the divergence operator generally have a one-dimesional left nullspace, so that one of the rows of the matrix is a linear combination of the others. The corresponding equation is redundant and can be eliminated.

For the special form (10.12), the condition (10.4b) reads

$$D\,[\mathbf{h}(\mathbf{u};\lambda) - G\mathbf{p}] = \mathbf{0}. \tag{10.13}$$

We thus have the linear equation

$$DG\mathbf{p} = D\mathbf{h}(\mathbf{u};\lambda) \tag{10.14}$$

which determines $\mathbf{p} = \mathbf{P}(\mathbf{u})$. The matrix $DG \in \mathbb{R}^{m\times m}$ is nonsingular by the assumption that the DAE is nonsingular. Equation (10.14) is a discrete version of the familiar Poisson equation for the pressure. The advantage of the special form (10.12) is that the validity of the representations $\mathbf{u} = \mathbf{U}(\boldsymbol{\alpha})$ and $\mathbf{p} = \mathbf{P}(\mathbf{u})$ is global.

Chapter 11

Application to Taylor-Couette Flow

The incompressible flow of a viscous fluid between two concentric rotating cylinders has been the subject of investigation since as early as 1890, when Couette [6] used such a setup to measure the viscosities of fluids. The existence of two flow regimes, laminar and tubulent, was known to Couette and he noted that viscosity measurements could only be performed in the laminar flow regime. Since then, many theoretical, experimental and computational studies have been conducted. For an excellent description of the history of these investigations, we refer the reader to [17].

Our primary goal in this investigation is to use the Taylor-Couette problem as a testing ground and example of the method in Chapter 10. A secondary goal is to develop a computer code based on our new method, which will later be used to obtain new understanding of the physical flow.

11.1 Problem Formulation

The flow configuration is described by the following physical quantities:

$$\begin{aligned} R_{inner} &= \text{radius of inner cylinder;} \\ R_{outer} &= \text{radius of outer cylinder;} \\ \omega_{inner} &= \text{angular velocity of inner cylinder;} \\ \omega_{outer} &= \text{angular velocity of outer cylinder;} \\ h &= \text{height of the cylinders;} \\ \nu &= \text{kinematic viscosity of the fluid.} \end{aligned}$$

In this study, we restrict ourselves to the infintely long cylinder case. That is, we assume that the ratio $h/(R_{outer} - R_{inner})$ is so large that end effects are negligible. So we assume the flow to be periodic in the axial direction with a wavelength L.

The flow is governed by the Navier-Stokes equations. In nondimensionalized form and cylindrical coordinates, they read:

$$\frac{\partial \vec{u}}{\partial t} = \vec{f}(\vec{u}; Re) - \nabla p, \tag{11.1a}$$

$$0 = \nabla \cdot \vec{u} = u_r + \frac{u}{r} + \frac{v_\theta}{r} + w_z, \tag{11.1b}$$

where $\vec{f}(\vec{u}; Re) = (f(\vec{u}; Re), g(\vec{u}; Re), h(\vec{u}; Re))^T$ with

$$f(\vec{u}; Re) = \frac{1}{Re}\left(\nabla^2 u - \frac{u}{r^2} - 2\frac{v_\theta}{r^2}\right) - \frac{u^2 - v^2}{r} - (u^2 + p)_r - \frac{(uv)_\theta}{r} - (uw)_z,$$

$$g(\vec{u}; Re) = \frac{1}{Re}\left(\nabla^2 v + 2\frac{u_\theta}{r^2} - \frac{v}{r^2}\right) - 2\frac{uv}{r} - (uv)_r - \frac{(v^2 + p)_\theta}{r} - (vw)_z,$$

$$h(\vec{u}; Re) = -\frac{uw}{r} - (uw)_r - \frac{(vw)_\theta}{r} - (w^2 + p)_z.$$

Here, ∇^2 represents the Lapacian operator

$$\nabla^2 = \frac{\partial^2}{\partial r^2} + \frac{1}{r}\frac{\partial}{\partial r} + \frac{1}{r^2}\frac{\partial^2}{\partial \theta^2} + \frac{\partial^2}{\partial z^2},$$

∇ is the gradient operator

$$\nabla = \left(\frac{\partial}{\partial r}, \frac{1}{r}\frac{\partial}{\partial \theta}, \frac{\partial}{\partial z}\right)^T,$$

$\vec{u} = (u, v, w)^T$ stands for the (scaled) velocity field, and

$$\begin{aligned} u(r, \theta, z) &= \text{velocity in the radial direction, } r, \\ v(r, \theta, z) &= \text{velocity in the azimuthal direction, } \theta, \\ w(r, \theta, z) &= \text{velocity in the axial direction, } z, \\ p(r, \theta, z) &= \text{pressure.} \end{aligned}$$

The domain of these equations is

$$\begin{gathered} R_1 \equiv \frac{\eta}{1-\eta} \le r \le \frac{1}{1-\eta} \equiv R_2, \\ 0 \le z \le \Gamma, \\ 0 \le \theta \le \frac{2\pi}{q}, \end{gathered}$$

where the integer q limits the wavelength in the θ-direction. Here we have introduced the Reynolds number

$$Re = \frac{R_{inner}\omega_{inner}(R_{outer} - R_{inner})}{\nu},$$

the aspect ratio of period to gap width

$$\Gamma = \frac{L}{R_{outer} - R_{inner}},$$

and the radius ratio

$$\eta = \frac{R_{inner}}{R_{outer}}.$$

We have scaled distances so that $R_2 - R_1 = 1$. Velocities are scaled by the tangential velocity of the inner cylinder. So the scaled angular velocity of the inner cylinder is

$$\omega_1 = \frac{1}{R_1} = \frac{1-\eta}{\eta}.$$

The scaled anlgular velocity of the outer cylinder is

$$\omega_2 = \frac{\omega}{R_2} = \omega(1-\eta),$$

where we have defined the ratio of tangential velocities of the two cylinders

$$\omega = \frac{\omega_{outer} R_{outer}}{\omega_{inner} R_{inner}} = \frac{\omega_2 R_2}{\omega_1 R_1} = \omega_2 R_2.$$

The problem is thus completely specified by the four parameters Re, η, Γ, and ω.

There has been excellent agreement between experimental and theoretical work, so that the Navier-Stokes equations appear to provide a good model for the physical behavior of the fluid.

For low Reynolds numbers Re, one observes a laminar solution, called Couette flow, which depends only on the radius. When Re is increased beyond a critical value Re_c, axisymmetric Taylor vortices appear. If Re is increased further, wavy Taylor vortices are observed. This wavy Taylor vortex solution is periodic in time and has the form of a travelling wave with one specific azimuthal frequency. At even higher Reynolds numbers, so-called modulated Taylor vortices, which have more than one characteristic frequency, occur. An important observation by Coles [5] was that wavy

Taylor vortex solutions are not unique: several "states" (characterized by the azimuthal and axial wavelengths) are possible for the same Reynolds numbers. Coles found that if one slowly increases or decreases the Reynolds number, transitions from one state to another take place abrubtly, discontinuously, and irreversibly. Futhermore, the transitions take place at repeatable Reynolds numbers.

Many numerical investigations of this problem have been conducted to determine the critical Reynolds numbers at which the first two transitions (to and from axisymmetric Taylor vortices) take place. However, the bifurcation to modulated wavy Taylor vortices has never been found computationally. It is our hope that RPM, used as described in Chapter 10, will help us find such a bifurcation.

11.2 Rotating Coordinate System

Wavy Taylor vortices are not steady flows and so they are not steady state solutions of (11.1). Rather, they are periodic solutions. However, it has been experimentally shown and computationally verified that these solutions have the form of travelling waves in the azimuthal direction. That is, the solution depends on θ and t only in the combination $\varphi = \theta - \Omega_0 t$. Wavy Taylor vortices are thus steady flows in a moving coordinate system which rotates in the θ direction with angular velocity Ω_0.

In order to represent wavy Taylor vortices as steady flows, we will thus introduce such a rotating coordinate system with angular velocity $\Omega(t)$. The

angular velocity of the coordinate system depends on the time t because we use a time integration procedure to compute the steady state. At a steady state in the rotating system (or a travelling wave in the nonrotating system), we have $\Omega(t) = \Omega_0 = constant$.

The azimuthal coordinate in the rotating frame of reference is

$$\varphi = \theta - \int^t \Omega(\tau)\, d\tau$$

so that $\partial/\partial\varphi = \partial/\partial\theta$. In the new coordinate system, the equations of motion (11.1) become

$$\frac{\partial \vec{u}}{\partial t} = \vec{f}(\vec{u}; Re) - \nabla p + \Omega(t)\frac{\partial \vec{u}}{\partial \theta}. \tag{11.2a}$$

$$0 = \nabla \cdot \vec{u}. \tag{11.2b}$$

For nonrotating flows which are steady state solutions in the original stationary frame of reference, we can use the formulation (11.2) with $\Omega(t) = 0$.

Since we have introduced an unknown rotation speed $\Omega(t)$, solutions of (11.2) are indeterminate in the sense that the azimuthal phase of such solutions is unknown. We can impose a scalar constraint to remove the indeterminacy and fix the phase of solutions. We use a constraint due to Doedel [9] which minimizes the change in phase as the solution changes with the time t. That is, we want to minimize with respect to Ω the function

$$H(\vec{u}, p, \Omega) \equiv \left\langle \frac{\partial \vec{u}}{\partial t}, \frac{\partial \vec{u}}{\partial t} \right\rangle,$$

where we use the notation

$$\left\langle \vec{\psi}_1(r,\theta,z), \vec{\psi}_2(r,\theta,z) \right\rangle \equiv \int_0^{\Gamma} \int_0^{2\pi/q} \int_{R_1}^{R_2} (\vec{\psi}_1)^T \vec{\psi}_2 \; r\, dr\, d\theta\, dz.$$

Using a simple variational argument, one obtains that the minimum occurs when

$$\Omega\langle\vec{u}_\theta, \vec{u}_\theta\rangle + \langle\vec{f} - \nabla p, \vec{u}_\theta\rangle = 0. \tag{11.3}$$

The rotation velocity Ω is therefore given by the formula

$$\Omega = -\frac{\langle\vec{f} - \nabla p, \vec{u}_\theta\rangle}{\langle\vec{u}_\theta, \vec{u}_\theta\rangle} \tag{11.4}$$

as long as $\vec{u}$ has some variation with θ. If $\vec{u}$ has no dependence on θ, then the flow is axisymmetric and the frame of reference is irrelevant, as all choices for Ω yield the same representation of the solution. In this case, both the numerator and the denominator in (11.4) are zero, and the rotation velocity Ω is arbitrary.

11.3 Boundary Conditions

In order to complete the specification of the problem, the following boundary conditions are used. In the axial and azimuthal directions, we impose periodicity, consistent with the geometry of the cylinders and the infintely long cylinder assumption. Thus, we have for all (r, θ, z) in the domain:

$$\vec{u}\left(r, \frac{2\pi}{q}, z\right) = \vec{u}\,(r, 0, z)\,, \tag{11.5a}$$

$$p\left(r, \frac{2\pi}{q}, z\right) = p\,(r, 0, z)\,, \tag{11.5b}$$

$$\vec{u}\,(r, \theta, \Gamma) = \vec{u}\,(r, \theta, 0)\,, \tag{11.5c}$$

$$p(r,\theta,\Gamma) = p(r,\theta,0). \tag{11.5d}$$

On the cylinder surfaces, we impose no-slip conditions. Following [28], we also use Neumann conditions on the pressure. The conditions on the inner cylinder, $r = R_1$, $\theta \in [0, 2\pi/q]$ and $z \in [0, \Gamma]$, then are

$$u(R_1,\theta,z) = w(R_1,\theta,z) = 0, \tag{11.6a}$$

$$v(R_1,\theta,z) = 1, \tag{11.6b}$$

$$p_r(R_1,\theta,z) = \frac{1}{R_1} + \frac{1}{Re}u_{rr} = \frac{1-\eta}{\eta} + \frac{1}{Re}u_{rr}. \tag{11.6c}$$

On the outer cylinder, $r = R_2$, $\theta \in [0, 2\pi/q]$ and $z \in [0, \Gamma]$, we have

$$u(R_2,\theta,z) = w(R_2,\theta,z) = 0, \tag{11.7a}$$

$$v(R_2,\theta,z) = \omega_2 R_2 = \omega, \tag{11.7b}$$

$$p_r(R_2,\theta,z) = \omega_2^2 R_2 + \frac{1}{Re}u_{rr} = \omega^2(1-\eta) + \frac{1}{Re}u_{rr}. \tag{11.7c}$$

In the pressure conditions, we have used that, on the cylinder surfaces, $u_r = 0$ due to the continuity equation (11.1b).

11.4 Discretization

We apply the method of lines to Equation (11.2) and the boundary conditions (11.5),(11.6) and (11.7) to obtain a DAE of the form (10.12). In order to accomplish this, we approximate all spatial derivatives by finite differences on a uniform grid with grid spacings

$$\Delta r = \frac{1}{n_r}, \tag{11.8a}$$

$$\Delta\theta = \frac{2\pi}{qn_\theta}, \tag{11.8b}$$

$$\Delta z = \frac{\Gamma}{n_z}, \tag{11.8c}$$

for some positive integers n_r, n_θ, n_z. The grid points are located at the points

$$r_j = R_1 + j\Delta r, \quad (j = 0, 1, \ldots, n_r);$$

$$\theta_k = k\Delta\theta, \quad (k = 0, 1, \ldots, n_\theta - 1);$$

$$z_l = l\Delta z, \quad (l = 0, 1, \ldots, n_z - 1).$$

We shall use subscript notation to indicate evaluation at one of these grid points. For example, we denote the velocity field at the grid point (r_j, θ_k, z_l) by $\vec{u}_{jkl} = (u_{jkl}, v_{jkl}, w_{jkl})^T$ and the pressure by p_{jkl}. We call the grid points with $j \in \{0, n_r\}$ *interior* grid points and the rest *boundary* grid points. There are $n_i \equiv (n_r - 1)n_\theta n_z$ interior grid points and $n_b \equiv 2n_\theta n_z$ boundary grid points.

All derivatives are approximated by differences of second order accuracy. In the interior, that is when $j \neq 0$ and $j \neq n_r$, we use centered differences. So, for example,

$$\left(\frac{\partial u}{\partial r}\right)_{jkl} \approx \frac{u_{j+1,kl} - u_{j-1,kl}}{2\Delta r},$$

$$\left(\frac{\partial^2 u}{\partial r^2}\right)_{jkl} \approx \frac{u_{j+1,kl} - 2u_{jkl} + u_{j-1,kl}}{(\Delta r)^2}.$$

At the cylinder surfaces, $j \in \{0, n_r\}$, one-sided differences are used. Thus, for example, for the pressure Neumann condition (11.6c) at the inner cylinder, we use

$$\left(\frac{\partial p}{\partial r}\right)_{0,kl} \approx \frac{-3p_{0,kl} + 4p_{1,kl} - p_{2,kl}}{2\Delta r},$$

$$\left(\frac{\partial^2 u}{\partial r^2}\right)_{0,kl} \approx \frac{2u_{0,kl} - 5u_{1,kl} + 4u_{2,kl} - u_{3,kl}}{(\Delta r)^2}.$$

In order to eliminate the indeterminacy in the pressure, we add the condition that, at $r = r_0 = R_1$, the average over the θ and z variables of the pressure is zero:

$$\sum_{k=0}^{n_\theta - 1} \sum_{l=0}^{n_z - 1} p_{0,kl} = 0. \tag{11.9}$$

Together with the Neumann conditions on the pressure (11.6c) and (11.7c), we now have n_b independent boundary conditions for the pressure.

The full MOL-discretized system of equations is thus composed of

- a discretized version of (11.2) at each interior grid point. This accounts for $4n_i$ independent equations.
- Equation (11.9) to fix the indeterminacy of the pressure.
- Equation (11.3) to fix the θ-phase of solutions.
- the boundary conditions (11.6) at each grid point with $j = 0$. This accounts for $4n_b$ equations.
- the boundary conditions (11.7) at each grid point with $j = n_r$. This accounts for $4n_b$ equations.

The periodic boundary conditions (11.5) are not included here because they have been incorporated into the discretization of (11.2). We thus have a total of $4(n_i + 2n_b) + 2$ equations. Only $4(n_i + 2n_b) + 1$ of these equations are independent because the $4n_b + 1$ equations (11.9), (11.6c), and (11.7c) constitute only $4n_b$ independent boundary conditions.

The unknowns are the values of $\vec{u}_{jkl}$ and p_{jkl} at each of the $n_i + n_b$ grid points, and the rotation speed Ω. We thus have a total of $4(n_i + 2n_b) + 1$ unknowns, the same as the number of independent equations.

In order to obtain a DAE of the form (10.12), we eliminate the rotation velocity Ω using (11.4) and the boundary values of $\vec{u}$ and p using (11.9) and the boundary conditions (11.6) and (11.7). The resulting system has $4n_i$ equations and unknowns, which are the values of $\vec{u}$ and p at the interior grid points. It is a DAE of the form (10.12) with $n = 3n_i$ and $m = n_i$. The vector $\mathbf{u}$ contains the interior components $\vec{u}_{jkl}$ and the vector $\mathbf{p}$ contains the interior components p_{jkl}. Specifically, $\mathbf{u} = (\mathbf{u_1}^T, \mathbf{u_2}^T, \mathbf{u_3}^T)^T$ with

$$\mathbf{u_1} \equiv (u_{100}, u_{101}, \ldots, u_{10,n_z-1}, u_{110}, \ldots, u_{1,n_\theta-1,n_z-1}, u_{200}, \ldots, u_{n_r-1,n_\theta-1,n_z-1})^T$$

$$\mathbf{u_2} \equiv (v_{100}, \ldots, v_{n_r-1,n_\theta-1,n_z-1})^T$$

$$\mathbf{u_3} \equiv (w_{100}, \ldots, w_{n_r-1,n_\theta-1,n_z-1})^T$$

and

$$\mathbf{p} \equiv (p_{100}, \ldots, p_{n_r-1,n_\theta-1,n_z-1})^T .$$

11.5 ODE Formulation

In order to apply RPM to solve our discrete equations, we must introduce a new parametrization and a constraint (10.6). The number of equations in the new constraint, and the number of new parameters, must be $n - m = 2n_i$.

We use a constraint of the form (10.11). To be specific, we use as the parameters $\boldsymbol{\alpha}$ the $2n_i$ components of $\mathbf{u_2}$ and $\mathbf{u_3}$. The corresponding constraint

(10.6) is

$$\mathbf{N}(\mathbf{u}, \boldsymbol{\alpha}) \equiv \boldsymbol{\alpha} - (0_{2n_i \times n_i}, I_{2n_i})\,\mathbf{u} = \mathbf{0}. \tag{11.10}$$

This constraint satisfies all the requirements in Section 10.2 for any consistent initial condition $(\mathbf{u}^0, \mathbf{p}^0; Re)$ and when n_r is odd. As we shall see, the centered difference discretization we use has properties which differ significantly depending on the parity of n_r. When n_r is even, the parameters $\boldsymbol{\alpha}$ must be chosen differently, but the overall method can still be applied.

With the aid of (11.10), we obtain an ODE formulation (10.9) (with $\lambda = Re$) of the DAE (10.12) corresponding to our discretization. Thus we are left with a dynamical system of the form

$$\frac{d\boldsymbol{\alpha}}{dt} = \mathbf{F}(\boldsymbol{\alpha}, \lambda).$$

11.6 Time Integration

We wish to find steady state solutions of the ODE (10.9). These steady state solutions will correspond to second order approximations of steady state solutions of (11.2), which may be travelling wave solutions of (11.1). In accordance with the RPM continuation method described in [16], we wish to integrate the ODE (10.9) for large times t, using RPM to accelerate and stabilize the convergence.

In order to avoid solving large linear systems, we use an explicit time stepping method. Specifically, we use the fourth order Runge-Kutta method with automatic step size control.

11.6.1 Switching Between DAE and ODE Variables

In evaluating the right hand side of (10.9), we must evaluate the functions $\mathbf{U}(\boldsymbol{\alpha})$ and $\mathbf{P}(\mathbf{U}(\boldsymbol{\alpha}))$. The evaluation of $\mathbf{U}(\boldsymbol{\alpha})$ is straighforward due to the simple form of the constraint (11.10).

We split the matrix D in (10.12b) into two parts so that

$$D = (D_1, D_2)$$

with $D_1 \in \mathbb{R}^{m \times n_i}$ and $D_2 \in \mathbb{R}^{m \times 2n_i}$. Similarly, we split the function $\mathbf{U}(\boldsymbol{\alpha})$ into two components:

$$\mathbf{U}(\boldsymbol{\alpha}) \equiv \begin{pmatrix} \mathbf{U}_1(\boldsymbol{\alpha}) \\ \mathbf{U}_2(\boldsymbol{\alpha}) \end{pmatrix},$$

where $\mathbf{U}_1(\boldsymbol{\alpha}) \in \mathbb{R}^{n_i}$ and $\mathbf{U}_2(\boldsymbol{\alpha}) \in \mathbb{R}^{2n_i}$. Now we have from the constraint (11.10) that

$$\begin{pmatrix} u_2 \\ u_3 \end{pmatrix} = \mathbf{U}_2(\boldsymbol{\alpha}) = \boldsymbol{\alpha}. \tag{11.11}$$

Using this result in (10.12b), one obtains the linear system

$$D_1 \mathbf{u}_1 = D_1 \mathbf{U}_1(\boldsymbol{\alpha}) = -D_2 \mathbf{U}_2(\boldsymbol{\alpha}) = -D_2 \boldsymbol{\alpha} \tag{11.12}$$

for the components of $\mathbf{U}_1(\boldsymbol{\alpha})$. In conjunction with the boundary conditions (11.6a) and (11.7a), we can solve (11.12) for those components.

The importance of the parity of n_r is now evident. The matrix D_1 is essentially a centered difference approximation of $(\partial/\partial r)$. This approximation has the property that D_1 is nonsingular if n_r is odd and singular when n_r is

even. (This can be shown using induction.) Therefore, when n_r is even, a different constraint (10.6) must be used.

This phenomenon does not cause instability in our computations when n_r is odd. That is, we do not detect any high frequency oscillations in the r-direction. However,

$$\det D_1 \to 0 \text{ as } n_r \to \infty, n_r \text{ odd},$$

so that D_1 becomes more and more ill-conditioned as n_r increases. Thus, our choice of parameters $\boldsymbol{\alpha}$ is not expected to yield good numerical results for very fine grids. A better choice of the constraint (10.6) is needed for fine grids. Besides changing the choice of parameters, we can also avoid this problem by changing the discretization of the continuity equation (11.2b). For example, a first order finite difference approximation can be used for the r-derivatives of u. Then we solve (11.12) using only *one* of the boundary conditions (11.6a) at $r = R_1$ or (11.7a) at $r = R_2$. The other condition will still be enforced when we solve for $\mathbf{p} = \mathbf{P}(\mathbf{u})$ as in (10.14). One might consider a method in which one boundary condition is enforced at odd time steps, and the other at even time steps.

The structure of the matrix D_1 is block diagonal, each (n_r-1)-by-(n_r-1) block along the diagonal is tridiagonal, and all blocks are the same. Therefore, the evaluation of $\mathbf{U}(\boldsymbol{\alpha})$ requires the solution of $n_\theta n_z$ tridiagonal linear systems, each with the same matrix of order $n_r - 1$.

11.6.2 Computing the Pressure

The function $\mathbf{P}(\mathbf{u})$ is the projection of a vector $\mathbf{u}$ onto the subspace of $\mathbb{R}^n$ defined by $D\mathbf{u} = \mathbf{0}$. In order to determine $\mathbf{P}(\mathbf{u})$, we solve the linear system (10.14). This system is a discretization of the familiar Poisson equation for the pressure. An efficient way to solve it is to employ the discrete Fourier transform (DFT) in the two periodic directions, θ and z. Given a vector $\mathbf{y} \in \mathbb{R}^{n_i}$ whose components y_{jkl} represent the values of a function $y(r, \theta, z)$ at our interior grid points, its (complex) DFT is denoted $\hat{\mathbf{y}}$ and its components are given by

$$\hat{y}_{jkl} = \frac{1}{\sqrt{n_\theta n_z}} \sum_{k=0}^{n_\theta - 1} \sum_{l=0}^{n_z - 1} \exp\left(\frac{2\pi i k \hat{k}}{n_\theta}\right) \exp\left(\frac{2\pi i l \hat{l}}{n_z}\right) y_{jkl}, \tag{11.13}$$

where $i = \sqrt{-1}$. In compact form, we write

$$\hat{\mathbf{y}} = F\mathbf{y},$$

where $F \in \mathbb{C}^{n_i \times n_i}$ is the nonsingular matrix of the coefficients in (11.13).

Instead of solving (10.14) directly, we solve it in the transform space. Thus we solve, instead of (10.14), the equivalent transformed system

$$FDGF^{-1}F\mathbf{p} = FD\mathbf{h}(\mathbf{u}; \lambda). \tag{11.14}$$

In practice, this means that we perform the following steps to obtain the solution $\mathbf{p}$:

- Compute $\hat{h} = FD\mathbf{h}$, the DFT of $D\mathbf{h}$, using the Fast Fourier Transform (FFT) algorithm.

- Solve $FDGF^{-1}\hat{\mathbf{p}} = \hat{\mathbf{h}}$ for $\hat{\mathbf{p}}$, the DFT of $\mathbf{p}$. This is an efficient procedure because the matrix $FDGF^{-1}$ is block diagonal, with blocks of size $(n_r - 1)$-by-$(n_r - 1)$ which are banded with bandwidth 5, so that only two superdiagonals and two subdiagonals are nonzero.

- Solve $F\mathbf{p} = \hat{\mathbf{p}}$ for the desired vector $\mathbf{p}$. This is done using an inverse FFT.

If the norm of the residual, $\|DG\mathbf{p} - D\mathbf{h}(\mathbf{u};\lambda)\|_2$, is too large (larger than some tolerance), then we use standard iterative improvement to obtain a better solution $\mathbf{p}$. In practice, we have found that one iterative improvement step is sufficient to make the residual negligible. Note that in order to be able to use the simplest version of the FFT algorithm, we require that both n_θ and n_z are integral powers of two.

11.7 Continuation Procedures

In order to obtain branches (parametrized by the Reynolds number Re) of steady state solutions of the ODE (10.9), we use the pseudo-arclength RPM continuation algorithm described in Section 7 of [16]. A summary of the algorithm is contained in Appendix A. In this Section, we do not discuss the details of that algorithm, since we use it with only minimal modification. However, the algorithm in [16] contains several adjustable parameters. Here, we discuss only our modifications and parameter adjustments of the algorithm presented in [16].

11.7.1 Increasing the Basis Size

We have slightly modified the method for increasing the size of the invariant subspace basis of the fixed point iteration. As suggested in Section 4.1 of [16], we use a window of four difference vectors. Schroff and Keller only used two, but suggested that using more would increase the accuracy of the basis. In addition, we substituted the Householder QR method for the modified Gram-Schmidt (MGS) method used in [16] to compute the QR factorization of those difference vectors. The reason for this change is that the Householder method, though more expensive, is more stable, especially when the vectors to be othonormalized are not very independent. For a comparison of QR factorization methods, we refer to reader to Chapter 5 of [10].

11.7.2 Parameter Settings

Several parameters in pseudo-arclength RPM continuation are adjustable. In this section, we discuss the settings we use.

The iteration in [16] corresponds to a "black-box" time integration over a small time interval Δt. We use $\Delta t = 0.5$ in all of our computations. In the automatic step size control in the fourth order Runge-Kutta method uses an error tolerance of 10^{-6}.

For increasing the size of the basis, the QR factorization of a few (in our case, four) difference vectors is computed. This is done if the iteration fails to converge after n_{max} iterations. We use $n_{max} = 50$. The size of the basis is decreased if some eigenvalues corresponding to the invariant subspace

spanned by the basis are less than some cut-off value δ, and we use $\delta = 0.5$. We point out that decreasing the basis size was never an issue because we never accumulated a basis which was too large to be efficient.

For the continuation algorithm, we used a pseudo-arclength stepsize of $\Delta s = 1$ in most cases. The condition for convergence is that the 2-norm of the residual $F(\alpha, \lambda)$ (see (10.9)) is less than the tolerance $tol = 10^{-8}$.

11.8 Numerical Experiments and Results

We performed numerical experiments with the laminar Couette flow solution branch as well as a Taylor vortex flow branch. The results of these experiments will serve to show that RPM, in conjunction with the theory of Chapter 10, is an effective method for computing solution branches of incompressible fluid flows such as the Taylor-Couette problem.

In order to compare our results with past investigations, particularly [28], we performed all experiments with the parameter values $\eta = 0.875$, $\Gamma = 2.54$, and $\omega = 0$. Thus, our experiments correspond to a configuration in which only the inner cylinder spins and the outer cylinder is at rest. Also, for the integer limiting the azimuthal wavelength, we used $q = 4$ in all our calculations.

11.8.1 Couette Flow

The Navier-Stokes equations (11.2) with the boundary conditions (11.5-

11.7) have the exact steady state solution

$$u = w = \Omega = 0, \tag{11.15a}$$

$$v = \frac{\eta}{1-\eta^2}\left(\frac{R_2}{r} - \frac{r}{R_2}\right), \tag{11.15b}$$

$$p_r = \frac{v^2}{r} \tag{11.15c}$$

for all Reynolds numbers Re. This is the laminar Couette flow, which is linearly stable for only small values of Re, less than the critical value Re_c. Our discretized system, for fine enough grids, displays similar behavior. An approximation to the Couette flow (11.15) is a solution for all Reynolds numbers, but the solution is linearly stable only for values of $Re < \overline{Re_c} \approx Re_c$.

Our continuation corrector is a time integration, and so we expect it to converge (for sufficiently small time step sizes) to the laminar flow as long as the Reynolds number remains in the stable regime, $Re < \overline{Re_c}$. In the stable regime, all the eigenvalues of $\mathbf{F}_{\boldsymbol{\alpha}}$ (evaluated at the laminar solution) have negative real part. At $Re = \overline{Re_c}$, one eigenvalue passes through zero. This eigenvalue has positive real part for $Re > \overline{Re_c}$ and causes the linear instability of the laminar flow. A time integration is expected to diverge from the laminar flow for Re greater than about $\overline{Re_c}$, regardless of how small the time step size is chosen.

RPM can be used to generate a hybrid iteration which will converge to the unstable laminar Couette flow at high Reynolds numbers. In addition, RPM can give us information on the unstable eigenvalue(s) and accelerate the convergence in the stable regime. If the fixed point iteration is of the form

$$\boldsymbol{\alpha}^{(n+1)} = \mathbf{G}(\boldsymbol{\alpha}^{(n)}, Re) \tag{11.16}$$

then RPM will compute a basis Z for an invariant subspace of the Jacobian $\mathbf{G}_{\boldsymbol{\alpha}}$. The eigenvalues of the small matrix $Z^T\mathbf{G}_{\boldsymbol{\alpha}}Z$ are a subset of the eigenvalues of $\mathbf{G}_{\boldsymbol{\alpha}}$ (see [16]). If all the (complex) eigenvalues μ of $\mathbf{G}_{\boldsymbol{\alpha}}$ lie within the unit disk $\{|\ \mu\ | < 1\}$, then the iteration is contracting. Eigenvalues with magnitude greater than one (outside the unit disk) cause instability.

We used RPM to compute the laminar solution branch for the range $100 \leq Re \leq 170$ with a resolution of $(n_r, n_\theta, n_z) = (31, 16, 32)$. We started at $Re = 130$ with the known Couette flow solution, to which we added the perturbation

$$u(r,\theta,z) = -\epsilon\frac{4(r-R_1)(r-R_2)}{(R_2-R_1)^2}\cos\left(\pi\left(1-\frac{2z}{\Gamma}\right)\right), \tag{11.17a}$$

$$w(r,\theta,z) = -\frac{\epsilon}{R_2-R_1}\sin\left(\frac{\pi}{2}\frac{(r-R_1)(r-R_2)}{(R_2-R_1)^2}\right)\sin\left(\pi\left(1-\frac{2z}{\Gamma}\right)\right), \tag{11.17b}$$

with $\epsilon = 0.001$. This is the same perturbation used by Schröder and Keller in [28]. The Couette flow solution is linearly unstable at $Re = 130$. This was confirmed by our time integration method, which diverged without the use of RPM.

But after 100 iterations, RPM isolated a single eigenvector of the iteration. This was enough to cause the iteration to converge, but the convergence was still slow. After 50 more iterations, another invariant subspace was isolated, this time of dimension three. After just one more iteration, the residual was well below the convergence criterion, and even below roundoff precision. Figure 11.18 shows the norm of the residual $\mathbf{F}(\boldsymbol{\alpha}, Re)$ plotted as a function of iteration number. Because the Couette flow solution is unstable at $Re = 130$, the residual actually increased before RPM isolated an invariant

subspace. This is a fine example of how RPM can stabilize unstable fixed point iterations.

We continued the solution branch in both directions of the Reynolds number. Before each continuation step, we added to the solution the same perturbation (11.17). Already having obtained a basis for a four-dimensional invariant subspace of the iteration, the convergence was much accelerated in both directions. In addition, the basis allowed us to compute, inexpensively, the four dominant eigenvalues of the iteration. Figure 11.19 shows the magnitudes of the three most dominant eigenvalues computed by RPM.

In the direction of decreasing Re, we found that eight or less iterations were sufficient to satisfy the convergence criterion at each continuation step. By monitoring the dominant eigenvalues of the iteration (see Figure 11.19), we were able to estimate the critical Reynolds numbers $\overline{Re}_c$ and Re_c at which Taylor vortices bifurcate from Couette flow. Initially, one eigenvalue has a magnitude greater than one, indicating instability. But as Re decreases, so does that eigenvalue. When the eigenvalue crosses the unit circle into the unit disk, the iteration becomes stable. This change of stability indicates that we have encountered a bifurcation. The location of the stability change is an estimate of $\overline{Re}_c$ and Re_c. For a resolution of $(n_r, n_\theta, n_z) = (31, 16, 32)$, we estimate $Re_c \approx 120$. The bifurcation of the continuous problem occurs at $Re_c = 118.2$ according to [8]. By increasing the resolution to $(n_r, n_\theta, n_z) = (63, 16, 64)$ near the bifurcation point, we obtain $Re_c \approx 118$.

Of course, the computed eigenvalues are only estimates, and their accuracy depends on the quality of the invariant subspace basis Z. If Z is indeed a basis of an invariant subspace of $\mathbf{G}_\alpha$, then the computed eigenvalues are

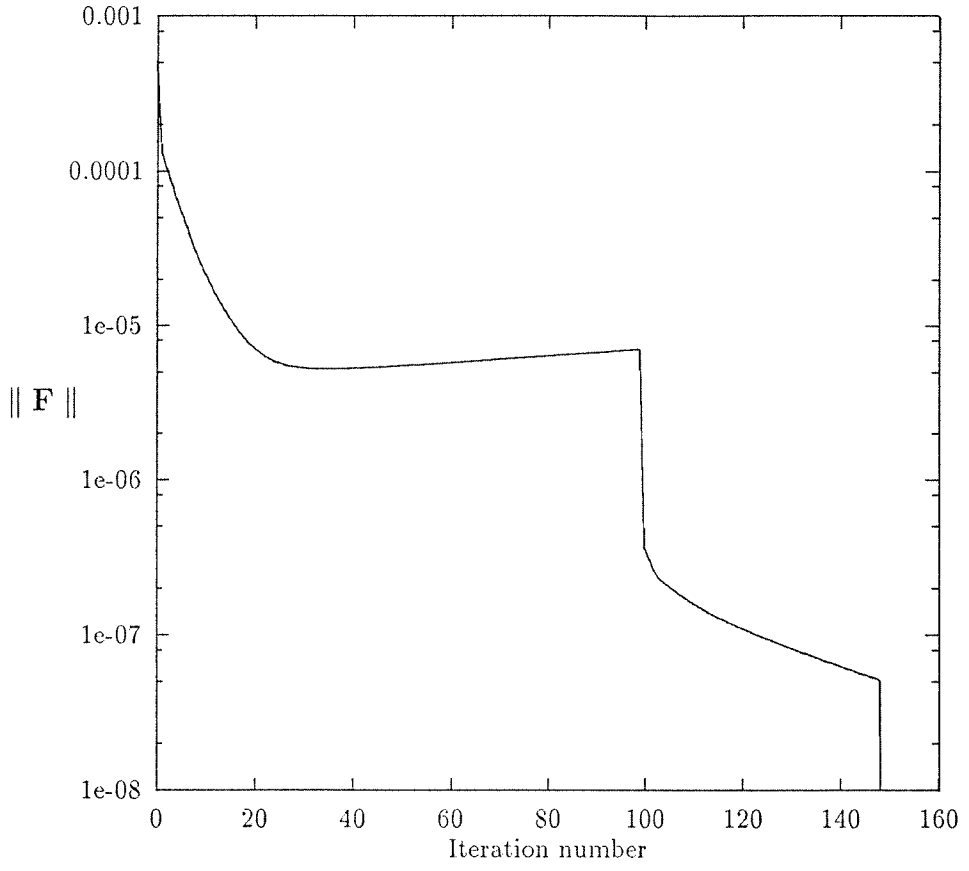

Figure 11.18: Norm of the residual $\mathbf{F}(\alpha, Re)$ as RPM converges to the laminar Couette flow solution at $Re = 130$. The residual actually increases before RPM isolates an invariant subspace because the solution is unstable.

exactly a subset of the eigenvalues of $\mathbf{G}_\alpha$. In reality, we only have a basis for an approximation to an invariant subspace, so the computed eigenvalues are only approximations to eigenvalues of $\mathbf{G}_\alpha$. So the eigenvalues computed by RPM should not be used to locate bifurcation points exactly, unless Z is a basis for a very good approximation to an invariant subspace (see Appendix A for how to test the quality of the invariant subspace). Nevertheless, we note that we obtain a very good estimate of the bifurcation point from the eigenvalues computed by RPM.

In the direction of increasing Re, we also found that convergence was significantly accelerated, so that eight to ten iterations were enough to satisfy the convergence criterion at each continuation step. At $Re \approx 140$, a second eigenvalue crossed the unit circle, turning unstable. This is shown in Figure 11.19 and indicates another bifurcation. We were able to continue through the bifurcation without problems.

Our Couette flow computations were a controlled experiment. They showed that RPM is an effective method for computing unstable steady states of a three-dimensional fluid dynamics problem. RPM also gave us information on the eigenvalues of the iteration Jacobian $\mathbf{G}_\alpha$, which allowed us to locate bifurcation points accurately.

11.8.2 Taylor Vortex Flow

Our Couette flow experiment was a somewhat artificial setting for using RPM. Couette flow does not vary with Re and so we added a perturbation at each continuation step. In realistic continuation problems, we do not, of

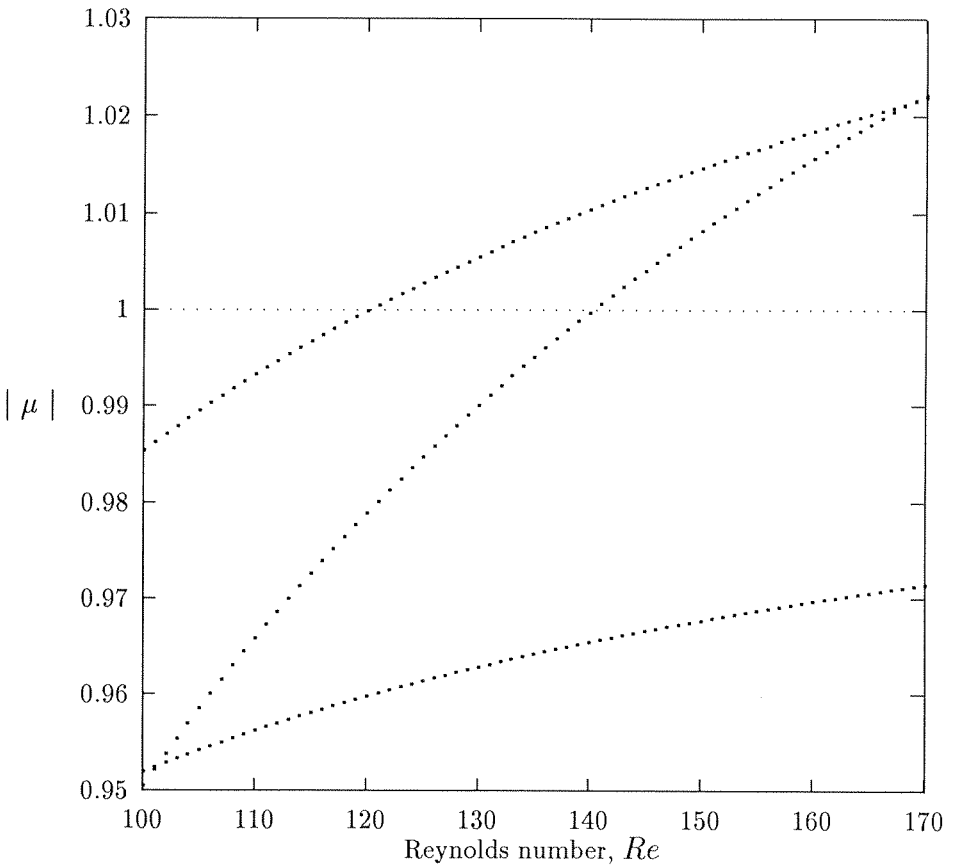

Figure 11.19: Magnitude of eigenvalues μ corresponding to dominant invariant subspace computed by RPM for laminar Couette flow. Eigenvalues μ with $|\mu| > 1$ cause linear instability.

course, introduce an artificial perturbation. Rather, the error to be corrected at each step is caused by the variation of the solution as the parameter value is changed.

In order to test RPM in such a more realistic setting, we used RPM to compute a Taylor vortex solution branch which bifurcates from Couette flow. To obtain a first Taylor vortex solution at $Re = 125$, we time evolved (without RPM) an initial condition obtained by adding a perturbation (11.17) to Couette flow with $\epsilon = 0.1$. Because the Couette solution is unstable at $Re = 125$, the time iteration converged to a stable Taylor vortex solution. We used a resolution of $(n_r, n_\theta, n_z) = (31, 16, 32)$.

When we were close to the Taylor vortex solution we turned on RPM to accelerate the convergence. Note that we could not use RPM from the start because RPM would have caught the instability and converged to the unstable Couette flow. After we turned on RPM, it took 100 iterations to isolate a three-dimensional invariant subspace, and the residual immediately dropped to well below the roundoff level. For subsequent continuation steps using the obtained basis, the convergence criterion was met after 97-114 iterations.

Figure 11.20 shows the streamlines of the axial and radial velocity components of our computed Taylor vortex solution at $Re = 125$. Starting with this solution, we used RPM continuation to obtain the Taylor vortex solution branch for $\overline{Re}_c \leq Re \leq 150$. In Figure 11.21, we plot $u^* = u(r^*, \theta^*, z^*)$ along the computed branch at $r^* = R_1 + \frac{1}{4}(R_2 - R_1)$, $\theta^* = 0$, and $z^* = \Gamma/2$. This should be compared to the upper branch (I) in Figure 7 of [28], and we see excellent agreement. Near the bifurcation point with Couette flow, we

reduced the continuation step size to 0.25. Interestingly, the solution merged into the Couette flow branch at the bifurcation point $Re = \overline{Re}_c$, instead of continuing into the other Taylor vortex branch (branch II in Figure 7 of [28]). In [28], Keller and Schröder attributed this to the phenomenon of perturbed bifurcation. We did not compute the other Taylor vortex branch because it is not relevant to this study of RPM.

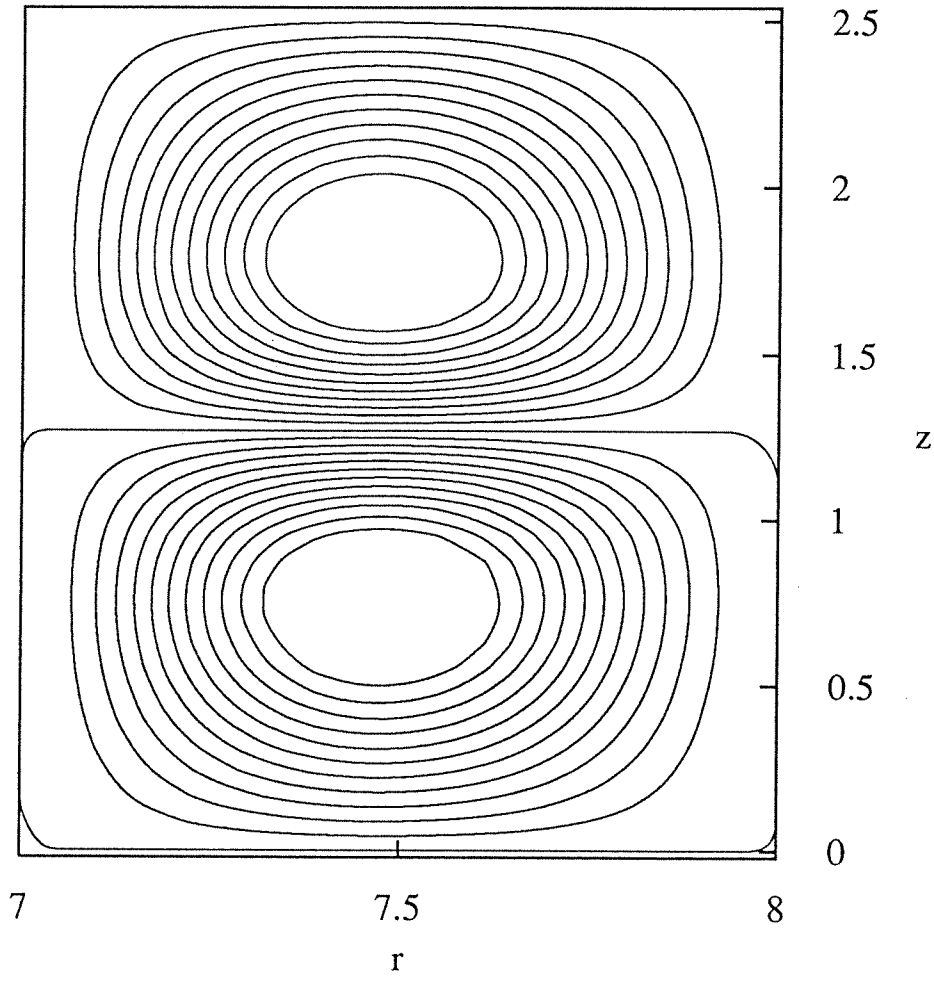

Figure 11.20: Streamlines of the radial and axial velocity components for a computed Taylor vortex solution at $Re = 125$, $\Gamma = 2.54$, $\eta = 0.875$, and $\omega = 0$. The (r,z)-plane shown is the cross-section with $\theta = \theta_0 = 0$. The flow is axisymmetric so that the solution is the same at all values of θ. The flow is counter-clockwise in the upper vortex and clockwise in the lower vortex.

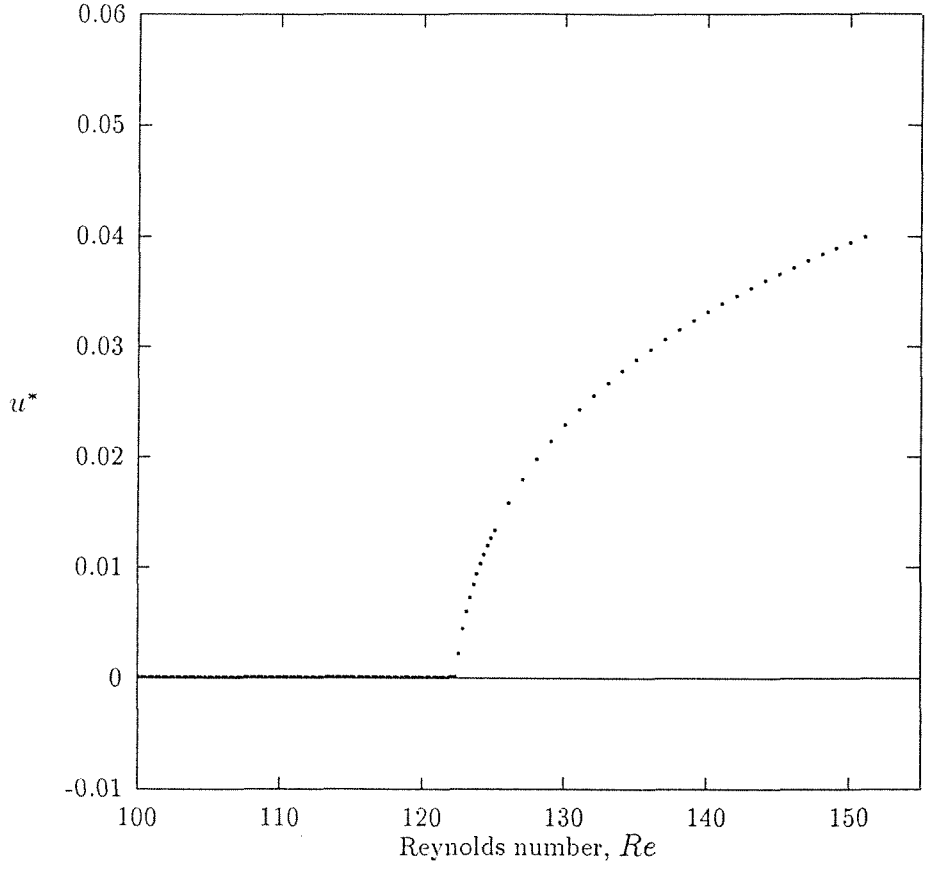

Figure 11.21: Radial velocity component u^* as a function of Reynolds number. This shows good agreement with branch I in Figure 7 of [28].

Chapter 12

Conclusions

We have demonstrated how the Recursive Projection Method of [16] can be applied to differential-algebraic systems by reducing them to ordinary differential equations. In particular, we showed that this approach yields a new method for computing steady state and travelling wave solution branches of the Navier-Stokes equations. As an example and test of this new method, we computed solution branches of the viscous flow between two concentric rotating cylinders. The method proved effective in this setting.

We emphasize that this method can be used in a great variety of settings other than fluid mechanics, in which differential-algebraic equations occur. Examples include constrained mechanical systems and electric circuit models.

A natural extension of this work is to use our new method in search of bifurcations from wavy Taylor vortex flows. The problem formulation in Chapter 11 includes a rotating frame of reference, which allows for the computation of travelling wave solutions. Thus, the method could be used

without modification to compute a wavy Taylor vortex solution branch. By monitoring the eigenvalues computed by RPM, we may be able to find a bifurcation from that branch. This could take us a step closer to understanding the state transitions observed by Taylor (see [17]).

A limitation of our method is that it can compute only steady state solutions or travelling wave solutions which are steady states in a moving frame of reference. However, in the study of fluid mechanics, one often wants to compute branches of periodic solutions. It would therefore be of great interest to develop a continuation method for this purpose.

Appendix A

The Recursive Projection Method

The Recursive Projection Method (RPM) was designed by Schroff and Keller [16] to recover convergence of fixed point iterations. Suppose we wish to compute equilibrium solution branches

$$\mathbf{u}^*(\lambda) = \mathbf{G}(\mathbf{u}^*(\lambda), \lambda) \tag{A.1}$$

of a nonlinear parameter-dependent fixed point iteration of the form

$$\mathbf{u}^{(\nu+1)} = \mathbf{G}(\mathbf{u}^{(\nu)}, \lambda), \tag{A.2}$$

where $\mathbf{G} : \mathbb{R}^n \times \mathbb{R} \rightarrow \mathbb{R}^n$ is smooth.

The local convergence (as $\nu \rightarrow \infty$) rate near a solution depends on the spectral radius of the Jacobian $\mathbf{G}_\mathbf{u}^* \equiv \mathbf{G}_\mathbf{u}(\mathbf{u}^*(\lambda), \lambda)$. The iteration (A.2)

converges locally as long as the eigenvalues μ of $\mathbf{G}_{\mathbf{u}}^{*}$ lie within the unit disk $\{|\mu| < 1\}$. This may the case for some interval of parameter values λ but not for parameter values outside this interval. RPM generates a modified hybrid iteration which restores convergence when one or more eigenvalues leave the unit disk. This is done by exploiting the fact that the divergence is due to only one or a few eigenvalues outside the unit disk. Even when all the eigenvalues are within the unit disk and the iteration converges, the convergence may be slow because some eigenvalues are close to the unit circle. RPM can also be used to accelerate convergence in such cases.

The purpose of this appendix is to provide a brief summary of RPM and the main results of [16]. For a more rigorous and detailed description of RPM, we refer the reader to [16].

A.1 The Hybrid Iteration

Suppose that the eigenvalues of $\mathbf{G}_{\mathbf{u}}^{*}$ are μ_j, $j = 1, \ldots, n$ and satisfy

$$|\mu_1| \geq |\mu_2| \geq \ldots \geq |\mu_n|.$$

Let $P \in \mathbb{R}^{n \times n}$ be a projector from $\mathbb{R}^n$ to the maximal invariant subspace of $\mathbf{G}_{\mathbf{u}}^{*}$, corresponding to the m largest eigenvalues $\mu_1, \mu_2, \ldots, \mu_m$. Then $Q \equiv I - P$ projects onto the orthogonal complement of that invariant subspace. We thus have, for each $\mathbf{u} \in \mathbb{R}^n$, the unique decomposition

$$\mathbf{u} = \mathbf{p} + \mathbf{q}, \mathbf{p} \equiv P\mathbf{u}, \mathbf{q} \equiv Q\mathbf{u}. \tag{A.3}$$

A Lyapunov-Schmidt decomposition is used to split the original problem into two parts:

$$\mathbf{p} = \mathbf{G_1}(\mathbf{p}, \mathbf{q}, \lambda) \equiv P\mathbf{G}(\mathbf{p} + \mathbf{q}, \lambda), \tag{A.4a}$$

$$\mathbf{q} = \mathbf{G_2}(\mathbf{p}, \mathbf{q}, \lambda) \equiv Q\mathbf{G}(\mathbf{p} + \mathbf{q}, \lambda). \tag{A.4b}$$

It is shown in [16] that the eigenvalues of

$$(\mathbf{G_2})^*_{\mathrm{q}} = Q\mathbf{G}^*_{\mathrm{u}}Q$$

are $\mu_{m+1}, \mu_{m+2}, \ldots, \mu_n$. Therefore, the iteration

$$\mathbf{q}^{(\nu+1)} = \mathbf{G_2}(\mathbf{p}, \mathbf{q}^{(\nu)}, \lambda) \tag{A.5}$$

converges if $|\mu_{m+1}|$ is less than one.

Now consider the hybrid iteration obtained by using

- the original fixed point iteration for $\mathbf{q}$ on (A.4b), i.e. (A.5), and
- Newton's method for $\mathbf{p}$ on (A.4a).

The new iteration is thus governed by:

$$\left(I - (\mathbf{G_1})^{(\nu)}_{\mathrm{p}}\right)(\mathbf{p}^{(\nu+1)} - \mathbf{p}^{(\nu)}) = \mathbf{G_1}(\mathbf{p}^{(\nu)}, \mathbf{q}^{(\nu)}, \lambda) - \mathbf{p}^{(\nu)}, \tag{A.6a}$$

$$\mathbf{q}^{(\nu+1)} = \mathbf{G_2}(\mathbf{p}, \mathbf{q}^{(\nu)}, \lambda). \tag{A.6b}$$

Here, $\mathbf{u}^{(\nu)} = \mathbf{p}^{(\nu)} + \mathbf{q}^{(\nu)}$ (different from $\mathbf{u}^{(\nu)}$ in (A.2)) is used to define

$$(\mathbf{G_1})^{(\nu)}_{\mathrm{p}} \equiv \frac{\partial}{\partial \mathbf{p}}\mathbf{G_1}(\mathbf{p}^{(\nu)}, \mathbf{q}^{(\nu)}, \lambda) = P\mathbf{G}_{\mathrm{u}}(\mathbf{u}^{(\nu)}, \lambda)P. \tag{A.7}$$

A convergence analysis in [16] shows that the Jacobian of the hybrid iteration (A.6) has a spectral radius of $|\mu_{m+1}|$.

A.2 RPM Continuation

The hybrid iteration can be used as the corrector in a predictor-corrector continuation algorithm which computes the desired solution branch $\mathbf{u}^*(\lambda)$. This algorithm is called RPM continuation.

For example, suppose we are interested in finding solution branches $\mathbf{u}^*(\lambda)$ of a nonlinear parameter-dependent system

$$\mathbf{F}(\mathbf{u}^*, \lambda) = \mathbf{0}, \tag{A.8}$$

where $\mathbf{F} : \mathbb{R}^n \times \mathbb{R} \rightarrow \mathbb{R}^n$. These solution branches are steady states of the dynamical system

$$\frac{d\mathbf{u}}{dt} = \mathbf{F}(\mathbf{u}, \lambda). \tag{A.9}$$

One way to compute these steady states is to integrate the dynamical system (A.9) for large times t. The time integration procedure can be viewed as a fixed point procedure (A.2). If the time integration converges, then it can be used as the corrector in the continuation method. However, the time integration will fail to converge if the eigenvalues of the $\mathbf{F}_\mathbf{u}^*$ lie outside the stability region of the time integration method. RPM can be used to recover convergence in such cases, and to accelerate the convergence rate even when the time integration converges. Of course, many other kinds of fixed point iterations, such as quasi-Newton methods, can be used in place of the time integration.

Note that the iteration (A.6) is well defined as long as the matrix $(I - (\mathbf{G_2})_\mathbf{p}^{(\nu)})$ remains nonsingular. Singularity of that matrix along a solution

branch indicates a critical point at which folds and bifurcations may occur [14]. If we encounter a critical point during coninuation in λ, we introduce a pseudo-arclength parameter s and a constraint

$$N(\mathbf{p}, \mathbf{q}, s) = 0.$$

This allows us to proceed beyond the most common type of critical point, a simple fold [14]. Schroff and Keller show in [16] that it is sufficient to perform the pseudo-arclength continuation in the small m-dimensional subspace and N can be chosen to be independent of $\mathbf{q}$.

A.3 Recursive Estimation of the Projectors P and Q

The hybrid iteration (A.6) requires the projectors P and Q. These are obtained by finding an orthonormal basis $Z \in \mathbb{R}^{n \times m}$ for the space $\mathcal{R}(P)$. The projectors P and Q are then given by

$$P = ZZ^T, \tag{A.10a}$$

$$Q = I - ZZ^T. \tag{A.10b}$$

RPM includes methods for increasing and decreasing the basis size m, as well as for maintaining the accuracy of the basis.

A.3.1 Increasing the Basis Size

The basis Z can be estimated directly from the iterates $\mathbf{q}^{(\nu)}$ of the algo-

rithm. If we define $\Delta \mathbf{q}^{\nu} \equiv \mathbf{q}^{(\nu)} - \mathbf{q}^{(\nu-1)}$, and if $\mathbf{u}^{(\nu)} = \mathbf{p}^{(\nu)} + \mathbf{q}^{(\nu)}$ is near $\mathbf{u}^*$ (i.e., $\| \mathbf{u}^{(\nu)} - \mathbf{u}^* \|_2 < \epsilon$), then

$$\Delta \mathbf{q}^{(\nu)} = (\mathbf{G_2})_{\mathrm{q}}^{*} \Delta \mathbf{q}^{(\nu-1)} + O(\epsilon^2) \approx \left((\mathbf{G_2})_{\mathrm{q}}^{*} \right)^{\nu} \Delta \mathbf{q}^{(0)}. \qquad \text{(A.11)}$$

Thus, the vectors $\{\mathbf{q}^{(\nu)}\}$ are, to a second order approximation in ϵ, a power iteration with the matrix $(\mathbf{G_2})_{\mathrm{q}}^{*}$. So as $\nu \rightarrow \infty$, these vectors lie in the dominant invariant subspace of $(\mathbf{G_2})_{\mathrm{q}}^{*}$, as long as $\Delta \mathbf{q}^{(0)}$ has a component in this direction.

If the iteration does not converged after say, n_{max} iterations, then we accumulate a window of r difference vectors

$$D \equiv \left[\Delta \mathbf{q}^{(\nu-r+1)}, \Delta \mathbf{q}^{(\nu-r+2)}, \ldots, \Delta \mathbf{q}^{(\nu)} \right],$$

which approximately span the dominant invariant subspace of dimension r. To get an orthonormal basis for the span of D, we compute the QR factorization of D to obtain $\hat{D} \in \mathbb{R}^{n \times r}$ with orthonormal columns and upper triangular $T \in \mathbb{R}^{r \times r}$ satisfying

$$D = \hat{D} T.$$

The decay of the diagonal elements T_{ii} of T shows how well separated the dominant invariant subspaces are. For example, if $|T_{11}| \gg |T_{22}|$, then a one-dimensional invariant subspace has been well isolated. The first column of $\hat{D}$ is thus added to the basis Z while the basis size m is incremented by one. Similarly, the remaining ratios $|T_{ii}/T_{i+1,i+1}|$ are examined. If $|T_{ii}/T_{i+1,i+1}| \gg 1$, then an invariant subspace of dimansion i has been isolated, and the corresponding columns of D can be added to Z.

In [16], a window of $r = 2$ difference vectors was used, and the QR factorization was computed using the "modified Gram-Schmidt" procedure [10]. However, Schroff and Keller point out in [16] that a larger window could be used. Also, the modified Gram-Schmidt method can be replaced with the QR method, which is slightly more expensive but also more stable, especially when the vectors in D are not very independent (see [10]).

A.3.2 Maintaining the Accuracy of the Basis

During the continuation process, the dominant invariant subspace of $\mathbf{G}_u^*$ will change and the accuracy of our basis estimate Z will deteriorate. It is therefore necessary to update the basis Z using a power iteration. This can be done very inexpensively after each continuation step, via

$$Z \leftarrow \text{orth}(\mathbf{G}_u^* Z).$$

Here, "orth($\mathbf{G}_u^* Z$)" represents an orthonormal basis for the range of $\mathbf{G}_u^*$, which is done using QR factorization. Because an approximation of $\mathbf{G}_u^* Z$ is required for executing the hybrid iteration, this does not require any additional function evaluations.

The accuracy of the basis Z can be monitored by evaluating the matrix

$$\mathcal{E} \equiv Q \mathbf{G}_u^* P,$$

which vanishes if Z spans an invariant subspace. If $\mathcal{E}$ becomes too large, one can perform additional power iteration steps. This, however, does require additional function evaluations. In practice, the one "free" power iteration has been found to be sufficient to keep the basis reasonably accurate.

A.3.3 Decreasing the Basis Size

As continuation progresses, eigenvalues which were once dominant may decrease in magnitude. The invariant subspace corresponding to such eigenvalues may have been included in the basis Z but should be deleted from the basis when the eigenvalue is no longer dominant.

This is important for two reasons. Firstly, the size of the basis m should be kept small, so that the method will operate efficiently. If m grows too large, the solution of linear systems in Newton's method may become too expensive. Secondly, the invariant subspace corresponding to non-dominant eigenvalues cannot be maintained well using power iterations. The accuracy of the basis Z will then deteriorate and this may cause poor convergence behavior.

In practice, we would like the basis Z to span an invariant subspace corresponding only to eigenvalues with magnitude greater than $1 - \delta$. The cutoff value δ is chosen so that eigenvalues within the disk of radius $1 - \delta$ do not cause slow convergence; this depends on the cost of function evaluations in the particular application. The eigenvalues of the m-by-m matrix

$$H \equiv Z^T \mathbf{G}_u^* Z$$

are the subset of the eigenvalues of $\mathbf{G}_u^*$ represented in Z. The eigenvalues and eigenvectors of the small matrix H are computed inexpensively after each continuation step. If only $\hat{m} < m$ eigenvalues of H have magnitude less than $1 - \delta$, then we compute a real basis $V \in \mathbb{R}^{m \times \hat{m}}$ for the corresponding

invariant subspace of H. Then we make the replacement

$$Z \leftarrow \text{orth}(ZV)$$

so that Z will be a good approximation to the $\hat{m}$-dimensional dominant invariant subspace of $\mathbf{G}_{\mathrm{u}}^{*}$.

Bibliography

[1] Uri M. Ascher, Peter A. Markowich, Paola Pietra, and Christian Schmeiser. A phase plane analysis of transonic solutions for the hydrodynamic semiconductor model. *Mathematical Models and Methods in Applied Sciences*, 1(3):347–376, 1991.

[2] K. E. Brenan, S. L. Campbell, and L. R. Petzold. *Numerical Solution of Initial-Value Problems in Differential-Algebraic Equations.* North-Holland, 1989.

[3] Leon O. Chua. *Introduction to Nonlinear Networks.* McGraw Hill, New York, 1969.

[4] Leon O. Chua and An-Chang Deng. Impasse points. Part I: Numerical aspects. *International Journal of Circuit Theory and Applications*, 17:213–235, 1989.

[5] D. Coles. Transition in circular couette flow. *J. Fluid Mech.*, 21:385–425, 1965.

[6] M. Couette. Etudes sur le frottement des liquides. *Ann. Chim. Phys.*, 6:433–510, 1890.

[7] M. G. Crandall and P. H. Rabinowitz. Bifurcation from simple eigenvalues. *J. Funct. Anal.*, 8:321–340, 1971.

[8] R. C. DiPrima and H. L. Swinney. Instabilities and transition in flow between concentric rotating cylinders. In H. L. Swinney and J. P. Gollub, editors, *Hydrodynamic Instabilities and the Transition to Turbulence*, page 139. Springer-Verlag, New York, 1981.

[9] E. J. Doedel. AUTO. In *Proceedings of the Tenth Manitoba Conference on Numerical Mathematics, Winnipeg, Canada, 1981*, page 265, Univ. of Manitoba, Winnipeg, 1984.

[10] Gene H. Golub and Charles F. van Loan. *Matrix Computations.* The Johns Hopkins University Press, 2nd edition, 1989.

[11] M. E. Henderson and H. B. Keller. Complex bifurcation from real paths. *SIAM J. Appl. Math.*, 50(2):460–482, April 1990.

[12] Michael E. Henderson. *Complex Bifurcation.* Ph.D. thesis, California Institute of Technology, Pasadena, California, 1985.

[13] Gérard Iooss and Daniel D. Joseph. *Elementary Stability and Bifurcation Theory.* Springer-Verlag, 1980.

[14] Herbert B. Keller. *Lectures on Numerical Methods in Bifurcation Problems.* Springer-Verlag, Tata Institute of Fundamental Research, Bombay, India, 1987.

[15] Herbert B. Keller and W. F. Langford. Iterations, perturbations and multiplicities for nonlinear bifurcation problems. *Archive for Rational Mechanics and Analysis*, 48:83–108, 1972.

[16] Herbert B. Keller and Gautam M. Schroff. Stabilzation of unstable procedures: the Recursive Projection Method. *SIAM J. Numer. Anal.*, 30(4):1099–1120, August 1993.

[17] E.L. Koschmieder. *Bénard Cells and Taylor Vortices.* Cambridge University Press, 1993.

[18] Shiu-Hong Lui. *Multiple Bifurcations.* Ph.D. thesis, California Institute of Technology, Pasadena, California, 1992.

[19] Roswitha März. Numerical methods for differential algebraic equations. *Acta Numerica*, pages 141–198, 1991.

[20] L. R. Petzold. A description of DASSL: A differential/algebraic system solver. In R.S. Stapleman et al., editor, *Scientific Computing*, pages 65–68. North-Holland, Amsterdam, 1983.

[21] Patrick J. Rabier. Implicit differential equations near a singular point. *J. Math. Anal. Appl.*, 144:425–449, 1989.

[22] Patrick J. Rabier and Werner C. Rheinboldt. A general existence and uniqueness theory for implicit differential-algebraic equations. *Differential and Integral Equations*, 4(3):563–582, May 1991.

[23] Patrick J. Rabier and Werner C. Rheinboldt. A geometric treatment of implicit differential-algebraic equations. Technical Report ICMA-91-162, Institute for Computational Mathematics and Computations, Dept. of Mathematics and Statistics, University of Pittsburgh, May 1991.

[24] Patrick J. Rabier and Werner C. Rheinboldt. On impasse points of quasilinear differential-algebraic equations. Technical Report ICMA-92-171, Institute for Computational Mathematics and Applications, Dept. of Mathematics and Statistics, University of Pittsburgh, April 1992.

[25] Patrick J. Rabier and Werner C. Rheinboldt. On the computation of impasse points of quasilinear differential-algebraic equations. Technical Report ICMA-92-172, Institute for Computational Mathematics and Applications, Dept. of Mathematics and Statistics, University of Pittsburgh, June 1992.

[26] Werner C. Rheinboldt. Differential-algebraic systems as differential equations on manifolds. *Mathematics of Computation*, 43(168):473–482, October 1984.

[27] Werner C. Rheinboldt. On the existence and uniqueness of solutions of nonlinear semi-implicit differential-algebraic equations. *Nonlinear Analysis*, 16(7/8):647–661, 1991.

[28] Wolfgang Schröder and Herbert B. Keller. Wavy Taylor-Vortex flows via multigrid-continuation methods. *Journal of Computational Physics*, 91(1):197–227, November 1990.